University of Wisconsin-Extension

GEOLOGICAL AND NATURAL HISTORY SURVEY
3817 Mineral Point Road
Madison, Wisconsin 53705

M.E. Ostrom, State Geologist and Director

GUIDE TO THE STUDY OF WATER MOVEMENT IN SOIL PEDONS ABOVE THE WATERTABLE

by

J. Bouma

Open-File Report 73-6
194 p.

This report represents work performed by the Geological and Natural History Survey, and is released to the open files in the interest of making the information more readily available. This report has not been edited or reviewed for conformity with Geological and Natural History Survey standards and nomenclature.

1973, First edition

GUIDE TO THE STUDY OF WATER MOVEMENT IN SOIL PEDONS ABOVE THE WATERTABLE

First Edition

Soil Survey Division
Geological and Natural History Survey
University of Wisconsin—Extension,
Madison, Wis. 53706

June 1973

Water movement through soil pedons above the water table

First Edition 1973

by J. Bouma
Assistant Professor of Soil Science, Wisconsin Geological and Natural History Survey, University-Extension, and Soils Department, College of Agricultural and Life Sciences, University of Wisconsin, Madison, Wisconsin 53706

TABLE OF CONTENTS

Page

N.B. THIS PUBLICATION IS REPRODUCED IN LIMITED QUANTITY AND IS AT THIS TIME MAINLY INTENDED FOR INTERNAL USE.

1. INTRODUCTION

Professional contacts between soil scientists specializing in soil survey, morphology and classification and those specializing in soil physics, have been too scarce in the past. Maybe that can explain why the former group likes to think of the latter as being composed of unpractical, theoretically motivated glass-bead minded, ivory, super specialists, while the latter from their view point look at the others as being empirically motivated generalists that shield their basic ignorance behind linguistically complicated classification and other schemes. Even if there is a grain of truth in these views, reality dictates the overriding fact that knowledge about basic transport phenomena in soils needs to be available to the soil surveyor or classifier so as to make his judgements on soil behavior more meaningful, while at the same time at least some soil physicists ought to know where to find certain soils and what a real soil looks like.

This guide is an attempt to discuss and illustrate some basic principles of soil morphology, that should be of interest to soil physicists and to discuss some simplified flow systems that should interest soil surveyors. In addition, some recent work in Wisconsin, discussing relationships between the two types of data and discussing future trends in the practical interpretation of soil maps, is included as well. This is only a first approximation and many changes will have to be made later.

Acknowledgement is made for many suggestions and contributions by W.R.Gardner (Univ. of Wisc.Madison, Soils Dept.),P.A.C.Raats, C.R.Amerman and Chr.Dirksen (ARS-USDA-Soils Dept.Univ.of Wis.) and F.D.Hole (Geol.Nat.Hist.Survey Univ.Ext. and Soils Dept.UW) Students contributing to different aspects included J.L.Anderson, J.L.Denning, W.G.Walker and D.J.van Rooijen.

2. Some basic morphological characteristics associated with water movement through soils.

2.1 INTRODUCTION

Movement of water in soil can only occur through voids, and shapes and sizes of these voids will therefore determine the rate of movement at any hydraulic gradient. Movement of water in soil is, of course, a physical process which is governed by characteristic constants as will be discussed in Chapter 3.

However, morphological soil studies, describing and measuring the occurrence, size and shape of voids in soil can be helpful to predict the rate and patterns of water movement as will be discussed in Chapter 5. In addition, movement of water may result in characteristic features in the soil such as cutans and iron mottling. Observation of such and other features may be helpful in providing indicators for the hydrodynamic processes in the soil. This chapter, then, will discuss methods to describe and measure soil morphological features.

The scheme of describing soil structure, as currently used in the United States, has been presented in the Soil Survey Manual (1951). Soil structure was defined as "the aggregation of primary soil particles into compound particles or clusters of primary particles, which are separated from adjoining aggregates by surfaces of weakness". An individual natural soil aggregate is called a "ped" in contrast to (1) a "clod", caused by

Table 2.1a

—*Types and classes of soil structure*

Class	TYPE (Shape and arrangement of peds)						
	Platelike with one dimension (the vertical) limited and greatly less than the other two; arranged around a horizontal plane; faces mostly horizontal	Prismlike with two dimensions (the horizontal) limited and considerably less than the vertical; arranged around a vertical line; vertical faces well defined; vertices angular.		Blocklike; polyhedronlike, or spheroidal, with three dimensions of the same order of magnitude arranged around a point.			
				Blocklike; blocks or polyhedrons having plane or curved surfaces that are casts of the molds formed by the faces of the surrounding peds		Spheroids or polyhedrons having plane or curved surfaces which have slight or no accommodation to the faces of surrounding peds	
		Without rounded caps	With rounded caps	Faces flattened; most vertices sharply angular	Mixed rounded and flattened faces with many rounded vertices	Relatively nonporous peds	Porous peds
	Platy	Prismatic	Columnar	(Angular) Blocky [1]	Subangular blocky [2]	**Granular**	**Crumb**
Very fine or very thin.	Very thin platy; <1 mm.	Very fine prismatic; <10 mm.	Very fine columnar; <10 mm.	Very fine angular blocky; <5 mm.	Very fine subangular blocky; <5 mm.	Very fine granular; <1 mm.	Very fine crumb; <1 mm.
Fine or thin	Thin platy; 1 to 2 mm.	Fine prismatic; 10 to 20 mm.	Fine columnar; 10 to 20 mm.	Fine angular blocky; 5 to 10 mm.	Fine subangular blocky; 5 to 10 mm.	Fine granular; 1 to 2 mm.	Fine crumb; 1 to 2 mm.
Medium	Medium platy; 2 to 5 mm.	Medium prismatic; 20 to 50 mm.	Medium columnar; 20 to 50 mm.	Medium angular blocky; 10 to 20 mm.	Medium subangular blocky; 10 to 20 mm.	Medium granular; 2 to 5 mm.	Medium crumb; 2 to 5 mm.
Coarse or thick.	Thick platy; 5 to 10 mm.	Coarse prismatic; 50 to 100 mm.	Coarse columnar; 50 to 100 mm.	Coarse angular blocky; 20 to 50 mm.	Coarse subangular blocky; 20 to 50 mm.	Coarse granular; 5 to 10 mm.	
Very coarse or very thick	Very thick platy; >10 mm	Very coarse prismatic; >100 mm	Very coarse columnar; >100 mm	Very coarse angular blocky; >50 mm.	Very coarse subangular blocky; >50 mm	Very coarse granular; >10 mm.	

[1] (a) Sometimes called *nut*. (b) The word "angular" in the name can ordinarily be omitted.
[2] Sometimes called *nuciform*, *nut* or *subangular nut*. Since the size connotation of these terms is a source of great confusion to many, they are not recommended.

Table 2.1b GRADE OF STRUCTURE

0. *Structureless.*—That condition in which there is no observable aggregation or no definite orderly arrangement of natural lines of weakness. ***Massive*** if coherent; ***single grain*** if noncoherent.

1. *Weak.*—That degree of aggregation characterized by poorly formed indistinct peds that are barely observable in place. When disturbed, soil material that has this grade of structure breaks into a mixture of few entire peds, many broken peds, and much unaggregated material. If necessary for comparison, this grade may be subdivided into *very weak* and *moderately weak*.

2. *Moderate.*—That grade of structure characterized by well-formed distinct peds that are moderately durable and evident but not distinct in undisturbed soil. Soil material of this grade, when disturbed, breaks down into a mixture of many distinct entire peds, some broken peds, and little unaggregated material. Examples are the loam A horizons of typical Chestnut soils in the granular type, and clayey B horizons of such Red-Yellow Podzolic soils as the Boswell in the blocky type.

3. *Strong.*—That grade of structure characterized by durable peds that are quite evident in undisplaced soil, that adhere weakly to one another, and that withstand displacement and become separated when the soil is disturbed. When removed from the profile, soil material of this grade of structure consists very largely of entire peds and includes few broken peds and little or no unaggregated material. If necessary for comparison, this grade may be subdivided into *moderately strong* and *very strong*. Examples of strong grade of structure are in the granular-type A horizons of the typical Chernozem and in the columnar-type B horizons of the typical solodized-Solonetz.

disturbance such as plowing or digging, (2) a "fragment", caused by rupture of the soil mass across natural surfaces of weakness and (3) a "concretion" caused by local concentrations of compounds that irreversibly cement the soil grains together.

Field descriptions of soil structure note: (1) the shape and arrangement of peds ("type" of structure), (2) the size of peds ("class") and (3) the distinctness and durability of the peds ("grade"). The usual sequence followed in structure description is: grade --- class --- type, for example: strong coarse prismatic structure. The structural pattern of a soil horizon also includes the shapes and sizes of soil pores as well as those of the peds themselves. However, the Soil Survey Manual (1951) does not provide specific terms to describe soil porosity. The classifications of types, classes, and grades of structure, as defined by the Soil Survey Manual, are summarized in table 2.1.

Soil morphological work by Kubiena (1938), Jongerius (1957), Johnson et al. (1962), and Brewer (1964), among others, indicated the need to:

1. Provide descriptive schemes for soil pores in which they are considered as separate individuals, and

2. develop schemes for characterizing unaggregated soil materials without peds that can not adequately be characterized by the terms "single grain" or "massive" of the Soil Survey Manual.

This text will present a summary of Brewer's system of classification of soil structure, to be illustrated with pictures of soil structures observed in soils in Wisconsin. In addition, some pedological features will be discussed that may be valuable for predicting hydrodynamic processes in soil.

Table 2.2

DEFINITIONS ACCORDING TO BREWER (1964)

Soil material is the unit of study; it is that unit in which the characteristics being studied are relatively constant, and it will vary in size with the kind and extent of development of those characteristics.

Soil Structure - The physical constitution of a soil material as expressed by the size, shape, and arrangement of the solid particles and voids, including both the primary particles to form compound particles and the compound particles themselves; fabric is the element of structure which deals with arrangement.

Skeleton grains of a soil material are individual grains which are relatively stable and not readily translocated, concentrated or re-organized by soil-forming processes; they include mineral grains and resistant siliceous and organic bodies larger than colloidal size (Brewer and Sleeman, 1960).

Plasma of a soil material is that part which is capable of being or has been moved, reorganized, and/or concentrated by the processes of soil formation. It includes all the material, mineral or organic, of colloidal size and relatively soluble material which is not bound up in the skeleton grains (Brewer and Sleeman, 1960).

A ped is an individual natural soil aggregate consisting of a cluster of primary particles, and separated from adjoining peds by surfaces of weakness which are recognizable as natural voids or by the occurrence of cutans (Brewer, 1960b)

Pedality. The physical constitution of a soil material as expressed by the size, shape, and arrangement of peds.

Primary Peds. The simplest peds occurring in a soil material; they cannot be divided into smaller peds, but they may be packed together to form compound peds of a higher level of organization.

Simple Packing Voids. These voids are due to random packing of single grains.

Channels. Channels are voids that are significantly larger than those which would result from normal packing of single grains, and have a generally cylindrical shape.

Vughs are relatively large voids, other than packing voids, usually irregular and not normally interconnected with other voids of comparable size; at the magnifications at which they are recognized they appear as discrete entities.

Planar voids are simply voids that are planar according to the ratios of their principal axes; by virtue of their shape and extent the constitute an obvious deviation from the normal packing of single plasma and skeleton grains in a soil material.

Compound Packing Voids. These voids result from packing of compound individuals, such as peds, which do not accomodate each other.

Basic structure refers to the size, shape and arrangement of simple grains (plasma and skeleton grains) and associated packing voids in primary peds or apedal soil material excluding pedological features other than plasma separations.

Matric structure refers to the size, shape and arrangement of simple grains (plasma and skeleton grains) and all voids in primary peds or apedal soil material, excluding pedological features other than plasma separations.

S-matrix of a soil material is the material within the simplest (primary) peds, or composing apedal soil materials, in which the pedological features occur; it consists of the plasma, skeleton grains, and voids that do not occur in pedological features other than plasma separations.

Primary Structure. The structure within an apedal soil material or within the primary peds in a pedal soil material; it is an integration of the size, shape, and arrangement of all the pedological features enclosed in the s-matrix and the basic structure, or structure of the s-matrix.

Secondary Structure. The size, shape, and arrangement of the primary peds, their interpedal voids, and associated interpedal pedological features in a soil material.

Tertiary Structure. The size, shape, and arrangement of the secondary peds of a soil material (compound peds resulting from the packing of primary peds), their interpedal voids and associated interpedal pedological features.

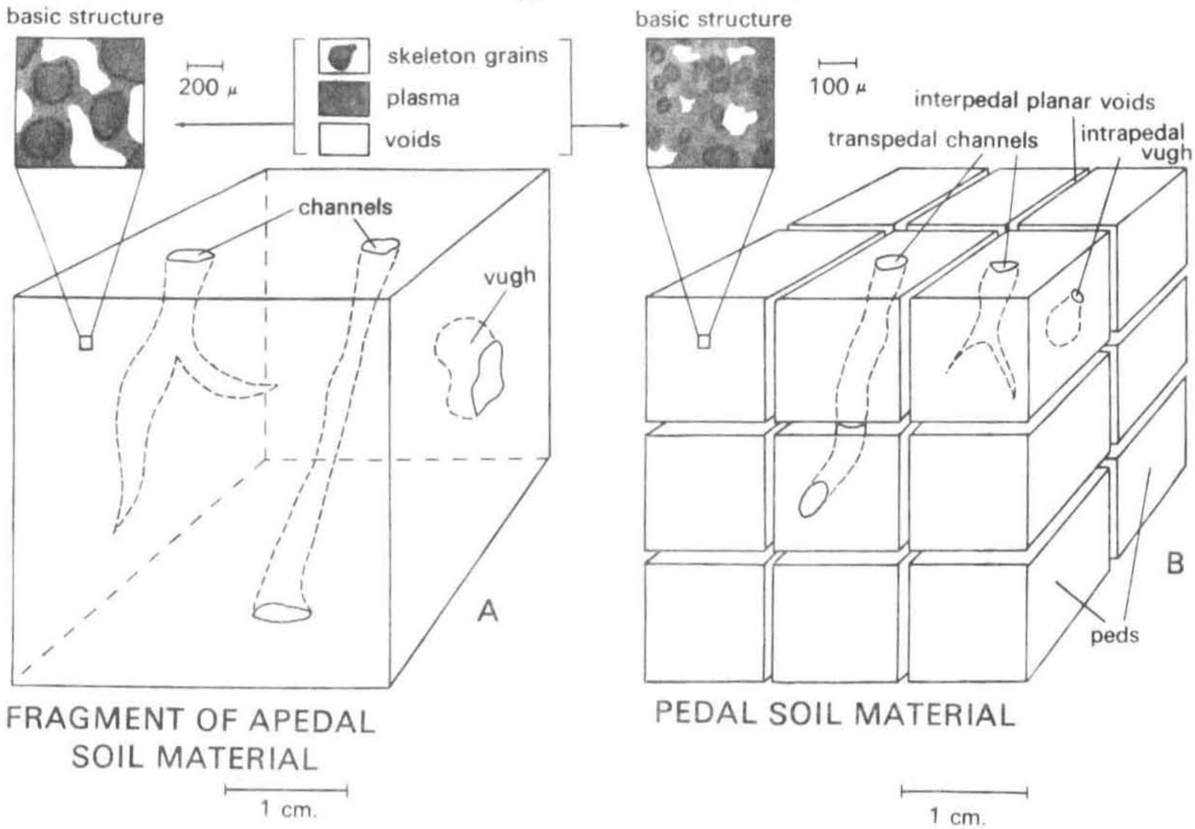

Fig. 2.1. Schematic drawings of apedal (left) and pedal (right) soil materials.

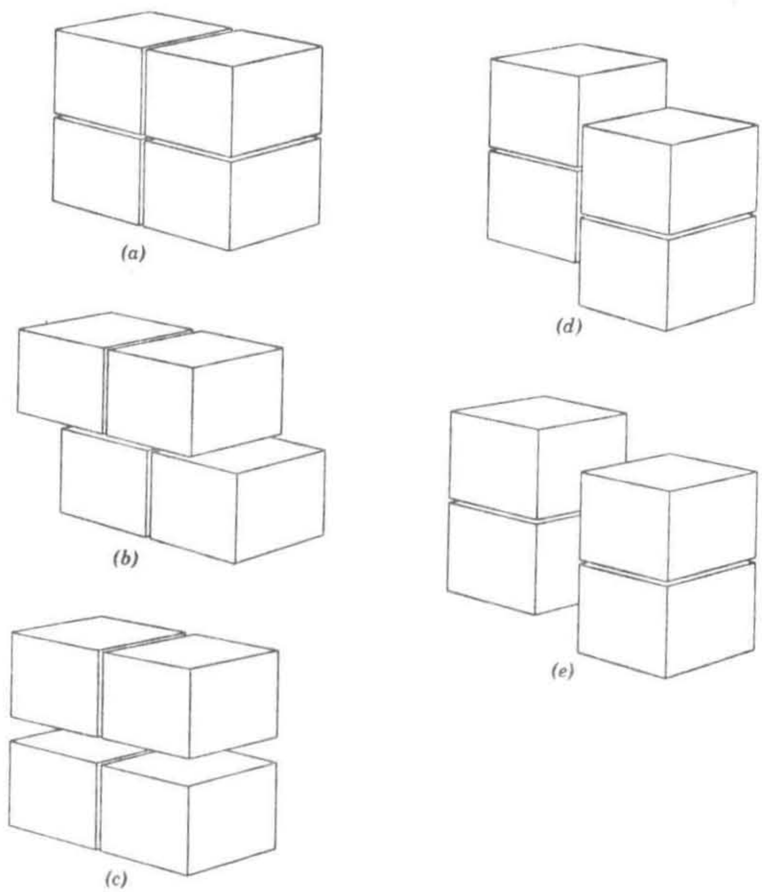

Fig 2.3(Brewer,1964) Systems of packing of cubes. (*a*) Normal. (*b*) Offset. (*c*) Bi-offset. (*d*) Faulted. (*e*) Offset faulted.

2.2. Soil structure description according to Brewer.

2.2.1. INTRODUCTION

Definitions of terms used by Brewer and discussed here have been placed in Table 2.2. to facilitate reading of this text. Brewer's definition of soil structure includes size, shape and arrangement of voids and primary particles, thus including the two omissions of the Soil Survey Manual (1951) discussed in the previous section. The term soil structure, as used in the Soil Survey Manual, referred to the type and degree of aggregation of soil materials. Brewer defines natural aggregation in terms of pedality. Pedal soil materials have peds, apedal soil materials don't. Fig. 2.1. illustrates these two different types of structure. Pores larger than simple packing pores, such as channels and vughs (table 2.2), may occur in an apedal soil mass in which the smallest individual mineral particles, defined as skeleton grains and plasma, determine the size and shape of the fine simple packing voids (Fig. 2.1, left picture). Peds usually occur in soil materials containing significant amounts of clay because of processes of swelling and shrinking due to wetting and drying. Sizes of simple packing voids in such pedal soil materials are usually much smaller than voids occurring in apedal soil materials with less clay (Fig. 2.1, right picture). The larger pores may be channels or vughs, as in apedal soil materials; interpedal voids are usually planar voids or compound packing voids.

Structures have to be characterized at different magnifications, starting with the primary particles, that may form peds, which, in turn, may be part of compound peds themselves. Different levels of structure have been distinguished (Table 2.2):

1. Basic structure (redefined here according to Bouma and Anderson, 1973).

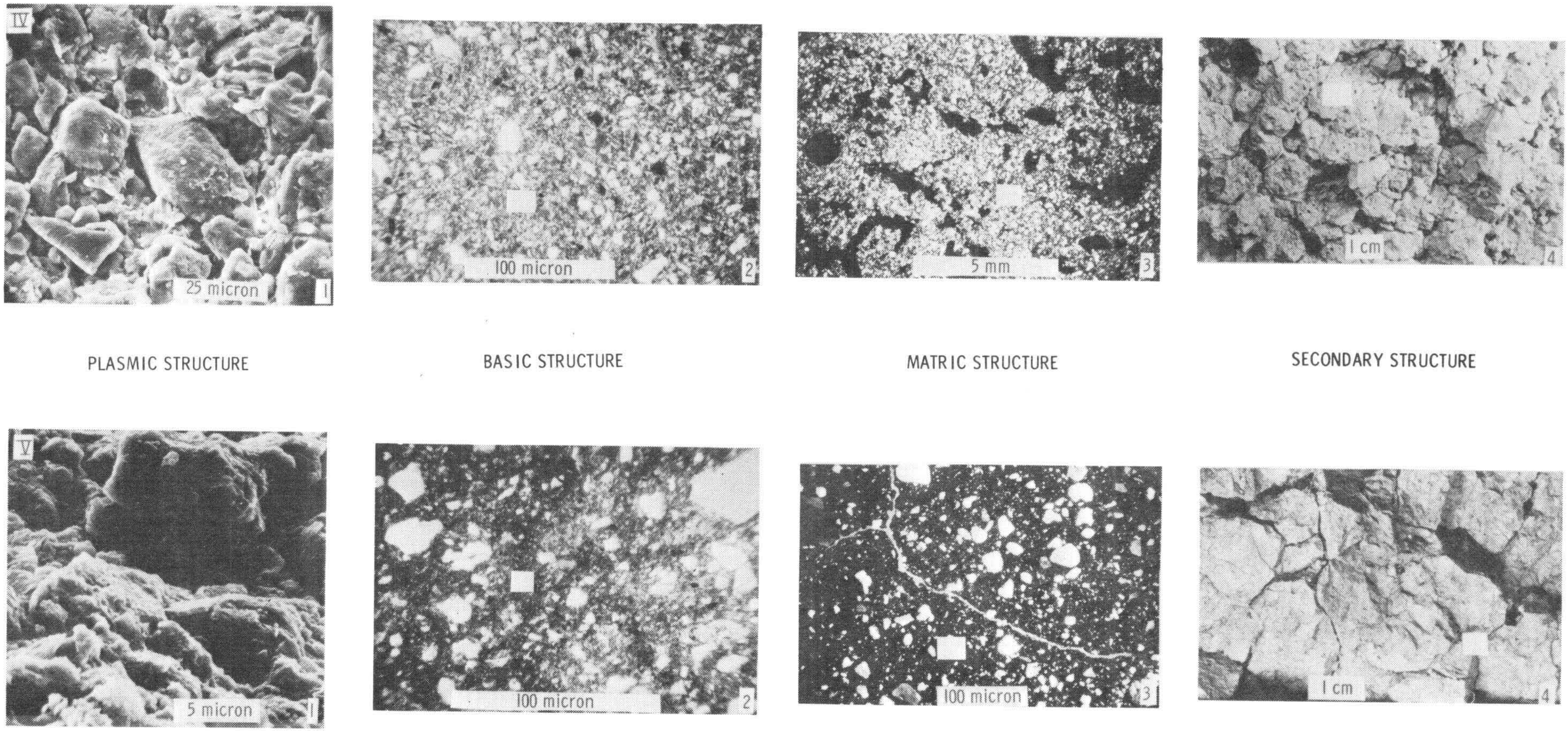

Fig. 2.2. Soil structure of apedal (I, II and III) and pedal (IV, V) soil materials, pictured at different magnifications. Pictures of plasmic structures were taken with a Scanning Electron Microscope (courtesy Dr. E.B. Sachs, USDA Forest Products Laboratory, Madison). Pictures of basic structures were made from thin sections as were pictures from matric structures in soils IV and V. Matric structures in soils I, II and III were taken from horizontal soil peels as were pictures from secondary structures in soils IV and V. Soil I is the C-horizon of a Plainfield loamy sand (loamy sand texture). Soil III is the IIC horizon of a Batavia silt loam (sandy loam texture) Soil IV is the B_2 horizon of a Batavia silt loam (silty clay loam texture) and soil V is the B_2 horizon of a Hibbing loam (clay texture). The little white areas in the pictures indicate the areas represented in the adjacent, left side, larger magnifications of the same horizon.

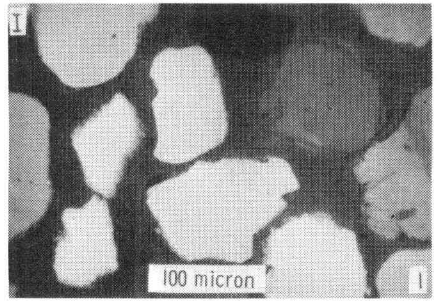

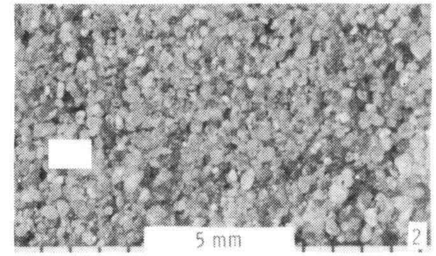

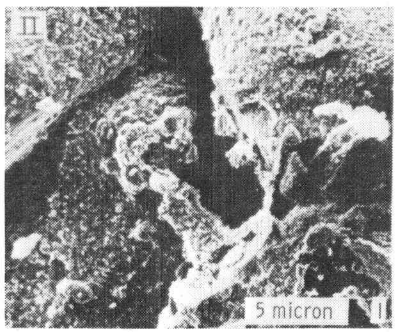

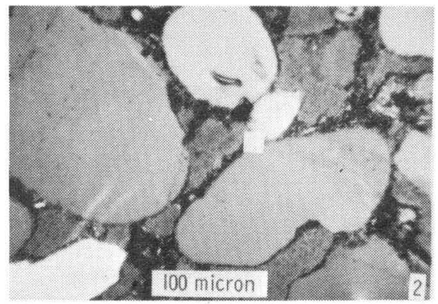

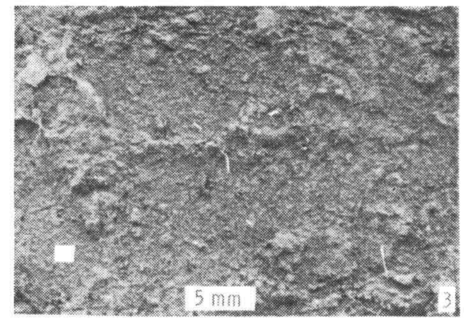

PLASMIC STRUCTURE

BASIC STRUCTURE

MATRIC STRUCTURE

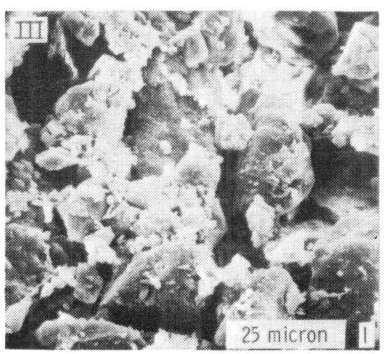

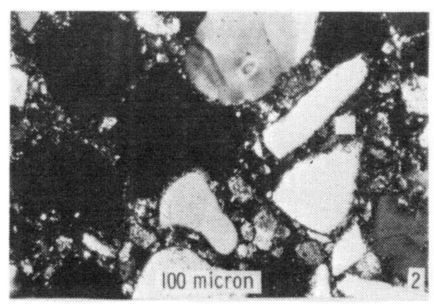

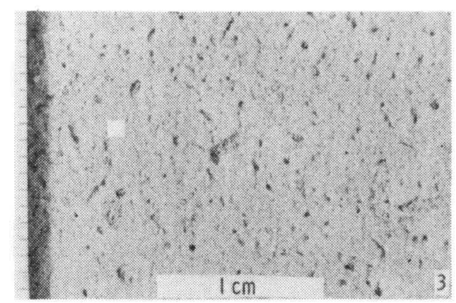

Descriptions of Pictures in Fig. 2.2.

I-1. Granular basic structure (simple packing voids between fine sand grains).

I-2. Granular matric structure. Voids larger than packing voids are not visible in the picture, so there is no essential difference between basic and matric structure.

II-1. Skelsepic plasmic structure, indicating orientation of clay-plates parallel to the skeleton grains.

II-2. Intertextic basic structure, indicating that plasma occurs between skeleton grains at points of contact, not filling simple packing voids.

II-3. Channelled intertextic matric structure. A few small channels are visible in the picture. However, their amount is low and the horizon could also be described as having an intertextic matric structure.

III-1. Argillasepic plasmic structure, indicating that the plasma grains (clay plates) are not mutually oriented.

III-2. Agglomeroplasmic basic structure, indicating an increased content of plasma as compared with II-2.

III-3. Channelled agglomeroplasmic matric structure. (Many round channels are visible in the picture).

IV-1. Argillasepic plasmic structure.

IV-2. Porphyroskelic basic structure. Plasma and skeleton grains form a dense S-matrix in which no larger pores are visible.

IV-3. Vughy porphyroskelic matric structure. Vughs and channels occur in a dense porphyroskelic S-matrix.

IV-4. Medium subangular blocky secondary structure with accomodating peds. Transpedal channels have to be quantified by field counts (see data in picture 10. Appendix of Chapter 2 for Batavia silt loam-B2).

V-1. Masepic plasmic structure. Plasma (clay) plates are mutually oriented. Thin sections would be needed to further investigate this.

V-2. Porphyroskelic basic structure.

V-3. Jointed porphyroskelic matric structure. Planar voids occur in the porphyroskelic S-matrix.

V-4. Medium prismatic secondary structure with accomodating peds. (See additional data in picture 13. (Appendix of Chapter 2 for Hibbing silt loam B2.)

Soil I is apedal C-horizon (sand) of Plainfield loamy sand; Soil II is apedal B-horizon (loamy sand) of the same soil; Soil III is apedal IIC horizon (sandy loam) of Batavia silt loam; Soil IV is pedal B2 horizon (silty clay loam) of Batavia silt loam and Soil V is pedal B2 horizon (clay) of Hibbing loam. (Descriptions of these soils are in Chapter 6.)

2. Matric structure (proposed by Bouma and Andersen, 1973 as the structure of the S-matrix).

3. Primary structure.

4. Secondary structure.

5. Tertiary structure.

The pictures in Fig. 2.2 illustrate different structures as they are visible at different magnifications. The number of pictures, in turn, shows the number of levels of magnifications necessary in each soil material to obtain a complete structure description. Complex structures, such as secondary or tertiary structures in a clay soil, need studies at more levels of magnification than the relatively simple structure of a sand without plasma. Specific techniques have to be used to observe soil structures, such as 1: scanning electron microscopy and microscopy in thin sections or in soil peels at high magnifications and 2: direct observation in hand specimens. Thus, attention is focused on the appropriate sizes of samples so as to make them representative for the soil material or the structure-level to be characterized. Relatively homogenous units of structure can be described using morphological analyses. Such units are defined as "the unit of study", the "soil material" (table 2.2). Necessary volumes of soil materials for study will increase as the size of structural phenomena increases or with increasing heterogenity. Assuming, then, that sufficiently large soil samples are available to be studied at all desired levels of magnification, the description schemes themselves remain to be defined.

2.2.2. Principles of structure analysis

Three elements are essential in descriptive systems of soil structure, as follows from the structure definition. These are: (1) size, (2) shape and (3) arrangement of the mineral particles and voids constituting a soil material. Brewer (1964) discusses sizes and shapes of mineral particles or aggregates in considerable detail (p. 17).

Size distributions of primary soil mineral particles can be determined by measuring the particle size distribution (the term "soil texture" is used in soil survey practices), which is a standard method based on Stokes' law. Size distribution of larger coherent mineral aggregates such as peds can be determined by sieving. A different procedure involves direct measurement, using morphometric techniques applied to thin sections, soil peels or hand specimen (Anderson and Binnie, 1961; Van der Plas, 1962; Bouma and Anderson, 1973). Specific techniques to measure pore size distributions in thin sections or size distributions and abundance of channels and planar voids in situ or in soil peels, will be discussed in Chapter 5.

Shapes of mineral grains, or aggregates, have been studied in great detail by sedimentologists (Pettijohn, 1957; Powers, 1953; Folk, 1955). This manual will be most concerned with shapes of peds, and these will be defined when discussing secondary structures. The element of shape has been integrated into the description of voids by distinguishing different "types" of voids, each of which with characteristic shapes, such as channels, packing voids, vughs, etc. Definitions of these different pore-types are given in Table 2.2.

Finally, the arrangement-aspect of structure is very important and rather complex. Brewer even defined a separate term: "soil fabric", which relates only to arrangement of primary and secondary particles, omitting their sizes and shapes which are part of the broader "soil structure" definition. Brewer discusses "arrangement" in his book at great length (p. 159), explaining that the term not only relates to (1) the arrangement of the constituents (plasma, skeleton grains and voids) with regard to each other, but also (2) with regard to specific reference features. There are two separate aspects of arrangement that apply to all the individuals in a soil material (mineral grains, voids and compound units) at all levels: distribution and orientation patterns. Descriptions of soil structures do usually (quite fortunately) not require a complete listing of all distribution and orientation patterns of all components. Rather, this descriptive scheme gives the morphologist a logical means to describe specific relevant features. Different aspects of 'arrangement" will be described in the following sections. For example, the arrangement of constituents with regard to each other (point 1 above) is very important when describing basic fabrics. When pedal soil materials are described the arrangement of peds with regard to alike and adjacent individuals (point 2 above) is most relevant.

A generalized approach will be used in this text to illustrate the use of Brewer's system for describing soil structure at the different levels of structure defined earlier. Emphasis will be placed on the description of pores. The reader is referred to Brewer's book for more details.

2.2.3. Description schemes for soil structure (See fig. 2.2 for examples of each type)

I. Plasmic structure. (Brewer, 1964, page 303)

Observed in: Scanning Electron Microscope (SEM) - pictures; thin sections.

To be noted: size and shape of plasma grains and their arrangement.

The latter can be described in terms of: (1) "sepic" (where elongated plasma grains, ("domains"), are mutually oriented in specific ways), (2) "asepic" where orientation of domains is at random or (3) isotropic when domains are invisible. (4) Crystic plasmic fabrics are composed of recognizable crystals and form a separate group.

Study of plasmic-structures is often of limited value in relation to flow of water through soils because: (i) plasma-pores are usually very small so flow of water can be expected to be very low, and (ii) study of structure of dry soil plasma as observed in a thin section may be highly unrepresentative of the structure that is formed after wetting due to swelling.

II. Basic structure. (Brewer, p. 170: related distribution pattern)

Observed in: thin sections, soil peels.

To be noted: size, shape and arrangement of plasma, skeleton grains and associated voids.

The arrangement of plasma and skeleton grains is very important as it determines the size, shape and continuity of the pores in basic structures. The most relevant aspect of arrangement is here the distribution pattern relating to the arrangement of the constituents (plasma, skeleton grains and voids) with regard to each other. Type-names have been suggested by Brewer, as derived from earlier terms proposed by Kubiena. Soil materials with only skeleton grains and very little plasma have a granular basic fabric; increasing content of plasma (which is often concentrated around grains and at points of contact between grains) is expressed by using the terms intertextic, agglomeroplasmic and porphyroskelic. Pictures of each of these basic fabrics are in Fig. 2.2.

III. Matric structure (Bouma and Anderson, 1973).

Observed in: thin sections, soil peels.

To be noted: size, shape and arrangement of plasma skeleton grains and associated voids and of voids significantly larger than packing voids occurring in primary peds or in apedal soil materials.

The matric structure, as defined here, is the structure of Brewer's S-matrix (p. 147), which is "the material within the simplest (primary) peds or composing apedal soil materials" (pedological features, to be discussed in one of the following chapters, occur in the S-matrix).

Nomenclature of matric structures can become quite complex (Brewer, p.321), but by emphasizing some important features rather than listing sizes, shapes and arrangements of all soil constituents, simplifications can be made. For example, a soil with an agglomeroplasmic basis structure, in which many channels occur would be described as having a channelled agglomeroplasmic S-matrix. It is advantageous to describe matric structures in terms of certain types of S-matrixes. Occurrence and abundance of pores larger than packing pores (channels, planar voids) can be studied with microscopic techniques applied to thin sections or soil peels or by applying direct counts to horizontal sections through pedons in situ (see Chapter 5 for some examples).

The primary structure relates to the occurrence of pedological features that will be discussed in the next chapter. The next category of soil structure is the secondary structure.

IV. Secondary structure.

Observed in: soil peels, hand specimen and in situ.

To be noted: size, shape and arrangement of peds and interpedal voids (and interpedal pedological features to be discussed later).

The Soil Survey Manual has provided a system to describe sizes and shapes of peds. Brewer's classification (p. 342) is more detailed and more specific. However, these classification schemes are more suitable for specialized research rather than for routine application in the field. This is certainly true for the size-analysis which requires, for example, extensive measurement of lengths of principal axes or planimetric determinations on thin sections. The shape-analysis introduces another, and more basic, problem associated with field application of detailed descriptive schemes. Introduction of many types of shape, some of them only differing in details, is rather unrealistic considering the natural variability occurring in the field and the inevitable lack of reproducibility that occurs when different investigators describe a similar soil. The more detailed the descriptive systems are, the more variability is bound to occur. The basic types of shape distinguished by Brewer (polyhedral, spheral and polyspheral) correspond essentially with those of the Soil Survey Manual. Shapes of peds, as defined in the Manual, would seem to be acceptable therefore for continued use. In specific cases, additions can be made following Brewer's system. The size

Table 2.3

Pedological Features. Recognizable units within a soil material which are distinguishable from the enclosing material for any reason, such as origin (deposition as an entity), differences in concentration of some fraction of the plasma, or differences in arrangement of the constituents (fabric).

Cutan. A modification of the texture, structure, or fabric at natural surfaces in soil materials due to concentration of particular soil constituents or in situ modification of the plasma; cutans can be composed of any of the component substances of the soil material.

Skeletan. These consist of skeleton grains adhering to the cutanic surface.

Argillan. An argillan is composed dominantly of clay minerals.

Matran. Matrans are composed of skeleton grains and plasma, and can be distinguished from the s-matrix by having more plasma and/or denser packing (modified after Brewer).

Neocutans. Neocutans are cutans that occur subcutanically immediately adjoining the natural surfaces with which they are associated.

Glaebule. A three dimensional unit within the s-matrix of the soil material, and usually approximately prolate to equant in shape; its morphology (especially size, shape, and/or internal fabric) is incompatible with its present occurrence being within a single void in the present soil material. It is recognized as a unit either because of a greater concentration of some constituent and/or a difference in fabric compared with the enclosing soil material, or because it has a distinct boundary with the enclosing soil material.

Nodules. Glaebules with an undifferentiated internal fabric; in this context undifferentiated fabric includes recognizable rock and soil fabrics.

Concretions. Glaebules with a generally concentric fabric about a center which may be a point, line, or a plane.

Papules. Glaebules composed dominantly of clay minerals with continous and/or lamellar fabric; they have sharp external boundaries. Most commonly they are prolate to equant and somewhat rounded.

and shape classification of the Soil Survey Manual was reproduced in Table 2.1. The arrangement of peds, as part of the structure concept, is described by Brewer in terms of three components: 1) Accomodation (Accomodated, Partially accomodated, and Unaccomodated), 2) Packing (Normal, Offset, Bi-offset faulted, see fig. 2.3.) and 3) Inclination (vertical, horizontal, inclined). This classification of arrangement is very useful as it refers to the very important pattern of planar pores in soils, which is essential for predicting permeability of pedal soil materials (Chapter 5).

Interpedal pores are usually adequately described by noting size, shape and arrangement of peds. If not, specific reference can be made to pore patterns using Brewer's terminology.

The Soil Survey Manual concept of "soil structure grade" is unsatisfactory as a soil morphological tool, as it is not only based on the visibility of peds *in situ* (which is quite dependent on the moisture status of the soil) but also upon their resistance to disturbance, e.g., mechanical strength. The latter property can be better described in terms of soil consistency, which has been adequately defined in the Soil Survey Manual as a function of the soil moisture content.

2.3. Pedological Features.

Study of pedological features may be useful to predict patterns of water movement in soils and of associated processes. Two types of features will be discussed here, viz. cutans and glaebules. All definitions are separately listed in Table 2.3. Pictures of secondary structures are presented in Chapter 2.5.

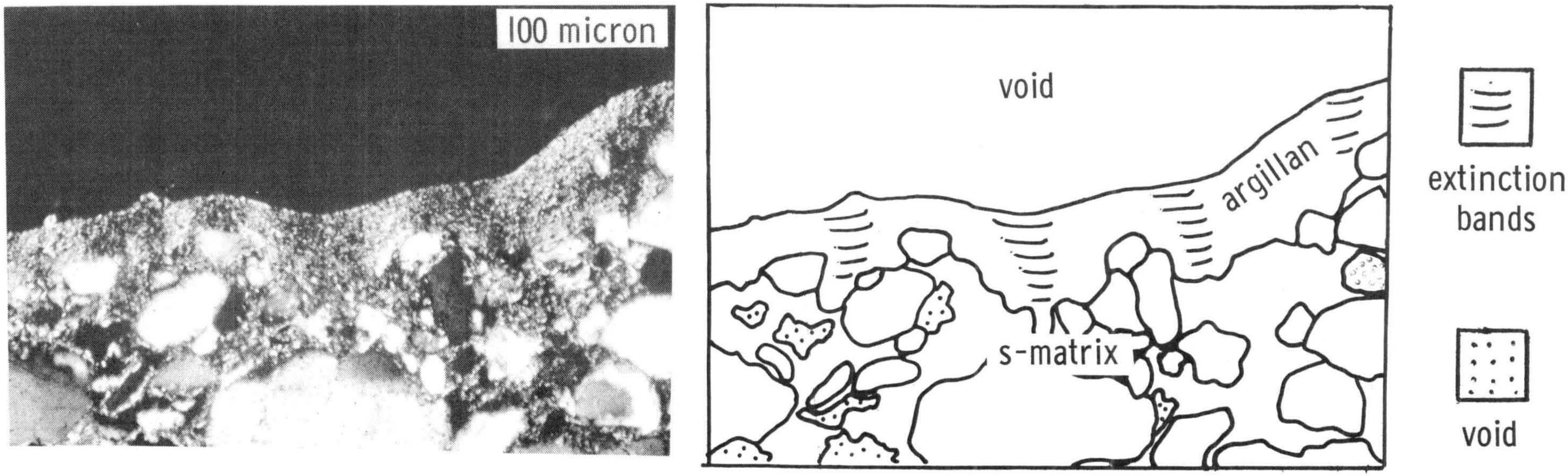

Fig. 2.4. Thin planar-void argillan with moderate orientation and a gradual boundary.

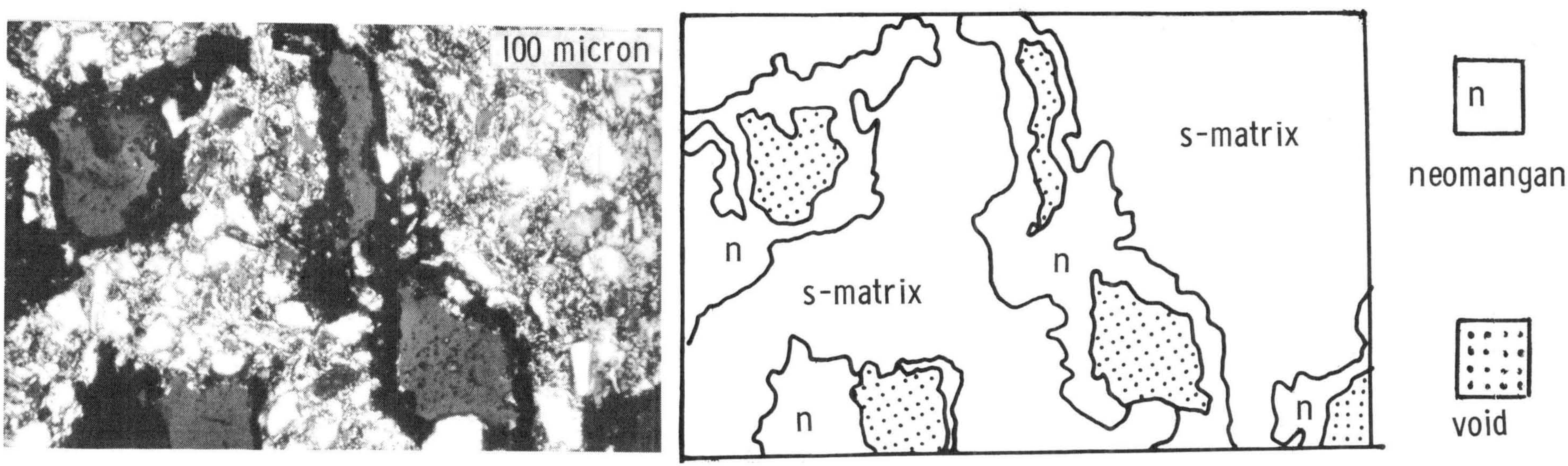

Fig. 2.5. Very thin channel mangan-neomangans with sharp boundaries.

2.3.1. CUTANS (Brewer, 1964, Chapter 10)

The definition of cutans can be found in Table 2.3. Type names are formed by adding -an to a term describing the nature of the cutanic material, for example: "argillan" is a cutan composed of clay minerals. Water moving through larger soil pores at relatively high velocities may carry suspended clay or silt particles downwards into the soil profile and may erode the walls of the pores as well. These particles will be deposited on the walls of channels or peds when water is absorbed deeper in the soil by the soil matrix. Such deposits, in turn, can then be considered as indicators for the type and intensity of the physical transport processes involved. For example, at high flow velocities, small as well as large grains are transported and sedimentation deeper in the profile will result in cutans with coarse components (matrans). When water flows very slowly, on the contrary, only fine particles will be moved that may form thin cutans in which the individual grains are mutually well oriented (argillan, Fig. 2.4). Skeletans are cutans composed of skeleton grains that accumulated on ped faces either because the fine particles were washed out (neoskeletan, Brewer, page 294) or because grains were transported downwards during periods of high flow. Sometimes, natural surfaces of peds in the field have a quite different appearance than ped interiors but microscopic analysis in thin sections may not reveal any accumulation of minerals at these surfaces. Then, the difference in appearance may be due to rearrangement of the plasma particles in a small zone at and just under the ped surface. Such cutans, then defined as "neocutans", have *in situ* modifications of the plasma. The neocutan considered here might be classified as a neostrian ("neo" because it occurs inside the ped adjacent to the voids and is not covering the ped and "strian" to indicate the striated orientation pattern of the plasma which results in a different light reflection).

Another very important type of cutan is composed of oxidized iron (red) or manganese (black) compounds. Such cutans may be indicative of redox potentials occurring in soils as induced by periodic saturation with water. Reduction of iron (Fe^{3+}) and manganese (Mn^{4+}) compounds may occur during soil saturation in the absence of free oxygen but in the presence of some energy source, such as soluble organic matter. Consideration of chemical equilibria has shown that Mn is reduced before Fe, while Fe is oxidized before Mn. This phenomenon is significant for the explanation of certain types of cutans occurring in poorly drained soils (Bouma and Van Schuylenborgh, 1967, 1969). Fig. 2.5 shows a mangan-neo mangan occurring in a poorly drained soil.

Detailed descriptions of cutans and neocutans require analysis of thin sections. In field descriptions, cutans can be described noting:

1. Color
2. Kind of surface affected and the area occupied
3. Kind of cutanic material and its thickness
4. Details on the internal structure of the cutan if observed
5. Sharpness of the boundary
6. Degree of separation (contrast in structure between cutanic and non-cutanic material)
7. Degree of adhesion (adhesion between the cutanic material and the cutanic surfaces).

Descriptions are included with pictures of cutans in Figs. 2.4 and 2.5.

Cutans or neocutans are either formed <u>in situ</u> or occur at the locations of deposition and both are associated with natural voids. Another important type of pedological features in the soil, the glaebules, are not necessarily associated with natural voids.

2.3.2. GLAEBULES (Brewer, 1964, Chapter 12)

The definition of different types of glaebules can be found in Table 2.3. Many types of glaebules have in common that they form a "different unit in an otherwise more or less homogeneous S-matrix."
For example, a ferran formed along a root channel, may become broken and mixed with the soil due to pedoturbation. Fragments of the cutans, scattered through the S-matrix, would then classify as glaebules. Detailed descriptions of glaebules require the use of thin sections. In the field the following descriptive scheme can be used, noting:

1. Color
2. Size and shape (for size classification, see Table 2.5)
3. Type name (for a listing of types, see Table 2.3)
4. Distinctness as a unit (sharpness of external boundary and ease of separation of the glaebule as a unit from the enclosing soil material)
5. Abundance in terms of few (0-2% of soil volume) common (2-20%) or many (larger than 20%), or preferably, by an exact count.

Table 2.5

(2) Absolute Size

Class Name	Class Limits
Extremely fine	<0.005 mm
Very fine	0.02–0.005 mm
Fine	0.1–0.02 mm
Medium	0.5–0.1 mm
Coarse	2–0.5 mm
Very coarse	10–2 mm
Extremely coarse	>10 mm–state actual size

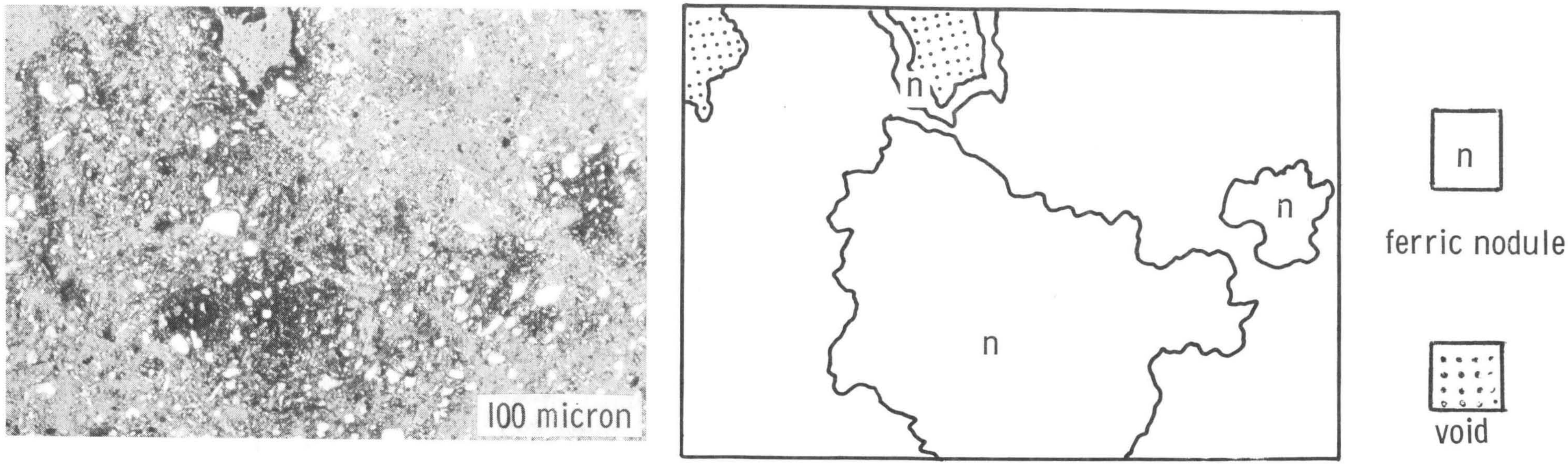

Fig. 2.6. Fine round iron-nodules with diffuse boundaries.

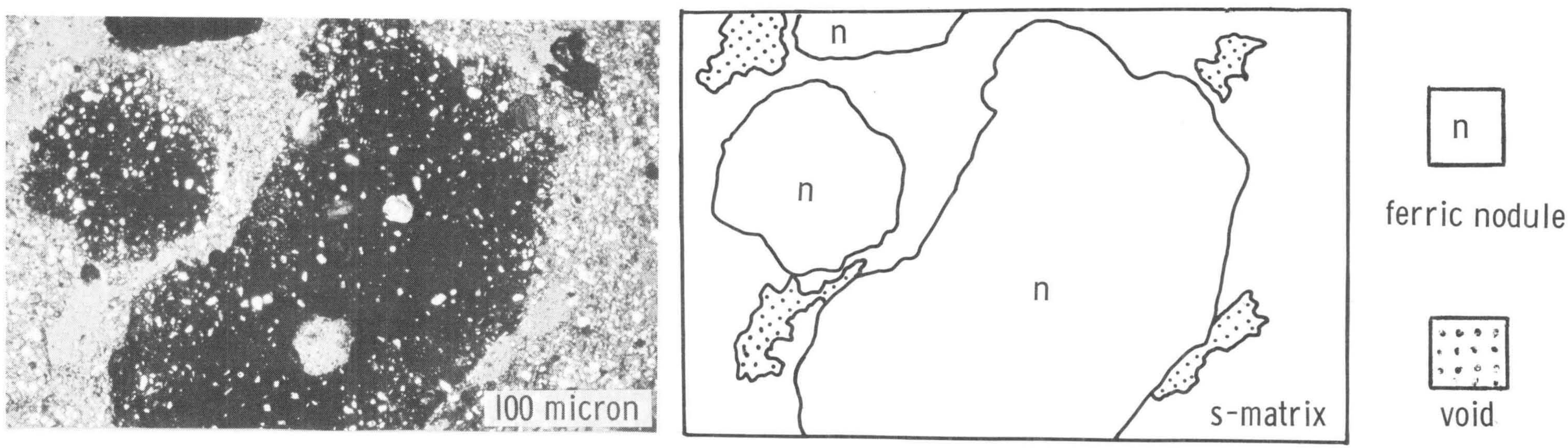

Fig. 2.7. Coarse round iron-nodules with sharp boundaries.

Descriptions are included with pictures of glaebules in Figs. 2.6 and 2.7. Systematic description of cutans and glaebules, to be discussed as pedological features, is to be preferred over the rather poorly defined system of describing "mottles" in the Soil Survey Manual.

2.4. CONCLUSION

A descriptive system has been discussed that can be used to define the size, shape and arrangement of the solid particles and voids in any soil material. Using these procedures, pore systems in soils and indicative pedological features can be represented by a meaningful description that will facilitate communication among scientists. However, direct use of this for predicting or explaining field moisture regimes, is not possible without considering basic physical principles that govern movement of water in soils.

2.5. Pictures of secondary structures

Topsoils (Pictures 1-6)

1. Tama silt loam (Typic Argiudoll). Horizontal section through A1 horizon (virgin soil) at a depth of 30 cm. Fine granular and subangular-blocky structure with partially accomodated peds. Physical data: Bulk density (B.D.) = 1.14; Porosity (P) = 48%; Particle density (P.D.) = 2.21. Texture: silty clay loam.

2. Tama silt loam (Typic Argiudoll). Horizontal section through B1 horizon below plow layer (cultivated) at a depth of 30 cm. Coarse subangular blocky structure with accomodated peds, 17 channels larger than 1 mm per 625 cm^2 (field count). Physical data: B.D. = 1.37; P = 47%; P.D. = 2.57. Texture: silty clay loam.

3. Plano silt loam (Typic Argiudoll). Horizontal section through the Ap horizon at 20 cm depth. Apedal coarse platy structure with accomodating fragments. Physical data: B.D. = 1.42; P = 43.8%; P.D. = 2.51. Texture: silty clay loam.

4. Batavia silt loam (Mollic Hapludalf). Horizontal section through the Ap horizon at 20 cm depth. Apedal soil material with a channelled porphyroskelic S-matrix. Physical data: B.D. = 1.42; P = 44.8%; P.D = 2.57.

5. Batavia silt loam (Mollic Hapludalf). Ap horizon. As picture 4; but showing a large worm channel with a worm-cast inside. Roots preferably follow such larger channels in compacted horizons. Texture: silt loam.

6. Batavia silt loam (Mollic Hapludalf). Structure transition between A2 (upper part of picture) and B2 (lower part). This soil peel was taken from a vertical section through the pedon. Peds become larger at increasing depths and change from subangular blocky to prismatic. Physical data: A2: B.D. = 1.44; P = 44.8%; P.D. = 2.57. B2: B.D. = 1.42; P = 45.0%; P.D. = 2.58.

<u>Subsoils</u> (Pictures 7-11)

7. Tama silt loam (Typic Argiudoll). Horizontal section through the B3 horizon at 80 cm depth (virgin soil). Fine subangular blocky structure with partially accomodated peds. 20 fine (1-2 mm diam.) and 3 medium (2-4 mm) vertical channels per 625 cm^2 (field count). Physical data: B.D. = 1.37; P = 47%; P.D. = 2.57. Texture: silty clay loam.

8. Tama silt loam. Horizontal section through the B3 horizon (cultivated soil) at 80 cm depth. Fine prismatic parting to fine subangular blocky structure with accomodated peds. 15 fine and 3 medium vertical channels per 625 cm^2. Physical data: B.D. = 1.43; P = 46%; P.D. = 2.67. Texture: silty clay loam.

9. Plano silt loam. Horizontal section through the B3 horizon (cultivated soil) at 80 cm depth. Medium prismatic structure with accomodating peds. 15 fine, 15 medium and 3 coarse (>4 mm) channels per 625 cm^2 (field count).

10. Batavia silt loam (Mollic Hapludalf). Horizontal section through the B2 horizon at 50 cm depth (cultivated soil). Medium subangular blocky with accomodated peds. 15 fine, 10 medium and 3 coarse vertical channels per 625 cm^2 (field count). Note worm channel in lower right corner. Physical data: B.D. = 1.42; P = 45%; P.D. =2.58. K-curve and moisture retention data are in Chapter 6. Texture: silty clay loam.

11. Batavia silt loam (as 10). Horizontal section through the B3g horizon at 120 cm depth. Coarse prismatic structure with accomodating peds. Physical data: B.D. = 1.53; P = 40.8%; P.D. = 2.62. Texture: silty clay loam.

<u>Subsoils</u> (Pictures 12 -15)

12. Batavia silt loam (B_{3g}) (as 11). Oblique view of a prism-face with traces of root-growth. Ped faces were wet when the soil was freshly exposed during excavation while the interior of the peds was moist, indicating water movement along ped faces (see Chapter 5).

13. Hibbing loam (Typic Eutroboralf). Horizontal section through the B2 horizon (40 cm depth). Medium prismatic strucutre with accomodated peds. Physical data: B.D. = 1.35; P = 51%; P.D. = 2.75. Texture: clay. For K-curve and moisture retention data, see Chapter 6.

14. Almena silt loam (Aeric Glossaqualf). Horizontal section through the B2 horizon (40 cm depth). Medium prismatic structure with accomodated peds. Physical data: B.D. = 1.60; P = 30.0%; P.D. = 2.29. Texture: silt loam. For K-curve and moisture retention data, see Chapter 6.

15. Batavia silt loam (as 10). End of a vertical worm channel is shown in the middle of the picture. Natural worm channels, when occurring as a continuous tube in a core can induce a very high core-permeability. The same channel may, however, <u>in situ</u> end as shown here, thus not contributing much to the K_{sat} of the whole horizon.

SOIL PEELS FROM TOPSOILS

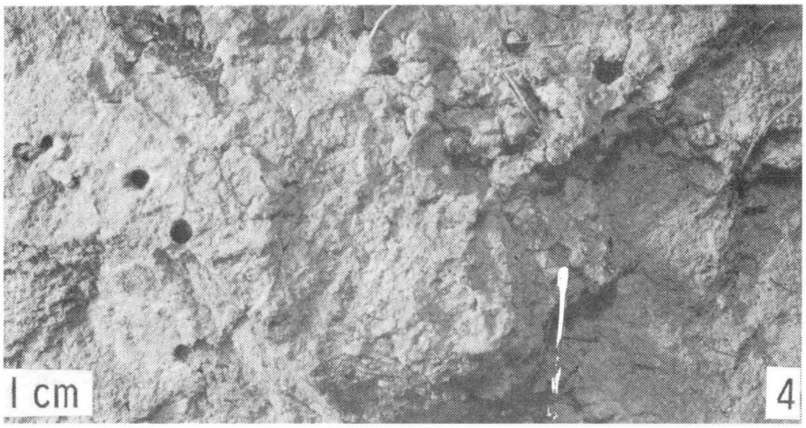
1 cm
4


1 cm
5


1 cm
6

SOIL PEELS FROM SUBSOILS

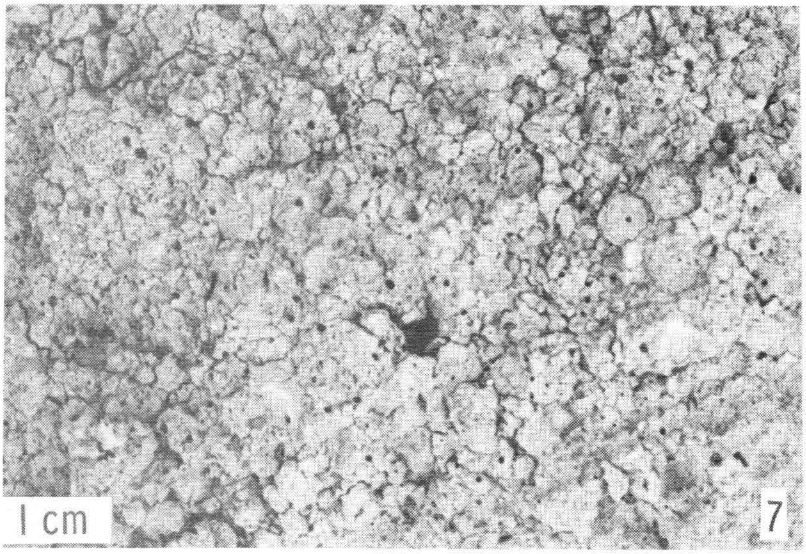

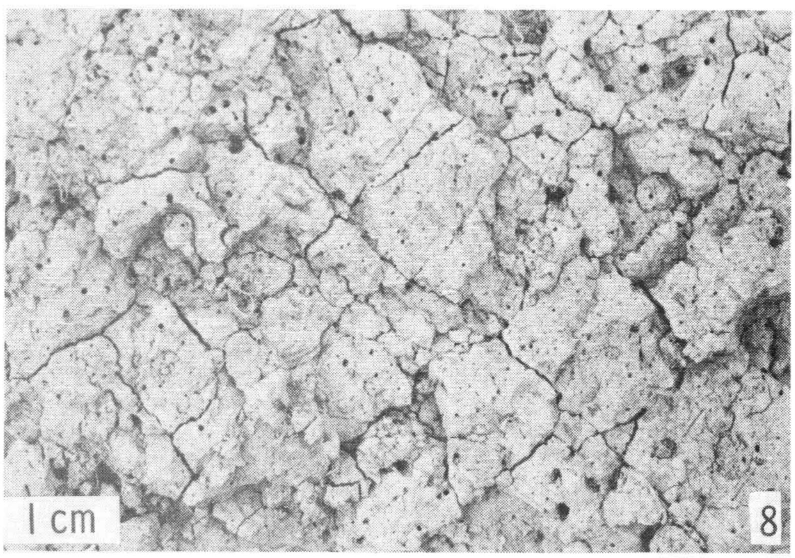

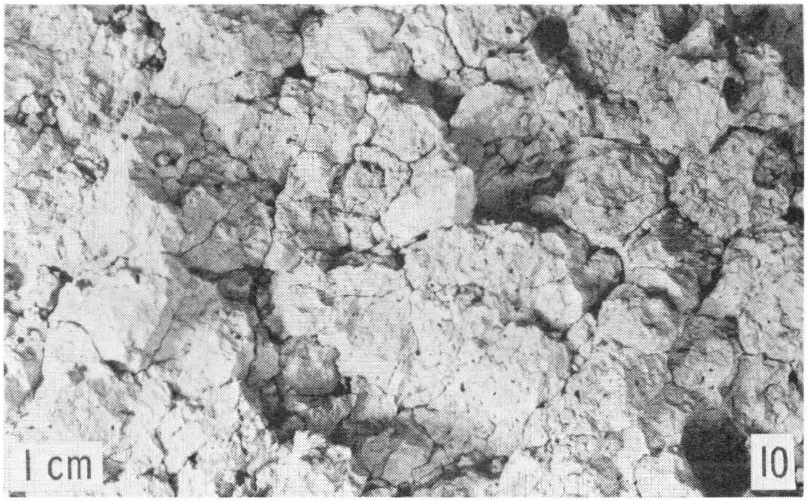
1 cm
10

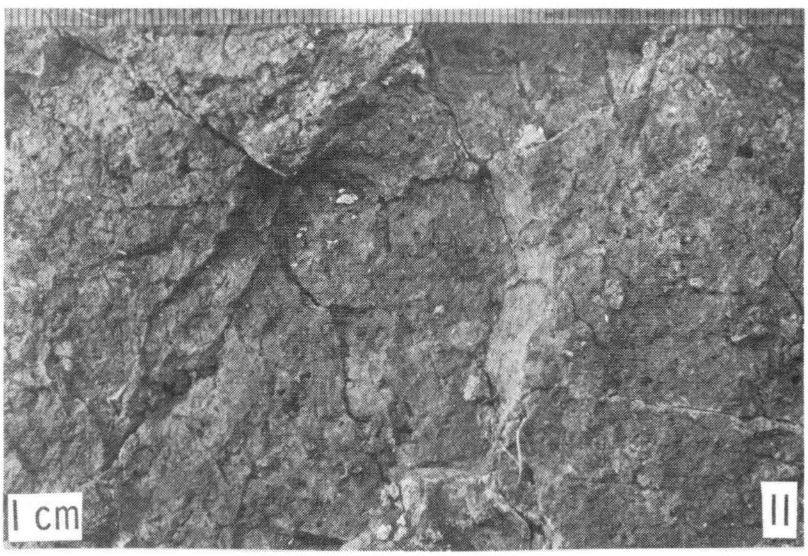
1 cm
11

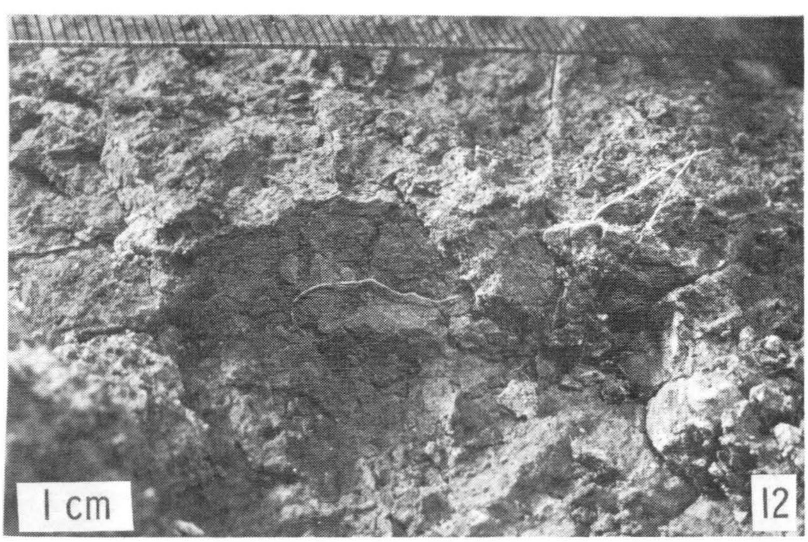
1 cm
12

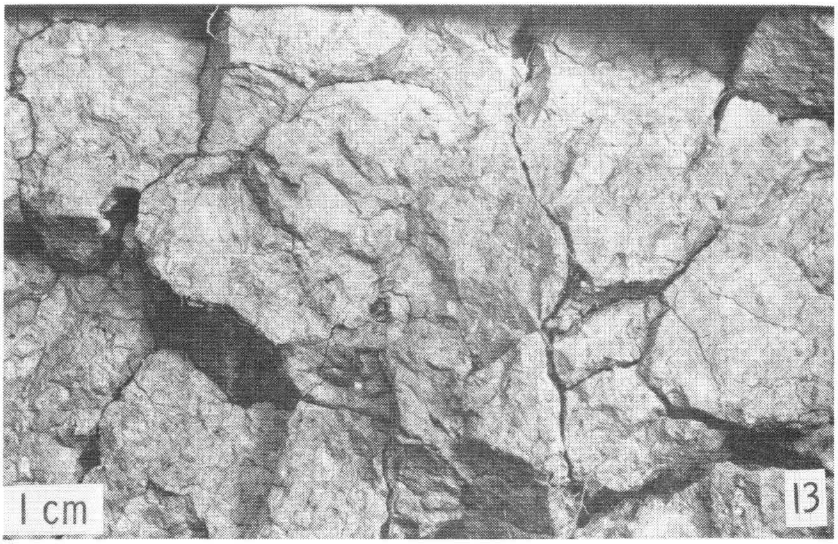
1 cm
13


1 cm
14

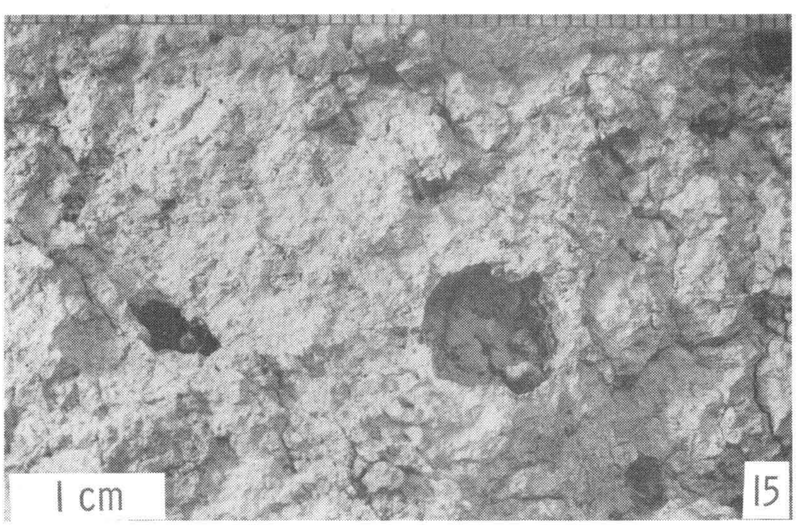
1 cm
15

2.6. LITERATURE CITED

1. Anderson, D.M. and R.R. Binnie (1961). Modal analysis of soils. Soil Sci. Soc. Amer. Proc. 25:499-503.

2. Bouma, J. and J.L. Anderson (1973). Relationships between soil structure characteristics and hydraulic conductivity in pedal soil materials. In: The Field Soil Moisture Regime. R.R. Bruce Ed., ASA Special Publication.

3. Brewer, (1964). Fabric and mineral analysis of soils. Wiley and Sons. 469 p.

4. Folk, R.L. (1955). Student operator error in determination of roundness, sphericity and grain size. J. Sed. Petrol. 25:297-301.

5. Johnson, W.M.; J.E. McClelland, S.A. McCaleb et al. (1960). Classification and description of soil pores. Soil Sci. 89: 319-321.

6. Jongerius (1957). Morphologic investigations of soil structure. Bodemkundige Studies no. 2. Wageningen.

7. Kubiena, W.L. (1938). Micropedology. Collegiate Press Iowa.

8. Pettijohn, F.J. (1957). Sedimentary Rocks (Harper Bros., New York).

9. Powers, M. (1953). A new roundness scale for sedimentary particles. J. Sed. Petrol. 23:117-119.

10. Van der Plas, L. (1962). Preliminary note on the granulometric analysis of sedimentary rocks. Sedimentology 1:145-157.

11. Bouma, J., Pons, L.J. and J. van Schuylenborgh. 1968. On soil genesis in temperate humid climate. VI. The formation of a glossudalf in loess (silt loam). Neth. J. Agric. Sci. 16:58-71.

12. Bouma, J. and J. van Schuylenborgh. 1969. On soil genesis in temperate humid climate. VII. The formation of a glossaqualf in a silt-loam terrace deposit. Neth. J. Agric. Sci. 17:261-271.

. Some basic physical characteristics associated with water movement through soils.

Several textbooks on soil physics have appeared in the last few years (Rose, 1966; Hillel, 1971; Baver and Gardner, 1973) and a discussion of the basic hydraulic properties of soils is central in each of them. This text will not repeat what is already in the literature but will present a simplified, and, if possible, non-mathematical approach intended to help the field soil scientist in applying soil physical concepts. The following subchapters will discuss three aspects:

1. Soil as a three-phase system
2. Physical characterization of liquid in soil materials and
3. Physical characterization of liquid movement in soil materials.

1. Soil as a three-phase system.

A soil sample consists of solid particles and voids, a fraction of which may be filled with liquid (Fig. 3.1). If we assume that the weight of solid particles is M, that of the water M_w, and that total weight is M_t grams, the corresponding volumes are: V_s, V_w, and V_t. Here also the volume of pores filled with air (V_a) has to be included, which contributes negligibly to weight but constitutes an important part of the total soil volume. The volume of the pores is $V_p = V_a + V_w$. The following characteristics are most commonly distinguished (see also Hillel, 1971). Methods of determination are discussed later in Appendix 7.2.

1. Particle density ρ; which is defined as:

$$\rho = \frac{M_s}{V_s} \ (gr/cm^3)$$

This value is used to calculate the volume of a certain dry weight of soil. Values are usually about 2.6 - 2.7 gr/cm^3.

2. Bulk density B.D. $= \frac{M_s}{V_t} = \frac{M_s}{V_a + V_s + V_w}$ (based on dry soil weight).

This value is always smaller than ρ, because V_a and V_w are also included. Sometimes bulk density is determined, including water:

$$\text{B.D. (wet)} = \frac{M_s + M_w}{V_t}$$

We will use B.D. (dry) exclusively because this is the value used to calculate θ_v from θ_w (see next subchapter).

Porosity is defined as $P = \frac{V_p}{V_t} = \frac{V_p}{V_p + V_w + V_s}$

and is normally expressed as a percentage. This value uses the total volume of all pores. Thus, no distinctions can be made between different types of pores with different functions in the soil fabric. Here, morphological analyses can be helpful.

Soil samples should be sufficiently large to represent the soil material to be characterized.

A description of soil structure is useful to estimate optimal sample size. For example, a pedal soil horizon with a fine blocky structure can be characterized with a smaller sample than one with a coarse prismatic structure because structural units in the former soil are so much smaller. A representative soil sample should at least contain about 20 structural units in pedal soil materials. This guide is quite practical for fine pedal soil materials but creates big problems when peds are very coarse or when structures are heterogeneous. An alternative in such cases is to define sub-types of structure, each of which to be considered as relatively homogeneous. By determining the relative importance of each subtype, the soil material as a whole can be characterized by summation of the characterizations of the subtypes.

3.2. Physical characterization of liquid in soil materials.

3.2.1. Introduction

Soil wetness can be expressed in two ways:

Percentage by weight: $$\theta_w = \frac{100 \cdot M_w}{M_s}$$

where M_s is determined after drying the soil at 105° C.

Percentage by volume: $$\theta_w = \frac{100 \cdot V_w}{V_s + V_a + V_w}$$

These two characteristics are interrelated as follows:

$$\theta_v = \frac{\theta_v \cdot \text{B.D. (dry)}}{\rho_w}$$

where ρ_w = density of water.

Soil volume is a relevant factor in several of the characteristics defined in 3.1. This volume may change when dry soil is wetted. Most soil materials containing clay will expand upon wetting which is mainly due to the mineralogical and chemical nature of the clay minerals and to chemical characteristics of the wetting liquid. Thus, it follows that B.D., and θ_v values will be affected. The saran-method has been developed to measure the amount of swelling at different moisture contents (see Appendix 7.2).

Soil wetness refers solely to the total amount of liquid in a soil sample. In addition, it is important to ascertain the distribution of water in the soil at different moisture contents, and to understand the natural laws that govern it. <u>As the moisture content of a soil sample decreases, water leaves the larger soil pores but remains in the finer ones.</u> This can be explained by considering the basic phenomena of liquid surface tension and capillarity. Surface tension occurs typically at the interface of a liquid and a gas. Molecules in the liquid attract each other from all sides. In the surface areas the molecules are attracted into the denser liquid phase by a force greater than the force attracting it into the gaseous phase. The resulting force draws the surface molecules downward, which results in a tendency for liquid to contract. Surface tension has the dimension of dynes/cm. Increased salt concentrations tend to increase the surface tension of water, whereas organic solubles like detergents tend to decrease it. Capillarity refers to the well known phenomenon of the rise of water into a capillary tube inserted in water, due to its surface tension. The finer the tube, the higher the capillary rise and the greater the negative pressures below the water meniscus in the tube. This negative pressure (p) is a result of the curvature of the meniscus, which increase as tubes become smaller,

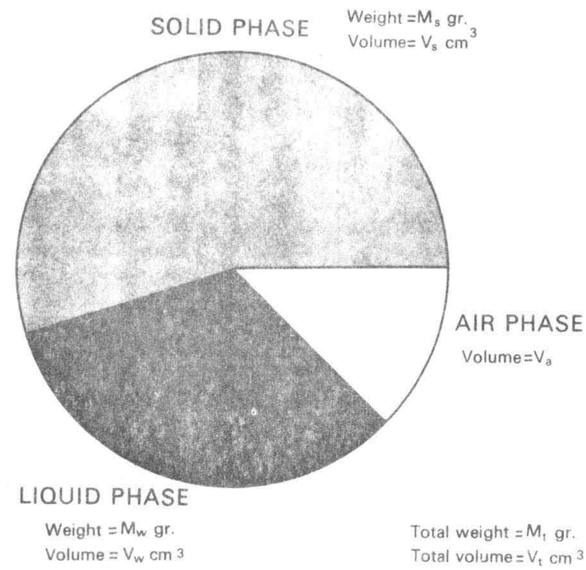

Fig. 3.1. Schematic diagram of the soil as a three-phase system.

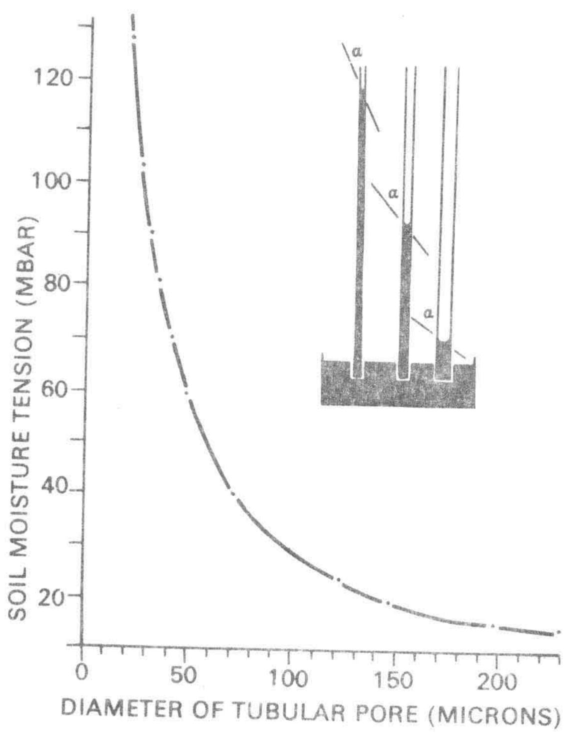

Fig. 3.2. Graphical expression of the relationship between tubular pore size and corresponding soil moisture tension.

and can be calculated (in dynes/cm^2) as follows (assuming that the contact angle between water and tube is zero):

$$P = \frac{2\delta}{r} \qquad (1)$$

Where δ = surface tension of the water (dynes/cm), and r = radius of the capillary. The height of capillary rise (cm) is:

$$h = \frac{2\delta}{\rho g r}$$

where ρ = density of the water (gr/cm^3) and g = gravitational constant (cm/sec^2). Function (1) can be pictured as a continuous graph, relating capillary radius to corresponding pressure (Fig. 3.2). The negative pressure below the meniscus in the water can thus be expressed in terms of height of capillary "pull", which is the force than can be exercised by the pore. Fig. 3.2 illustrates that fine pores can exercise a larger "pull" than large pores. For example, a cylindrical pore radius of 100 micron corresponds with a relatively low capillary rise of 28 cm water, a radius of 30 micron with a relatively high 103 cm. These figures imply that it takes a larger force (more energy) to remove water from a small pore as compared with a large one, which, in turn, implies that water in small pores has a higher potential level of energy than that in the large pores.

To represent the porosity of a certain soil material as a bundle of capillaries, with a characteristic size range is, of course, an unrealistic model as real pores in the soil have a much more complex configuration with varying sizes and discontinuities, as was illustrated in Chapter 2. This representation cannevertheless be helpful to visualize flow phenomena in soils, particularly when soil moisture contents are relatively close to saturation.

A more scientific expression of the common observation that water flows downhill is one stating that water moves from points where it has a higher to points where it has a lower energy status. The energy status is referred to as the "water potential", a central concept in soil physics. A thorough and clear discussion of this concept has been given by Rose (1966) and only a brief summary will be presented in this text. The total potential (or energy per unit quantity) of water (Ψ) is defined as the mechanical work required to transfer unit quanitity (e.g., unit mass or unit volume) of water from a standard reference state ($\Psi = 0$) to the situation where the potential has the defined value. The total potential of water (which in the following will be expressed in terms of energy per unit of weight because this results in the simplest expression) is composed of several components, which will now be discussed separately.

3.2.2. 1. <u>Pressure potential (P)</u>

Water in unsaturated soil occurs only in the finer pores and not in the larger ones because the total amount of available water is insufficient to fill all the pores while the smallest pores can "pull" strongest and thus get filled, thereby excluding the larger ones. The pressure in the water is then less than that of the local atmosphere. As the available amount of water decreases, the diameter of water-filled pores decreases and the moisture pressure becomes more negative. It is convenient, but not necessary, to refer to a negative (less than atmospheric) pressure as a "tension" or "suction". This potential is referred to as the <u>matric</u> or <u>capillary potential</u> M. Expressed per unit weight the dimension of the matric potential becomes:

$$P/\rho g = \frac{g \cdot cm \cdot t^{-2} \cdot cm^{-2}}{g \cdot cm^{-3} \cdot cm \cdot t^{-2}} = cm$$

The matric potential is the most important component of the pressure potential in most cases because soils above the water table are usually unsaturated. The soil water is at a pressure higher than one atmosphere if submerged beneath a free water surface. The potential associated with this has been called the submergence potential (S) by Rose, 1966. The submergence and matric potentials are mutually exclusive possibilities, if either of them is non-zero, the other must be zero. Finally, another possible cause of pressure change in soil water is a change in the pressure of the air adjacent to it (pneumatic potential G). Gas pressures in natural soil will usually not be different from the atmospheric pressure. In summary:

$$P = M \text{ (or S)} + G \text{ (cm)}$$

3.2.3. 2. Gravitational potential (Z)

The gravitational potential is due to the attraction of every body on the earth's surface towards the center of the earth by a gravitational force equal to the weight of the body. To raise this body against this attraction, work must be done, and this work is stored by the raised body in the form of gravitational potential energy (Z) which is determined at each point by the elevation of the point relative to some arbitrary reference level. Therefore:

$$Z = M \cdot g \cdot z$$

where Z is the gravitational potential energy of a mass M of water at a height z above a reference and g = acceleration of gravity. This potential, expressed per unit weight, becomes: Z = z (in cm).

The osmotic potential (O) describes the effect of solutes on the total potential of soil water and is important for the study of water movement into and through plant roots and for studies of evaporation and vapour movement. This component-potential will not be discussed further here as it does not significantly affect the mass-movement of water through soil between tensions of 0 and 100 cm which is of most interest in the context of this review.

The total potential (Ψ) of soil water at any place in the soil is thus equal to the sum of the component-potentials P, Z, and O. Theory of water flow uses the hydraulic potential (cm), which is the sum of the pressure and gravitational potentials previously defined. It is common to refer to the hydraulic potential in terms of the "hydraulic head (H)". (cm).

At zero tension all pores in the soil are filled with water (assuming that isolated air pockets do not exist). With increasing soil moisture tension progressively smaller pores will empty as the capillary force they can exercise becomes insufficient to retain water against the suction applied. The rate of decrease of water content in a soil sample upon increasing tension is characteristic for each soil material as it is a function of its pore size distribution. This simplified discussion assumes that the S-matrix is rigid and that water extraction does not result in soil shrinkage, thereby releasing water without creating empty voids. This is, however, an important process in clayey soils. Use of the saran-method (Appendix), can yield data on volume changes of soil upon desaturation. Techniques are available (Appendix 7.2) to experimentally determine the so-called 'soil-moisture-retention-curve" which gives the water content of the soil at any given tension. Figure 3.3 shows

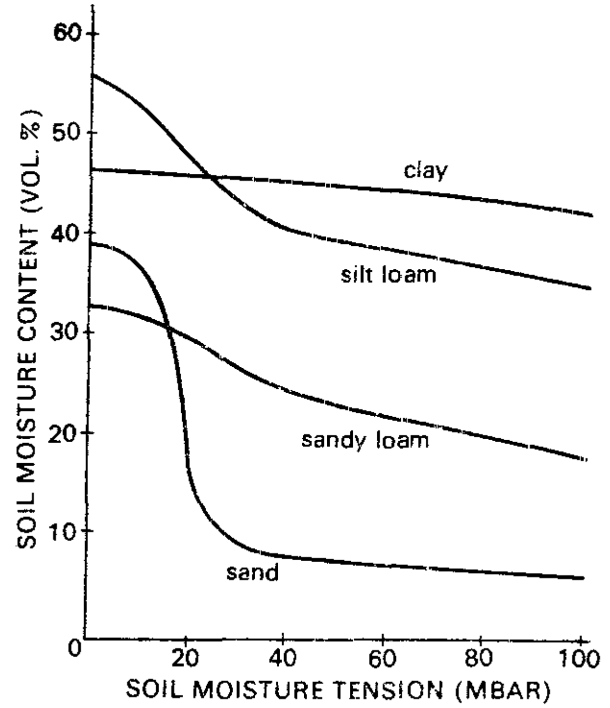

Fig 3.3 Soil moisture retention curves, relating soil moisture content to moisture tension, for four different soil materials.

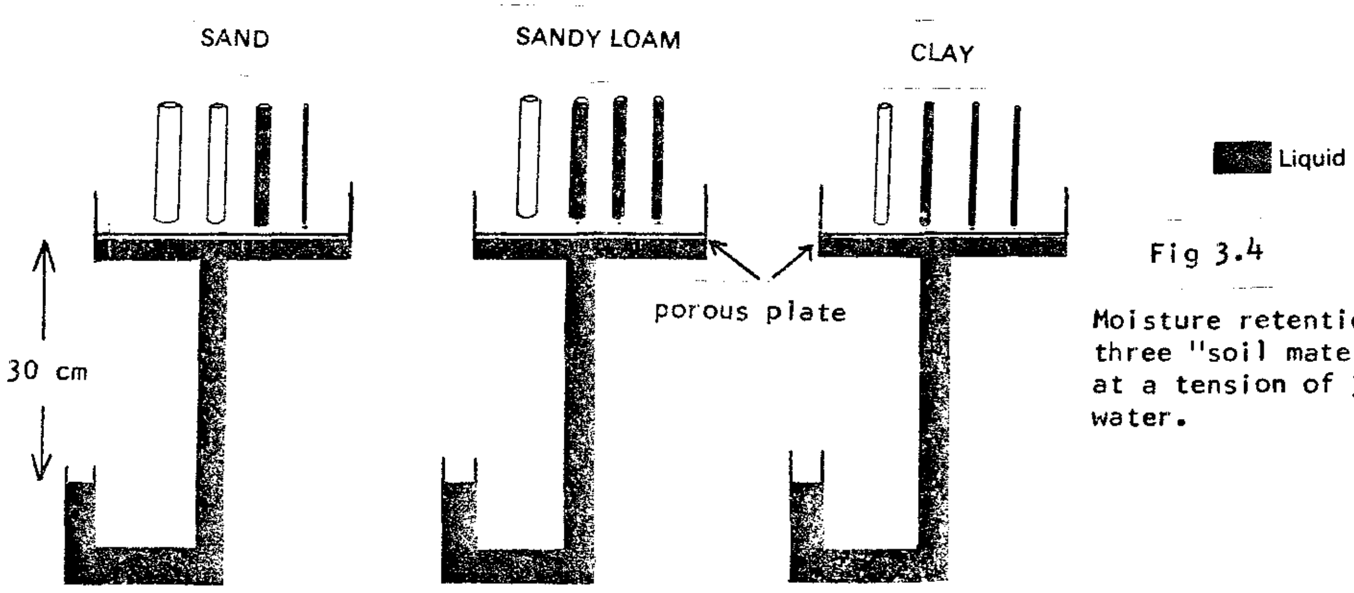

Fig 3.4

Moisture retention in three "soil materials" at a tension of 30 cm water.

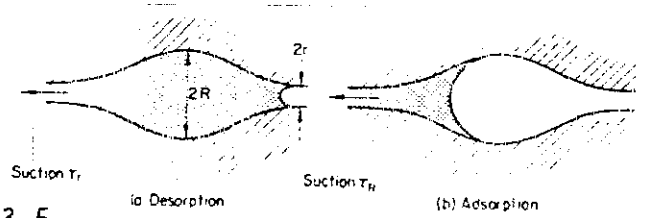

Fig 3.5 Cross-section through an idealized void of maximum effective radius R, interconnected with the rest of the pore space through two channels, of effective radius r.

(From:Rose. 1966)

such curves for a sand (see Soil I in Fig. 2.2), a silt loam (See Soil IV in Fig. 2.2), and a clay soil (see Soil V in Fig. 2.2), demonstrating the effect of their different pore types. These pore types are schematically represented in Fig. 3.4. The sand has many relatively large pores that drain at relatively low tensions, whereas the clayey soils release only a small volume of water, because most of it is strongly absorbed in very fine pores. The silt loam has more coarse pores than does the clay soil.

Moisture contents in a soil sample are different at corresponding tensions depending on whether the moisture content was reached by desorption of an initially wetter sample or by adsorption of an initially drier sample. This phenomenon is referred to as hysteresis, and can be illustrated using Fig. 3.5. The water-filled void (left) will drain (desorption) if the tension exceeds P_r where $P_r = 2\gamma/r$ and r = radius of the smallest pore "neck" in the system. The whole void will fill (adsorption) if the tension is less than P_R where R = maximum diameter of the void itself. It follows that the water content of a soil will be greater on desorption than on adsorption at any given tension, because $P_r > P_R$.

3.3. Physical characterization of water movement in soil materials.

The amount of flow through a soil sample is proportionate to the drop of the hydraulic head per unit distance in the direction of flow. This, basically, is Darcy's law as stated for a one-dimensional steady-state condition of flow:

$$V = K \cdot \frac{\Delta H}{L} \qquad (2)$$

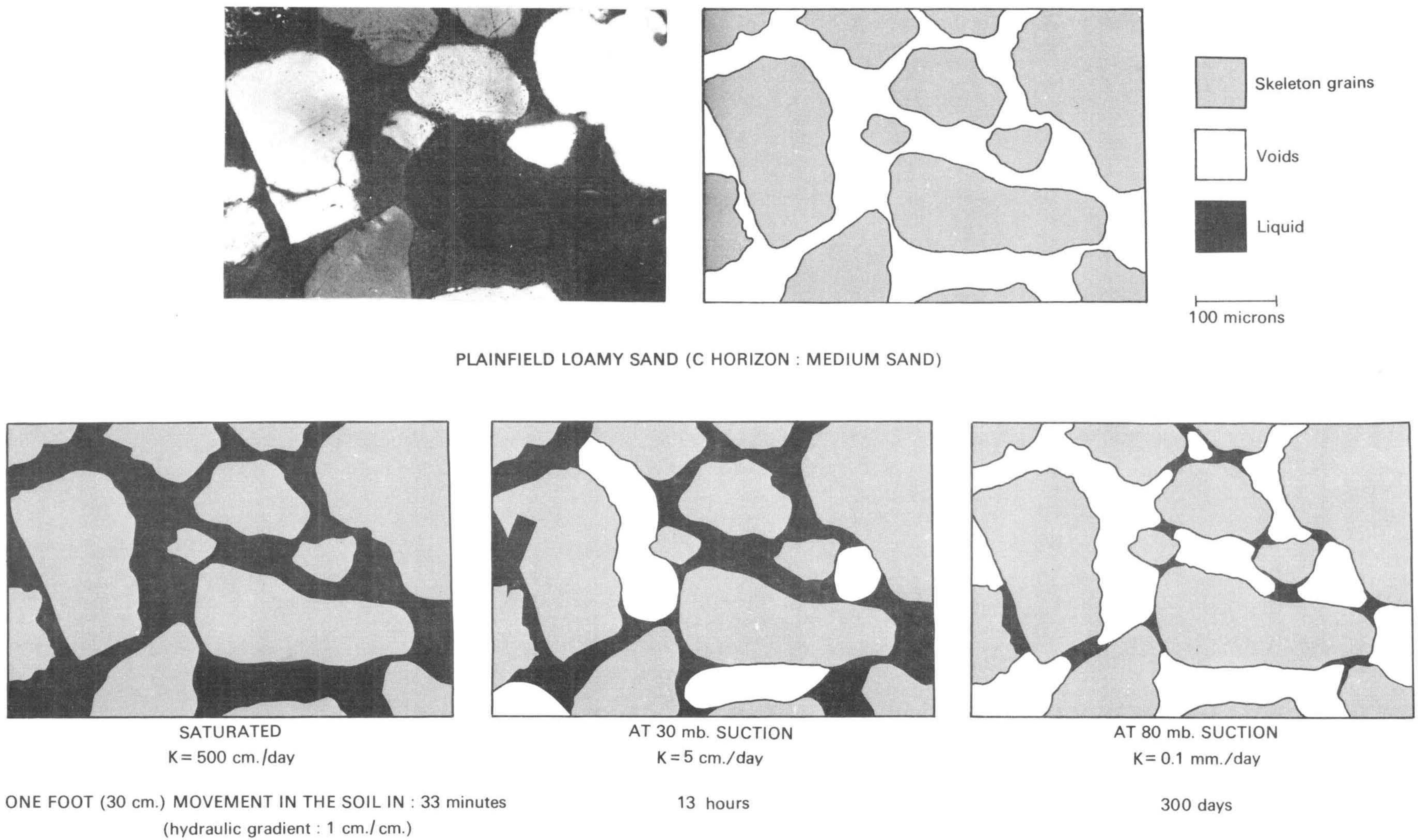

Fig.3.6 Occurrence and movement of liquid in a saturated and unsaturated sand (C horizon of Plainfield loamy sand).

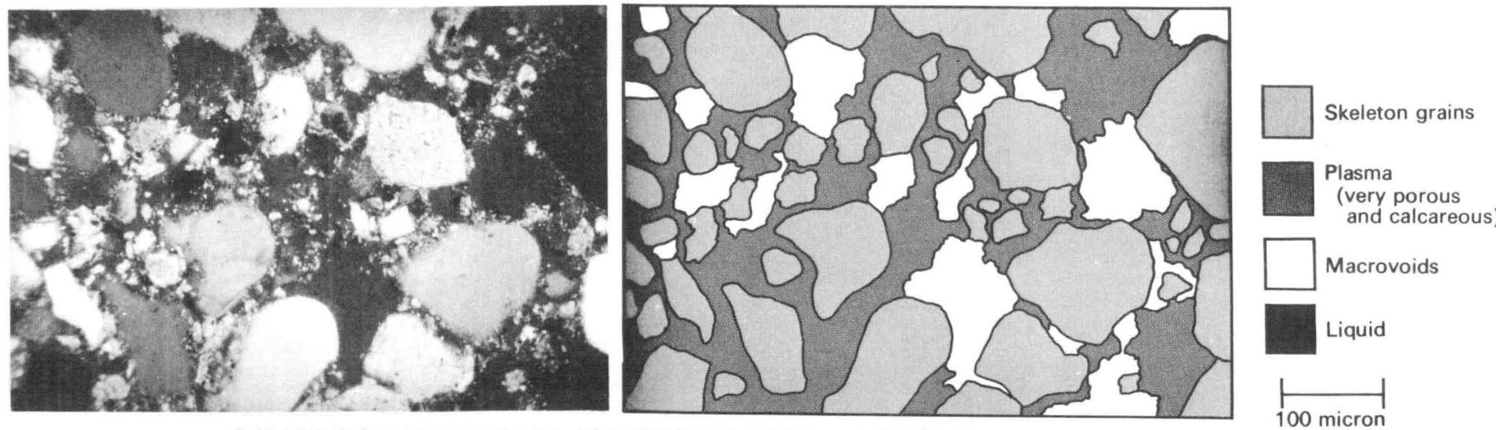

SAYBROOK SILT LOAM (IIC STONY SANDY LOAM TILL)

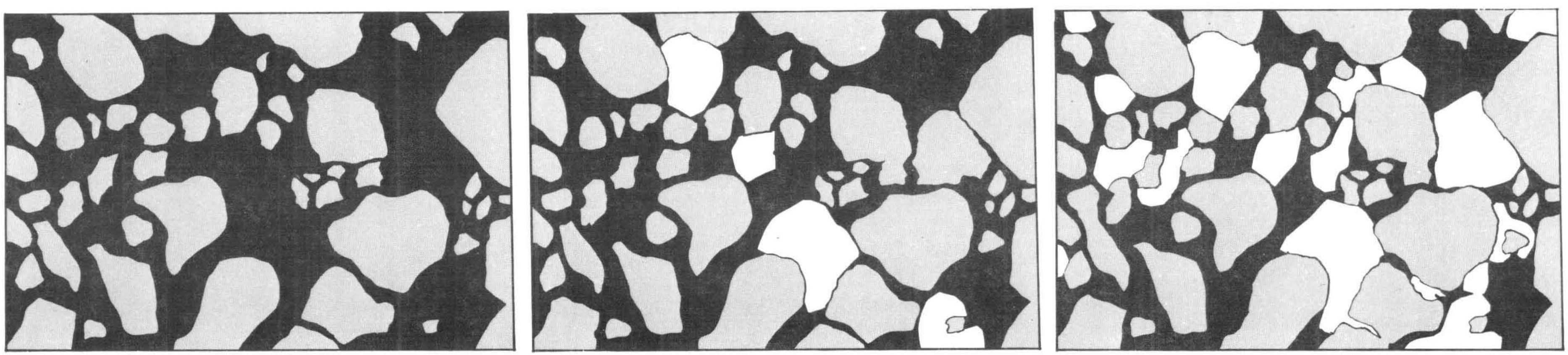

SATURATED
K= 80 cm./day
ONE FOOT (30 cm.) MOVEMENT IN THE SOIL IN : 3 hours
(hydraulic gradient : 1 cm / cm)

At 30 mb. SUCTION
K = 7cm/day
30 hours

At 80 mb. SUCTION
K = 7mm/day
8 days

Fig.3.7 Occurrence and movement of liquid in a saturated and unsaturated sandy loam (IIC horizon of a Saybrook silt loam).

where V = flux ($cm \cdot t^{-1}$) of water $[= Q/(A \cdot t)]$, which is the volume (Q) of water flowing through a cross-sectional area A per time t. K is the hydraulic conductivity ($cm \cdot t^{-1}$) and H/L is the hydraulic gradient (dimensionless). This equation applies to both saturated and unsaturated soils, for steady-state conditions of flow.

The flux V is measured per unit cross-sectional area. Part of that area (at least 40%) is occupied by the solid phase, which implies that the real velocity of flow in the soil pores itself is larger than V. If the soil would be composed of simple capillary tubes, with a specific size, calculations of the real flow velocity in those pores would be easy. However, pores vary in shape, width and direction, and the actual flow velocity in the soil pores is variable. At best, therefore, one can refer to some "average" velocity (v) that can be calculated on the basis of the water-filled porosity at each tension.

$$v = \frac{q}{\varepsilon_w}$$

where ε_w is the water filled porosity, as derived from the moisture retention curve. At unit hydraulic gradient, we find:

$$v = \frac{K}{\varepsilon_w}$$

Using these relationships, travel times at different moisture contents during steady-state flow can be estimated for different soil horizons if a K-curve is available. This was done (in Figs. 3.6 and 3.7) for three moisture contents for the C-horizon of a Plainfield loamy sand (Soil I, Fig. 2.2) and the IIC horizon of the Batavia silt loam (Soil III, Fig. 2.2). According to equation (2), flow rates in a given soil material at a certain moisture content can vary

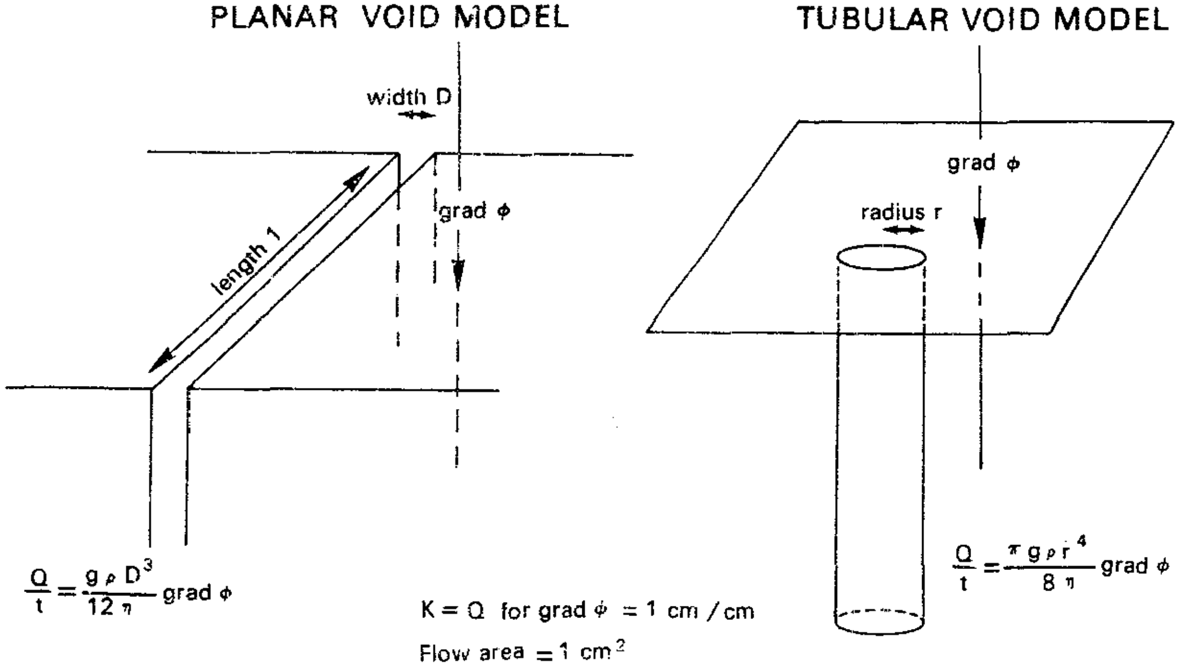

Fig. 3.8. Relationships between sizes of tubular and planar voids and flowrates at defined hydraulic gradients.

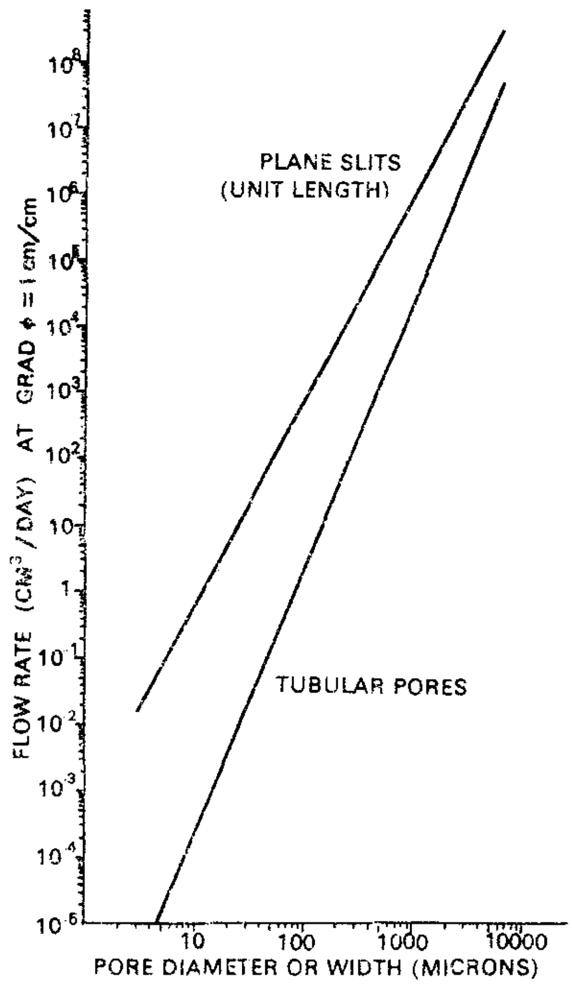

Fig. 3.9. Graphical expression of flow rates through tubular or planar voids as a function of pore size at a hydraulic gradient of 1 cm/cm.

considerably with varying hydraulic gradient. The hydraulic conductivity (K), however, is defined as the flux at unit gradient, and can, therefore, be considered as a characteristic value for the soil. Methods for measuring hydraulic conductivity K in the field will be discussed in the Appendix. These include:

1) Bouwer double-tube method for measurement of K of saturated soil (Appendix 7.3).

2) The crust test (Appendix 7.4) and the instantaneous profile method (Appendix 7.5) for measuring K of unsaturated soil.

K curves of different soil materials vary widely due to different pore size distributions in the soils.

Physical equations have been developed for certain types of pores to relate pore sizes to flow rates at a given hydraulic-head gradient (Childs, 1969). For a cylindrical pore of radius r we find:

$$Q/t = \frac{\pi g \rho r^4}{8\eta} \cdot \text{grad } \phi \text{ (Fig. 3.8)} \qquad (3)$$

For a plane silt of width D, and unit length:

$$Q/t = \frac{g \rho D^3}{12\eta} \cdot \text{grad } \phi \text{ (Fig. 3.8)} \qquad (4)$$

where Q/t = flow rate ($cm^3/cm^2/sec$), ρ = density of water (gr/cm^3), g = gravitational constant (cm^2/sec), η= viscosity (dyne/cm), grad ϕ = hydraulic gradient (cm/cm). These equations are graphically expressed in Fig. 3.9, demonstrating the great effect of pore size on flow rates. For example, these graphs show that a tubular (cylindrical) pore with a diameter of 100 microns will conduct about 2 cm^3/day at a gradient of 1 cm/cm (8 cm^3/day at a gradient of 4 cm/cm). A plane silt with a width of 100 micron (and unit length)

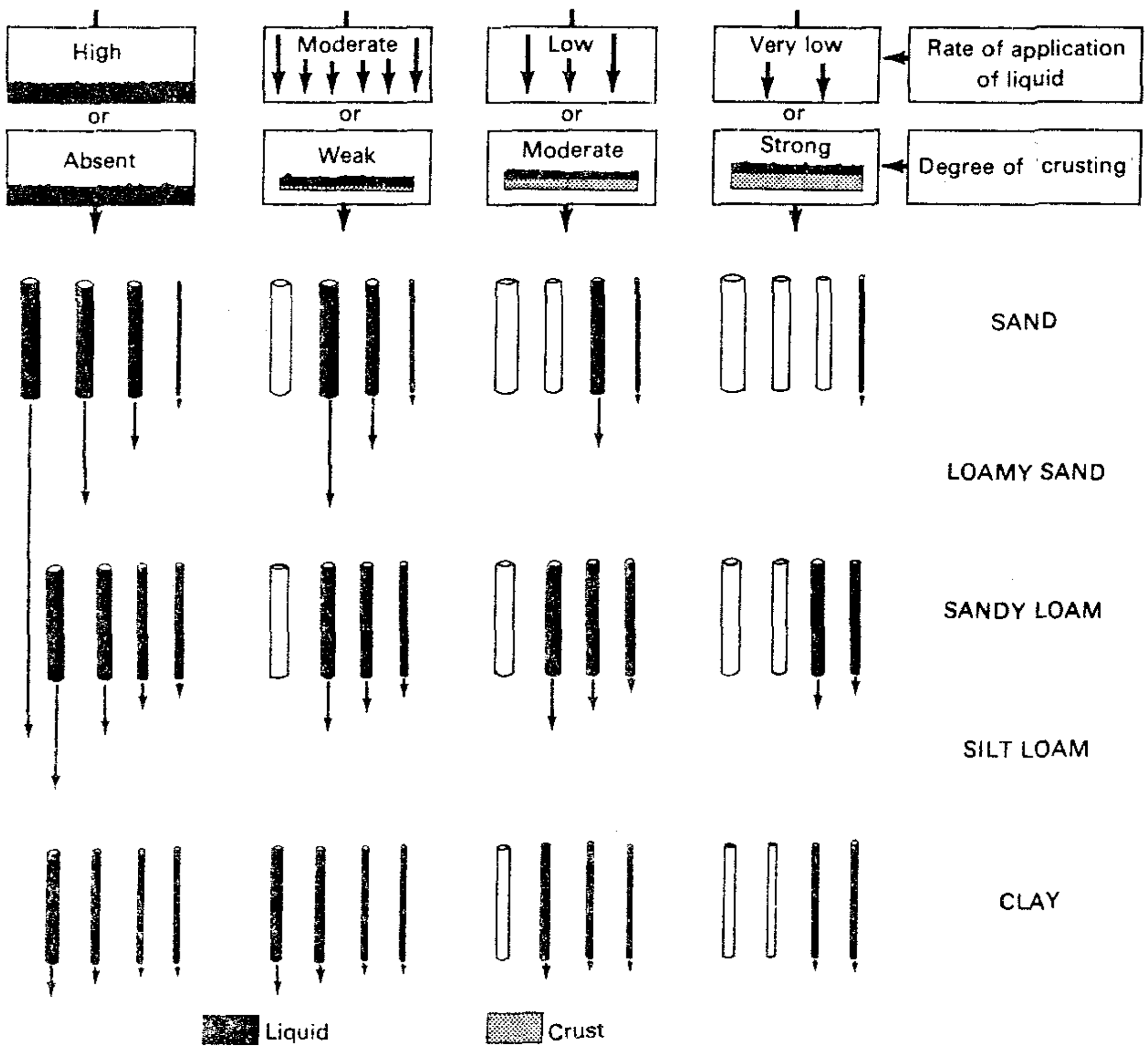

Fig. 3.10 Schematic diagram showing the effect of increasing degree of crusting or decreasing rate of application of liquid on the rate of percolation through three "soil materials".

will conduct 700 cm^3/day. A plane slit with a length of 4 cm will conduct 8400 cm^3/day if the gradient is 3 cm/cm . (12 x 700 cm^3/day).

Morphological studies (Chapter 2) attempt a classification of pore types, among which cylindrical channels and planar voids figure prominently. It appears possible, at least for some soils, to calculate K values from morphometric data, using Equations (3) and (4) that relate pore size to permeability (Chapter 5). A physical method was introduced by Marshall (1958) to calculate K values from moisture retention data, following an equation which relates pore sizes to K values, including a pore interaction model. Pore sizes are indirectly derived from the moisture retention curve, using Equation (1). This procedure, and its limitations, will be discussed in Appendix 7.6. The dominant effect of pore sizes on permeability is evident when K values of a soil material are compared, that are measured at different degrees of saturation. Unsaturated soil below an infiltrating surface may have different causes, such as the occurrence of a physical barrier to flow or an inflow rate which is lower than the saturated hydraulic conductivity. We may assume three different soil materials, with pore size distributions schematically represented in Fig. 3.10. The uppermost "soil" is coarse porous like a sand, the lowest one is fine porous (like a clay). Without any physical barrier (a "crust") on the soil surface and with a sufficient supply of water, all pores are filled and each will conduct water downward as a result of the potential gradient of 1 cm/cm, due to gravity. The larger pores will conduct much more water than the smaller ones (see Equation (3) and Fig. 3.9.). Suppose a weak crust forms over the top of the tubes. Pores will only fill with water if the capillary force they can exercise is strong enough to "pull" the water through the crust. The larger the pore, the smaller the capillary

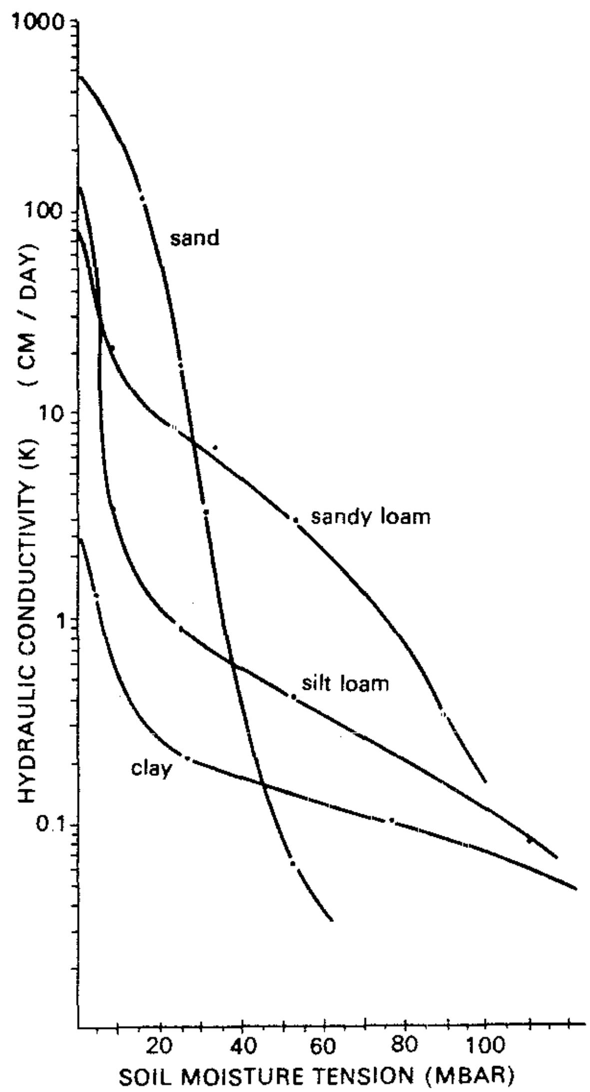

Fig. 2.11 Hydraulic conductivity (K) as a function of soil moisture tension measured <u>in situ</u> with the crust test procedure.

force that can be exercised (Equation 1). Therefore, larger pores will empty first at increasing crust resistance, creating unsaturated soil and soil moisture tensions (Chapter 3.2) which, in turn, leads to a strong reduction in the hydraulic conductivity of the soil.

With no crusts present, similar processes can occur, when the rate of application of water to the capillary system is reduced. With abundant supply, all pores are filled. As this supply (which is supposed to be divided evenly over the infiltrating pore system) is decreased, insufficient water is available to keep all pores filled during the downward movement of the water (it is assumed here that pores are horizontally interconnected). Larger pores will empty first, as they conduct most liquid while at the same time, they exercise only relatively small capillary forces. Thus in this system, a certain size of pore can only be filled with water if smaller pores have an insufficient capacity to conduct away the applied water.

The degree of reduction in K upon desaturation and increasing soil moisture tension is thus characteristic for the pore-size distribution. Coarse porous soils have a relatively high saturated hydraulic conductivity (K_{sat}); but K drops strongly with increasing tension. Fine porous soils have a relatively low K_{sat}, but K decreases more slowly upon increasing tension. Experimental curves, determined in the field with the crust test show such patterns for natural soil. Fig. 2.11 shows curves for the C-horizon of the Plainfield loamy sand (sand; Soil I, Fig. 2.2 in Chapter 2); the IIC horizon of Batavia silt loam (sandy loam; Soil III, Fig. 2.2); the B2 horizon of the Batavia silt loam (silt loam; Soil IV, Fig. 2.2) and the B2 horizon of the Hibbing loam (clay; Soil V, Fig. 2.2). The curves for the pedal silt loam and clay horizons demonstrate the physical effect of the occurrence of relatively large interpedal planar voids and transpedal root and worm channels. Soil structure inside the peds is very fine porous (see Fig. 2.2) and these fine pores hardly contribute to flow. The large structural pores give relatively high K_{sat} values (140 cm/day for the silt loam), but these pores are not filled with water at low tensions and K values for these pedal soils drop, therefore, very strongly between saturation and 20 mbar (1.5 cm/day for the silt loam). These phenomena, showing relationships between pore size distributions and K, are schematically represented in Fig. 3.10.

In summary, then, the higher the "crust" resistance, or the lower the steady rate of application of water, the higher the soil moisture tension in the underlying soil, and the lower the water content and the relevant hydraulic conductivity (K). These characteristics apply to steady state conditions in a one-dimensional system, where, at a hydraulic gradient of 1 cm/cm, flow rates are equal to the hydraulic conductivity. More complex flow systems, for example those where the moisture content is changing with time, need more complex mathematical expressions.

Some of these expressions will be discussed because the principles involved are part of flow models to be discussed in later chapters. The steady-state processes, discussed so far, are already quite helpful and the not-mathematically inclined reader may want to omit the following.

Darcy's law can be written as:

$$V = -K \frac{\partial H}{\partial Z} = -K \frac{\partial}{\partial Z}(M + Z) = -K \frac{\partial M}{\partial Z} - K \tag{5}$$

for downward flow, where H = hydraulic head (cm), M = soil moisture pressure expressed per unit weight (in cm) and Z = vertical coordinate (positive upwards). If water contents are changing during flow processes, it is convenient to

introduce the soil-water diffusivity D which is defined as:: $K \cdot \frac{\partial H}{\partial \theta}$;
the latter of both terms being the slope of the moisture retention curve.
To introduce D, the Darcy equation can be written as:

$$V = -K \cdot \frac{\partial M}{\partial \theta} \cdot \frac{\partial \theta}{\partial z} - K$$

(this is a mathematical trick: multiplying with $\partial\theta$ and dividing by $\partial\theta$ does not change the value of the product on the right hand side of the equation, but creates the opportunity to introduce D)

$$V = -D \frac{\partial \theta}{\partial z} - K \tag{6}$$

Measurement of moisture conditions in the field usually relate to the moisture content θ at different times and depths and not to flow rates as such. It is therefore advantageous first to differentiate this equation with respect to z, as follows:

$$\frac{\partial v}{\partial z} = \frac{\partial}{\partial z} \cdot \left(D \frac{\partial \theta}{\partial z}\right) - \frac{\partial K}{\partial z} \tag{7}$$

and then to apply an equation of liquid conservation:

$$\frac{\partial \theta}{\partial t} = - \frac{\partial v}{\partial z} \cdot \text{(downward flow)}$$

which expresses the requirement that the change in water content per unit time of any small volume of soil equals the net flow of liquid across the boundaries of this volume. It does, in fact, state that water cannot be lost during the flow into and through any small volume of soil. Substitution in equation (7), results in:

$$\frac{\partial\theta}{\partial t} = \frac{\partial}{\partial z} \left(D \cdot \frac{\partial\theta}{\partial z}\right) + \frac{\partial K}{\partial z} \tag{8}$$

This equation forms the basis for the analysis of vertical entry or drainage of water in insaturated soil.

It is possible to avoid using D values in describing unsteady flow through soil, by transforming the above equation as follows:

$$\frac{\partial\theta}{\partial t} = \frac{\partial}{\partial z} \left(D \cdot \frac{\partial\theta}{\partial z} + K\right)$$

$$\frac{\partial\theta}{\partial t} = \frac{\partial}{\partial z} \left(K \cdot \frac{\partial M}{\partial\theta} \cdot \frac{\partial\theta}{\partial z} + K\right)$$

$$= \frac{\partial}{\partial z} \left[K \cdot \left(\frac{\partial M}{\partial z} + \frac{\partial Z}{\partial z} \right) \right]$$

$$= \frac{\partial}{\partial z} \left[K \cdot \frac{\partial}{\partial z} (M + Z) \right]$$

$$\frac{\partial\theta}{\partial t} = \frac{\partial}{\partial z} \left[K \cdot \frac{\partial H}{\partial z} \right]$$

These equations will be used in later chapters to discuss processes of unsteady flow.

3.4. LITERATURE CITED

1. Baver, L.D., W.H. Gardner and W.R. Gardner. 1972. Soil Physics. John Wiley. 498 p.

2. Bybordi (1968). Moisture profiles in layered porous materials during steady state infiltration. Soil Sci. 105:379-383.

3. Hillel, D.I. (1971). Soil and water: physical principles and processes. Academic Press. p. 288.

4. Peck, A.J. (1971). Redistribution of water after infiltration. Austr. J. Soil Sci. 9:59-71.

5. Rose, C.W. (1966). Agricultural Physics. Pergamon Press - Oxford.

4. Application of the flow theory to specific examples.

These applications assume the availability of K-curves and of moisture retention data (for methods, see Appendix), and will be concerned with problems of increasing complexity starting with saturated flow.

4.1. One dimensional steady saturated flow.

4.1.1. One layer

Fig. 4.1. illustrates flow of water through a soil core under saturated conditions. The soil in the ring has a height of 10 cm, and 1 cm water is ponded on top. Assume that water is leaving this ring at a flow rate of 5 cm/day while the 1 cm head is maintained at the top. The question to be answered is: what is the K_{sat} value of the soil in the core? Following Darcy's law ($V = K \cdot \Delta H/L$), we need to know ΔH in order to calculate K, since $L = 10$. H is composed of P (pressure potential) and Z (gravitational potential). It is advantageous to obtain differences in P and Z between top and bottom of the core separately and then adding them up. The alternative would be to calculate $\Delta\,(P + Z)$ for the top and for the bottom and then to determine the difference. This approach is without problems for saturated flow but confusion often results for flow under unsaturated conditions when pressure values may be negative. For the simple case discussed, we find: $\Delta P = 1$cm, $\Delta Z = +10$, and thus $\Delta H = 11$. (Reference level for G at bottom of core and $P = 0$ at bottom of core, because outflow occurs under atmospheric pressure). It follows that $K = 5/1.1 = 4.55$ cm/day. The values for the

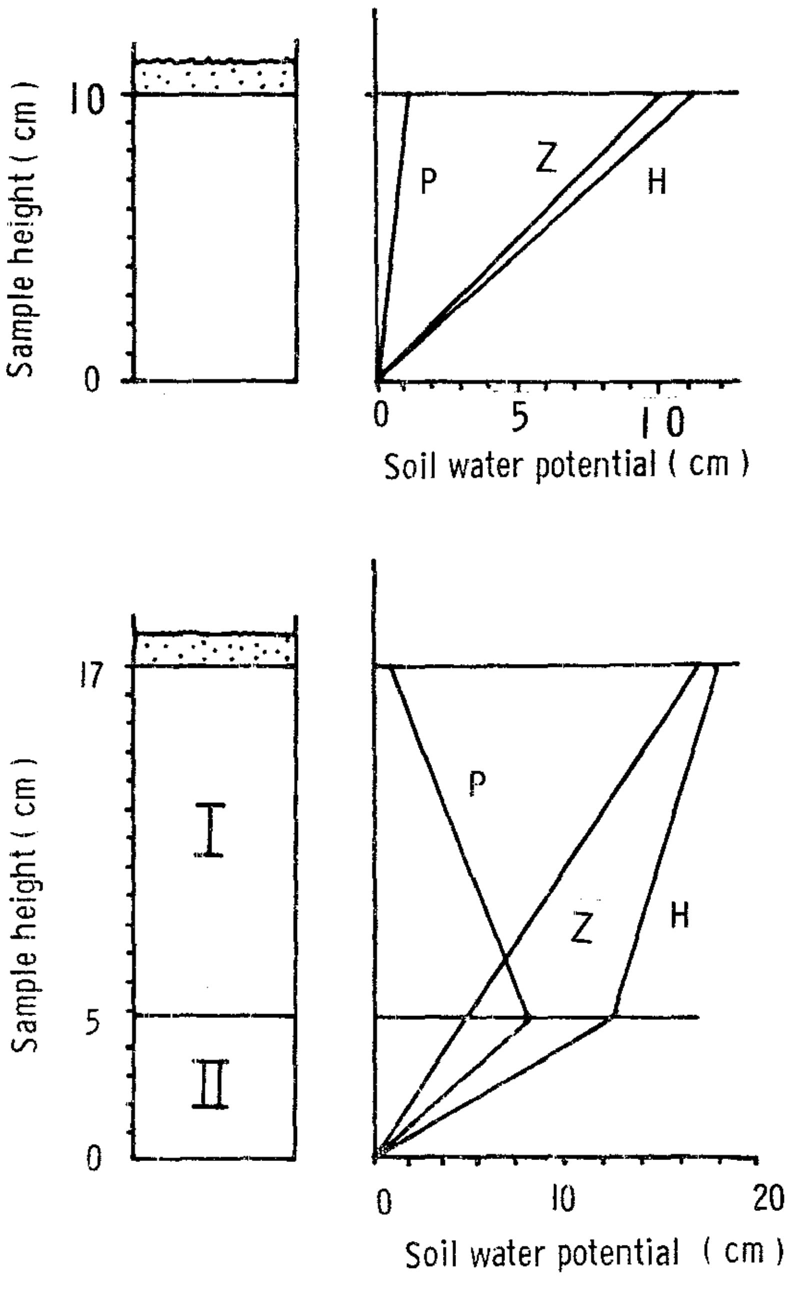

Fig. 4.1. Moisture conditions in cores during steady saturated flow.

pressure, the gravitational and the total potential have been pictured in Fig. 4.1 for different positions inside the core.

4.1.2. Two layers

A slightly more complicated situation is found when steady saturated flow occurs through a soil core that has two layers with different K_{sat} values. Fig. 4.2 shows two layers, (12 and 5 cm thick) of soil in a core, with one cm of water ponded on top. Assume $K_{sat}(I) = 10\ K_{sat}\ (II)$. Question: what are the values for the different potentials in this flow system at steady-flow conditions.

The flow rate can again be expressed as: $V = K \cdot \frac{\Delta H}{L}$. V can only be constant if $\Delta H/L$ varies inversely as K. This means that the slope of the H-potential line should be ten times as steep in I as compared with II. We know the two end points of the H-potential line (Top: P = +1, Z = +20 if the reference level is taken at the bottom of the 20 cm high core. Therefore: H = +21. Bottom: Z = 0, P = 0 since outflow occurs). The H-potential line can now be constructed using the proper slopes. The Z-potential line in known as it varies from zero at the bottom to =20 at the top. The P-potential line can be constructed from the other two, subtracting Z from H. The P line shows that pressure increases with depth until the interface with layer II is reached.

4.2. One dimensional steady unsaturated flow.

4.2.1. One layer

The flow conditions in a homogeneous soil material are very simple and have been discussed already in Chapter 3.3, that dealt with water movement through

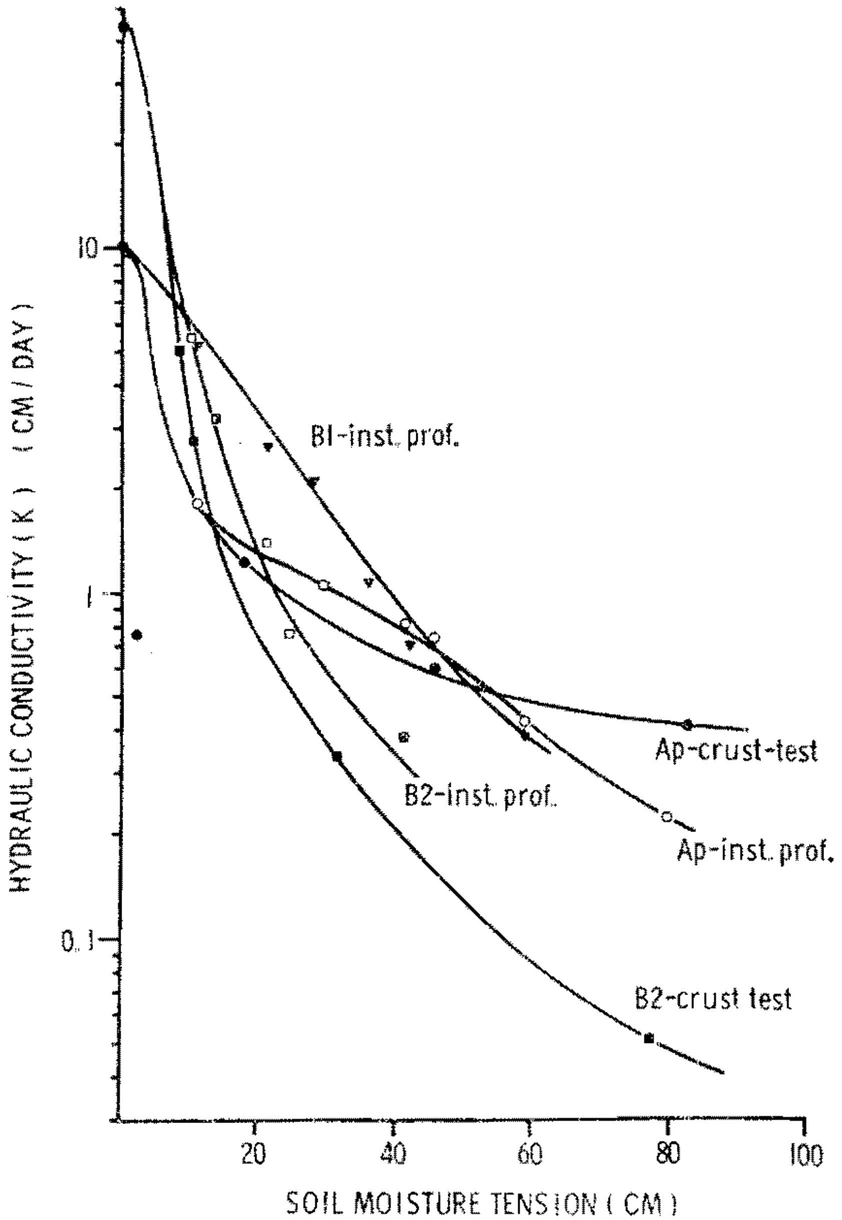

Fig. 4.3. Hydraulic conductivities for the Ap and B2 horizon of the Batavia silt loam determined in situ with the crust test. (The figure also includes curves determined with the instantaneous profile method, see Appendix 7.5.)

soil. Any given steady flow rate that is lower than the saturated hydraulic conductivity of a soil material corresponds with a characteristic soil moisture tension because it is related to its particular pore-size distribution. Flow occurs only by forces of gravity expressed by the gravitational potential Z because the pressure potential P (or better the matric potential M because pressures are negative) is constant at all depths under conditions of steady flow. Fig. 4.3 (same as Fig. 7.14 in Appendix 7.5) gives the hydraulic conductivity curves for the Ap and the B2 horizon of a Batavia silt loam (Typic Argiudoll) measured in situ with the crust test at the Charmany UW Exp. Farm in Madison, Wisconsin. Curves like these make it possible to predict moisture tensions (and corresponding phase distributions if moisture retention data are available) at steady flow rates (unrealistically assuming that the horizons are of semi-infinite depth, see next section). For example, tensions at a steady flow rate of 1 cm/day would be 20 cm in the B2 and 30 cm in the Ap. At 5 mm/day these tensions would be 26 and 58 cm respectively. Soil horizons, of course, are not semi-infinite and interferences of underlying horizons strongly influence tensions with depth. These effects can be calculated using an approach published by Bybordi (1968).

4.2.2. Two or more layers.

Darcy's law can be written as:

$$V = -K\left(1 + \frac{dh}{dz}\right)$$

where z is the vertical direction (cm), K is the hydraulic conductivity (cm/day) and h = soil moisture potential (cm). This equation can be integrated as follows:

$$Z_n = - \int_0^{h_n} \frac{dh}{1 + \frac{V}{K}} \qquad \text{(Byboardi, 1968)}$$

where Z_n is the height above a horizon boundary (or a water-table level) at which the pressure h_n is experienced. So by choosing a steady-velocity V for the flow system and by reading appropriate K values from the K-curves for the different layers, a complete profile of Z vs h may be plotted if a sufficiently high number of different limits h_n is used. This method will be illustrated by using K-data for the two surface horizons of the Batavia silt loam (Fig. 4.3). (Crust test data).

We assume that the B_2 extends very deep and that only flow from the Ap into the deep B2 will be considered.

At a steady flow rate of 4 mm/day, the tension in the B2 is 30 cm. This tension will occur, therefore, at the boundary of Ap and B2. However, a steady flow rate of 4 mm/day represents a tension of 83 cm in the Ap. Tensions are always continuous in a soil and an abrupt change from 83 cm to 30 cm tension at the interface of the horizon is therefore not possible. The integration procedure is used now to calculate tensions in the Ap in the transition zone between 30 and 83 cm. The basic question is as follows: At what height h above the boundary does a tension occur of, for example, 40 cm (to construct a tension curve for the transition zone, small intervals have to be used). Thus: $h_n = 40$ cm, $V = 0.4$ cm/day and $K = 0.7$ cm/day (= K at 40 cm tension in the Ap, read from Fig. 4.3) $dh = 40\text{-}30 = 10$ cm. Since downward flow is considered, V has a negative sign.

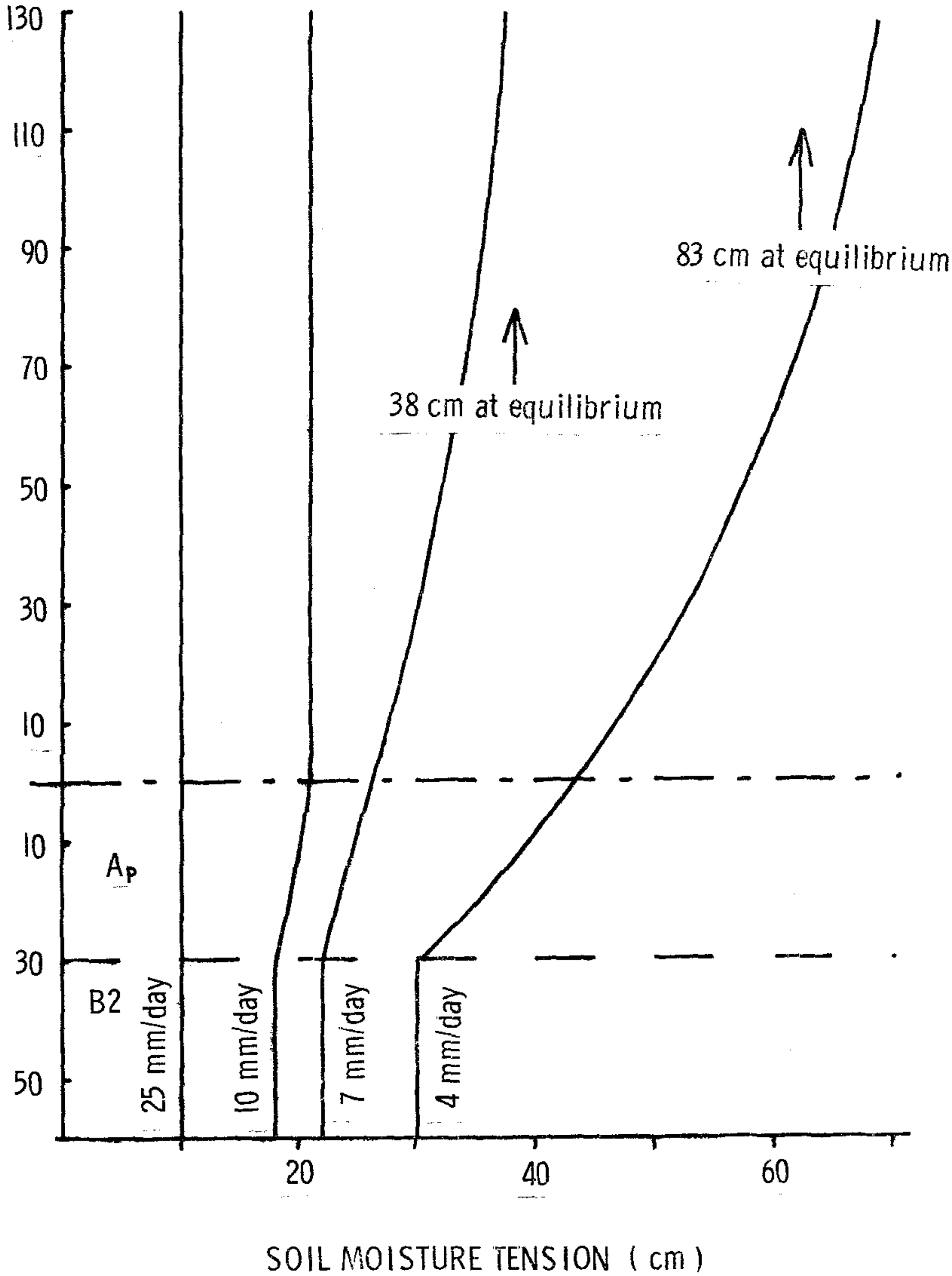

Fig. 4.4. Calculated moisture tensions in the B2 and Ap of a Batavia silt loam at four steady-flow rates, using Byb●rdi's approximation. The real Ap was 30 cm thick. Curves are extended above this surface to show tensions if the Ap had been much thicker.

Thus:

$$Z_n = -\int_{30}^{40} \frac{10}{1 - \frac{0.4}{0.7}} \quad . \quad \underline{Z_n = 23.3 \text{ cm}}$$

Result: at 23.3 cm above the boundary of A_2 and B_2, a tension of 40 cm occurs at a flow rate of 4 mm/day. The next point could be to calculate a tension of 50 cm as follows:

$$Z_n = -\int_{40}^{50} \frac{10}{1 - \frac{0.4}{0.6}} \quad . \quad Z_n = 28 \text{ cm}$$

which gives a total distance of 51.3 cm. This integration can be continued until a tension of 83 cm is reached which is the equilibrium tension at the given flow rate.

A part of the complete calculated curve is in Fig. 4.4, where other curves for additional flow rates were also calculated. Note the curve for a flow rate of $2\frac{1}{2}$ cm/day, when tensions in both horizons are 10 cm. Horizons are often not deep enough to reach equilibrium tensions corresponding with steady flow rates. This is certainly true of the A_p just discussed. Whatever its depth, theoretical tensions at the soil surface can be estimated (assuming all the time that there is no evaporation) by drawing a horizontal line at any desired depth in the A_p and by reading the tensions at that level from the calculated curves.

A special case of the two-layer flow system occurs when very thin layers with different hydraulic properties occur in a flow system. An example will be discussed concerning thin crusts on top of infiltrative surfaces (Hillel, 1971).

Assuming steady infiltration (as will be occurring during the crust-test measurement to be discussed in Appendix 7.4, the flux through the crust (q_c) should be equal to the flux in the subcrust soil (q_s).

$$q_c = q_s \quad \text{or} \quad K_c \left(-\frac{dH}{dz}\right)_c = K_s \left(-\frac{dH}{dz}\right)_s$$

where K_c and K_s are hydraulic conductivities of the crust and the subcrust soil respectiviely with dH/dz the hydraulic head gradient in both materials. The hydraulic-head gradient will be approximately unity at steady state infiltration as the gradient of soil moisture tension decreases with increasing wetting depth. Assuming flow in the soil thus to result only from gravitational forces:

$$q = K_{s(M)} = K_c \cdot \frac{H_o + M + z_c}{z_c}$$

where $K_{s(M)}$ is the unsaturated K of the subcrust zone at a moisture tension of M cm water; H_o is the positive hydraulic head imposed on top of the crust by the ponded water and z_c is the thickness of the crust. Crusts may be very thin relative to the tension induced in the subcrust soil ($-z_c \ll M$). The same may hold for H_o if water is only very shallowly ponded on top of the crust ($-H_o \ll M$). Then it follows:

$$q = K_c \cdot \frac{M}{z_c} = K_{s(M)}$$

or

$$\frac{K_{s(M)}}{M} = \frac{K_c}{z_c} = \frac{1}{R_c} \qquad (R_c = \text{ hydraulic crust resistance}).$$

Thus, the ratio of the K of the subcrust soil to its tension is approximately equal to the ratio of K_{sat} of the crust to its thickness. The latter ratio can also be expressed as $\frac{1}{R_c}$ where R_c is hydraulic crust resistance. Use of R_c may be very helpful in analyzing natural crusts, the thickness of which may be difficult to measure. The R_c value follows of course, from Darcy's law as applied to a crust, for example:

$$q = K_c \cdot \frac{\Delta H}{z_c} \quad \text{or} \quad q = \frac{K_c}{z_c} \cdot \Delta H = \frac{\Delta H}{R_c}$$

Knowing the depth of ponded water on top of the crust (H_o), the subcrust tension (M) and thickness of the crust z_c, ΔH can be determined as: $H_o + M + z_c$. When the flux q is known, resistance R_c of the crust can be determined. K_c can only be calculated if the thickness of the crust is known. The hydraulic resistance (R_c) may be particularly useful to predict hydraulic effects of crusts on different soils by considering, again, the assumption of steady gravitational flow in the subcrust soil:

$$q = K_{s(M)} = \frac{M}{R_c}$$

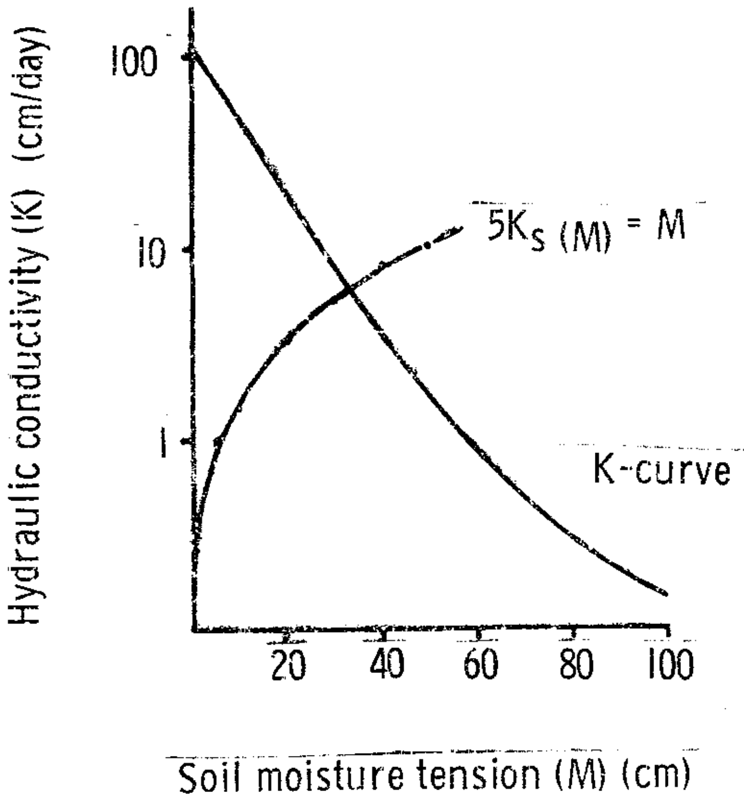

Fig. 4.5. Calculation of moisture tension and associated flow rate induced by a thin crust (R_c = 5 days) in a soil with a known relationship between hydraulic conductivity (K) and moisture tension

If the K-curve of the subcrust soil is available ($K_{s(M)}$), it is possible to calculate the steady-flow rate q in any subcrust soil on the basis of a known R_c value for the crust. For example, assume a crust with R_c = 5 days on top of a soil with a K-curve pictured in Fig. 4.5. Question: what are subcrust tension and infiltration rate under steady-state conditions? It follows from the above description that $R_c = \frac{M}{K_{s(M)}} = 5$. A line can be drafted in Fig. 4.5 describing $5\,K_{s(M)} = M$. The point where this line crosses the K-curve gives the required values for subcrust tension and infiltration rate. It should be pointed out that the assumptions of steady-state gravitational flow under a very small hydraulic head (H_o) may not apply under many conditions occurring in nature. But analysis of the problem becomes complicated then, and these simplified calculations may be quite meaningful for applied work.

4.3. One-dimensional unsteady unsaturated flow.

Flow conditions considered so far in this chapter were steady-state, which implies that moisture contents and tensions did not change with time and location in the flow system. This condition may occur in the field in deeper soil horizons or during extended infiltration through impeding layers, such as crusts. Generally, though, flow velocities will be constantly changing in the upper soil horizons as periodic rainshowers add water to the soil while water is extracted by evapotranspiration and deep drainage. This means that the general flow equation cannot generally be solved analytically. Phillip (1957) developed a mathematical-analytical method to describe horizontal and vertical infiltration of water into soil. Discussions of this procedure are in the literature. When infiltration takes place under shallow ponding conditions into an initially dry soil, the soil moisture tension gradients in the topsoil are at first much greater than the gravitational gradient, and the initial vertical infiltration rate will be relatively high to decrease with time to a lower rate as the wetting zone increases in depth, thereby reducing the hydraulic gradient. The final infiltration rate at steady state equals the saturated hydraulic conductivity (hydraulic gradient = 1 cm/cm) of the soil when no crusts are present. This final infiltration rate is independent of the initial moisture content of the soil. But the initial infiltration rate is strongly affected by it, because this rate is mainly determined by the gradient of the soil moisture tension, which will be lower as the original moisture content is higher. Lower gradients result in lower flow rates, thus giving lower initial infiltration rates when the initial soil moisture content was high. Of great practical interest in areas without irrigation is the problem of infiltration followed by redistribution of limited quantities of water, as may be added to the soil by a single shower. Infiltration of, for example, a few centimeters of water usually proceeds rapidly in most soils, unless strong soil crusting occurs. This water will then flow downwards in the soil, wetting the soil first, followed by drying as the wetting front moves downwards and no new water is added on top. Physically, these conditions are very difficult to describe because flow rates and tensions change continuously and strong hysteresis processes (Chapter 3.2) are involved because wetting (moisture adsorption) and drying (moisture desorption) occur within a relatively short time-span. A complex numerical computer analysis can be made to analyse the problem for any particular situation with well defined boundary conditions. However, an attractive approximate analysis was published recently by Peck (1971) that will be summarized here. Results from a field test of this method for the Ap of the Batavia silt loam will be presented.

4.3.1. The Peck-approximation for redistribution of water after infiltration

After infiltration of a certain quantity of water into a soil, the moisture content (θ) and the water potential (ψ) increase during redistribution to maximum values (θ_* and ψ_* respectively) and then decrease. The maxima occur at greater depths at ever greater times. At the time the maxima are at depth $z = z_*$, the soil is drying in the zone above z_* and wetting in the region below z_*. The plane $z = z_*$ which moves downwards into the profile, is referred to as the transition plane.

Fundamental to the analysis is the development of an expression for the function θ_* (z). The mean moisture content ($\bar{\theta}$) in the drainage region $0 \leq z \leq z_*$ is defined as:

$$\bar{\theta} = \left(\frac{1}{z_*}\right) \int_0^{z_*} \theta \, dz$$

$$(\bar{\theta} - \theta_o) \cdot z_* = \int_0^{z_*} (\theta - \theta_o) \, dz = Q_* \qquad (1)$$

Where: θ_o = initial moisture content which should represent a state of semi-equilibrium. Q_* may be identified as that part of the infiltrated water (Q) which is instantaneously in the draining zone $0 \leq z \leq z_*$. The following transformations can be made:

$$(\bar{\theta} - \theta_o)z_* = Q_*$$

$$(\theta_* - \theta_o) \cdot (\bar{\theta} - \theta_o)z_* = Q_* \cdot (\theta_* - \theta_o) \cdot \frac{Q}{Q}$$

or $$(\theta_* - \theta_o) \cdot z_* = \alpha Q \qquad (2)$$

Where:

$$\alpha = \frac{\beta Q_*}{Q} \quad \text{and} \quad \beta = \frac{(\theta_* - \theta_o)}{(\bar{\theta} - \theta_o)}$$

The contribution of hysteresis to redistribution is thus incorporated in the factors α and β. Empirical data is necessary to obtain these values. Peck analysed several papers on the topic and suggests $\alpha = 0.70$ $\beta = 0.78$. Equation (2) gives the moisture content in the transition plane θ_* as a function of the depth z_* of this plane in the soil. The only element left to be defined is time, and this can be achieved by differentiating equations (1) and (2). Details are to be found in Peck's paper. The final equation is as follows:

$$\frac{d\theta_*}{dt} \approx - \frac{(\theta_* - \theta_o)}{\alpha Q} \left[D \cdot \frac{(\theta_* - \theta_o)^2}{\alpha Q} + K \right] \qquad (3)$$

Table 4.1: Results of Peck-calculation of redistribution of water after infiltration into the A_p of a Batavia silt loam. The infiltrated quantity of water (Q) was 1 cm., the initial moisture content (θ_o) was 0.38 cm^3/cm^3 $\alpha = 0.70$ ($\alpha Q = 0.7$).

INPUT				OUTPUT		
θ_*	$\theta_* - \theta_o$	K	D	Time	Z_*	$\bar{\theta}$
(cm^3/cm^3)	(cm^3/cm^3)	(cm/day)	(cm^2/day)	(days)	(cm)	(cm^3/cm^3)
0.49	0.11	5.5	484	0.004	6.4	.521
0.48	0.10	4	332	0.008	7.0	.508
0.47	0.09	3	264	0.013	7.8	.495
0.46	0.08	1.8	234	0.022	8.7	.483
0.45	0.07	1.4	238	0.033	10.0	.470
0.44	0.06	1.1	231	0.051	11.7	.457
0.43	0.05	1	260	0.072	14.0	.444
0.42	0.04	0.8	240	0.130	17.5	.431
0.41	0.03	0.75	288	0.208	23.3	.418
0.40	0.02	0.68	340	0.400	35.0	.406
0.39	0.01	0.60	579	1.02	70.0	.393
0.385	0.005	0.55	550	2.45	140.0	.386

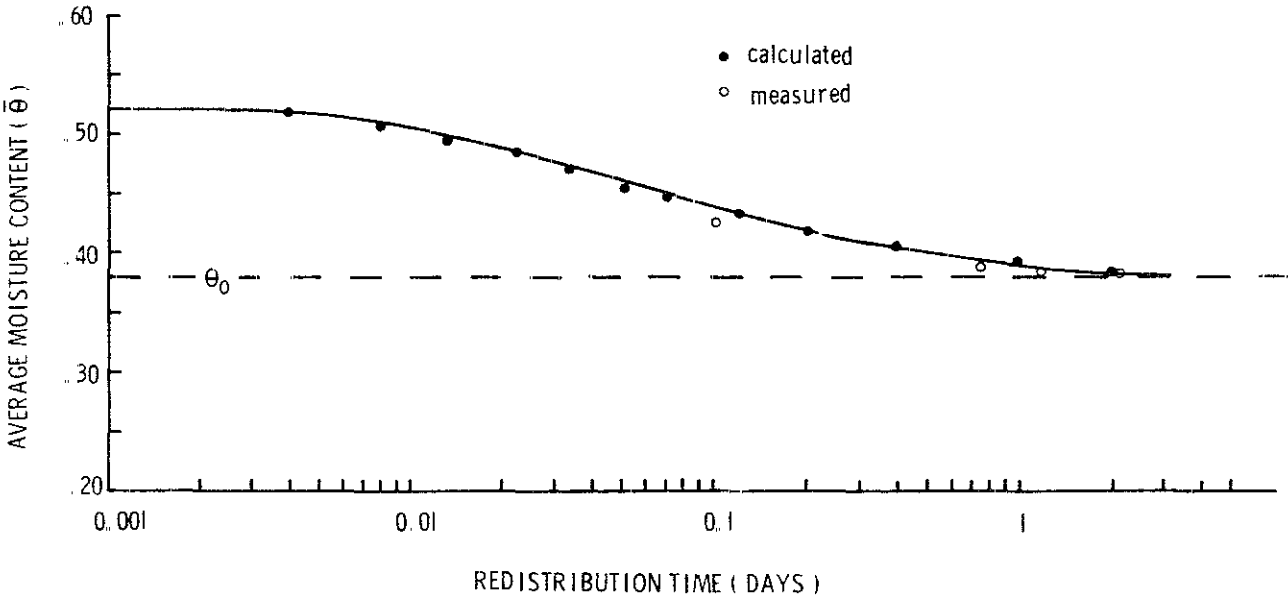

Fig. 4.6. Redistribution of one cm of liquid after infiltration into the Ap horizon of a Batavia silt loam. The measured values were compared with values calculated with the Peck-procedure.

given values of α (constant = 0.70), Q (= infiltrated quantity of water) and Θ_o (initial moisture content) and the functions D (Θ) (diffusivity) and K(Θ) (hydraulic conductivity) for wetting from Θ_0, Equation (3) can be used to approximate $d\Theta_*/dt$, and thus $dt/d\Theta_*$ for each value of Θ_*, including the one at t = 0, when all water has just infiltrated ($\Theta_* = \Theta_{sat}$). The $dt/d\Theta_*$ value can then be used to calculate t values, by substituting the proper $d\Theta_*$ value (in our example $d\Theta_* = 0.01$). The value for β (= 0.78) can be used to calculate $\overline{\Theta}$ (the average moisture content above the transition plane). Finally, z_* values are easily obtained from Equation (2).

A programmable USDA-ARS Hewlett-Packard calculater was used to write a simple program, that printed out values for t, z_*, and $\overline{\Theta}$. Results for the A_p of the Batavia silt loam are presented in Table 4.1. The moisture adsorption curve was used to calculate diffusivity (D) values from K values, measured in situ with the crust test. The slope of the absorption curve ($dP/d\Theta$) was graphically determined and then multiplied with the appropriate K value to obtain the corresponding D.

A field experiment was made applying one cm of water to the A_p horizon. Tensiometers are installed below the surface at 6, 12, 18 and 24 cm. The initial moisture content of the A_p horizon was 38% and rather constant throughout because the soil had been covered with plastic. Tensions during redistribution were followed with time and the average moisture content of the A_p horizon was graphically represented in Fig. 4.6. The calculated moisture contents ($\overline{\Theta}$) were plotted in the same figure and show that the method gave good agreement here for periods exceeding 2 hours.

4.3.2. Computer techniques using numerical methods to describe unsteady flow systems

As discussed, flow of water under natural conditions in the field will usually be unsteady as periodic rain showers add water to the soil intermittently, while surface crusting may inhibit infiltration and induce runoff. In the soil, water is extracted by plants to considerable depths in the growing season and by evaporation at the soil surface. In addition, deep downward drainage will remove water from the root zone. These processes occur concurrently, though each of them will peak at different times. Drying and wetting will occur simultaneously in different parts of the profile at the same time, which implies that hydraulic gradients and flow rates will vary widely at any given time. The picture is even more complicated because of hysteresis phenomena. Simplified approximate methods such as the one of Peck (1971) may give insight into some of these processes without going into complicated mathematical or numerical methods. Details of these procedures are in the literature, but it is advantageous to discuss the principles of numerical analysis to illustrate its potential and its limitations. C.R. Amerman (*in* Hillel, 1971) gave a very clear description of the topic, which will be followed in this context. One example of a very simple numerical analysis, describing a steady-state system with saturated flow with a known solution, will be worked out to illustrate the procedure. Modelling involves three phases:

1. Construction of a mathematical model of soil-water flow. For this, the partial differential equation discussed earlier can be used:

$$\frac{\partial \theta}{\partial t} = \frac{\partial}{\partial x} \left(K \frac{\partial H}{\partial x}\right) + \frac{\partial K}{\partial z}$$

Since K is a function of θ, this equation cannot be solved directly.

2. Modelling of the mathematical equation by means of a system of finite-difference equations and

3. Modelling of the finite-difference system by means of a digital computer using iteration procedures.

Example of finite-difference model of steady, saturated flow

(See C.R. Amerman in Hillel, 1971)

Assume saturated flow in a core with lenght L (L = 8). This is a very simple situation that can be solved analytically. A small layer of water is continuously supplied to the surface of the core, so that the positive pressure on the top surface of the core is effectively zero. A pressure of zero is also maintained at depth L where water flows from the core at atmospheric pressure. Since the pressure on both boundaries is zero, the pressure at every point in the soil is zero as well and the hydraulic head gradient is entirely gravitational (1 cm/cm). The hydraulic head at any point between $z = 0$ and $z = L$ is simply z, which is the elevation of that point (cm) with respect to some datum. In this example, the bottom of the core will be taken as $z = 0$. The flow equation for one-dimensional saturated flow reduces to:

$$\frac{\partial}{\partial x}\left(\frac{\partial H}{\partial x}\right) = 0 \qquad (1)$$

Now the finite-difference form for this equation has to be written for every node, except for those at the top and bottom of the core, where H is known. Adjacent nodes are separated by 1 cm intervals.

Assume three adjacent nodes: i - 1 is the upper, i the middle and i + i the lower node. Then:

$$\frac{\partial}{\partial x}\left(\frac{\partial H}{\partial x}\right) \backsimeq \frac{1}{\Delta x}\left(\left.\frac{\partial H}{\partial x}\right|_1 - \left.\frac{\partial H}{\partial x}\right|_2\right)$$

$$\left.\frac{\partial H}{\partial x}\right|_1 = \frac{H_{i+1} - H_i}{\Delta x} \qquad \left.\frac{\partial H}{\partial x}\right|_2 = \frac{H_i - H_{i-1}}{\Delta x}$$

Thus:

$$\frac{\partial}{\partial x}\left(\frac{\partial H}{\partial x}\right) \backsimeq \frac{H_{i+1} - 2H_i + H_{i-1}}{\Delta x^2} \tag{2}$$

and by substitution the right side of (2) into (1) we find:

$$H_{i+1} - 2H_i + H_{i-1} = 0$$

and

$$H_i = \frac{H_{i+1} + H_{i-1}}{2} \tag{3}$$

Table 4.2: Example of iteration procedure as part of a numerical analysis of steady saturated flow (see text)

Z		i_1	i_2	i_3	i_4	i_5	i_6	i_7	i_8
8	8	8	8	8	8	8	8	8	
7	0	4	5	5.5	5.81	6.03	6.20	6.33	
6	0	2	3	3.62	4.06	4.40	4.66	4.86	
5	0	1	1.75	2.31	2.76	3.12	3.40	3.64	
4	0	0.5	1.0	1.46	1.83	2.15	2.42	2.65	
3	0	0.25	0.62	0.91	1.18	1.43	1.65	1.85	
2	0	0.125	0.33	0.53	0.72	0.90	1.05	1.18	
1	0	0.062	0.16	0.26	0.36	0.45	0.52	0.59	
0	0	0	0	0	0	0	0	0	

L = 8 cm.

The completed model consists of Equation (3) for all interior nodes of the solution mesh and the two boundary conditions: $x = 0$, $H = 0$ (bottom core) and $x = 8$, $H = 8$ (top core). The operation of this model is quite simple. We arbitrarily assume the value of H to be zero at every node; except for $x = L$ where $H = 8$. Now start at the first node beneath the surface and solve for H_7 using $H_{i-1} = 8$. The value of H_i (= 4) will be the first estimate of H at node no. 7. Then, the second node below the surface is considered, where the value to use for H_{i-1} is the one just calculated for that node. This operation can be repeated for each interior node in the solution mesh. For results, see Table 4.2. In this simple case the answer to the problem is known. The figures in Table 4.2 show that after 7 "runs" (also called "iterations") H values are still not corresponding to the real H values in the system but they are approaching these values. Several hundred iterations are usually required to obtain realistic estimates of the real H-distribution. The iteration procedure is stopped as soon as the difference between results of successive iteration "runs" is sufficiently small. Stopping calculations requires therefore a, by nature, arbitrary decision as to required accuracy. A computer is necessary to make these calculations. The procedures described here are essentially similar for the more complicated, unsteady, unsaturated flow (Amerman, 1971 in Hillel, 1971). This simple example illustrates a major aspect of numerical analysis; namely that the operator has to select some initial distribution of the dependent variable (in our example H), while known boundary values (here: $H = 0$ and $H = 8$) are <u>essential</u> to the calculation procedure. The latter requirement makes this method rather specific: certain flow geometries can be calculated but each new one needs a new program. Good agreement has been reported for flow processes in soil columns using numerical techniques (see references in Chapter 6).

5. Relationships between soil structure and hydraulic conductivity.

Research has been conducted in the years 1970 through 1972 in the Soil Survey Division of the Wisconsin Geological and Natural History Survey in cooperation with the Soils Department, College of Agricultural and Life Sciences, on relationships between soil structure as characterized with morphometric techniques and hydraulic conductivity (K). Three papers on this topic are in press at this time or have been submitted and abbreviated versions of these papers will be presented in this chapter in the context of the general discussion of hydraulic behavior of soil pedons. The three papers are:

1. J. Bouma and J.L. Anderson (1973). Relationships between soil structure characteristics and hydraulic conductivity, in: R.R. Bruce. Ed. The Field Soil Moisture Regime. ASA-Special Publication, based on the Syposium at the ASA-meetings, New York, 1971.

2. J.L. Anderson and J. Bouma (1973). Relationships between saturated hydraulic conductivity and morphometric data of an argillic horizon. In press. Soil Sci. Soc. Amer. Proc.

3. J.L. Denning and J. Bouma. 1973. A comparison of hydraulic conductivities calculated with morphometric and physical methods. Soil Sci. Soc. Amer. Proc. (Submitted for publication).

5.1. RELATIONSHIPS BETWEEN SOIL STRUCTURE CHARACTERISTICS AND HYDRAULIC CONDUCTIVITY IN PEDAL SOIL MATERIALS

ABSTRACT

Relationships between soil structure, as characterized by morphometric methods, and hydraulic conductivity (K) were explored for four pedal soil horizons. Morphometric analysis was shown to have a specific function in studying the occurrence of pore types, such as planar voids and channels, that constitute only a small fraction of total pore volume, but strongly affect K_{sat}. Results were used to construct simple models of natural soil structures. A planar-void model, assuming vertical plane continuity, was used to calculate K_{sat} of the four natural pedal soil materials. Results obtained were close to experimental values, measured *in situ* by the double-tube method.

5.1.1. INTRODUCTION

Questions about the physical behaviour of soil types, and in particular their capacity to transmit water, are becoming more specific as soil maps are increasingly used.

Field methods are available to measure hydraulic conductivity (K), of saturated and unsaturated soil well above the groundwatertable (Bouwer, 1961, 1962, Bouwer et al., 1964, 1967; Boersma, 1965; Gardner, 1970; Bouma et al., 1971b). Such methods are preferable to those requiring sampling of "undisturbed" cores in the field and subsequent measurement in the Laboratory (Klute, 1965). The field techniques require instrumentation and are laborious. Hydraulic field characterization of major horizons is too costly to be applied to all soils represented on a soil map. An alternative could be to study horizons of benchmark soils and to extrapolate measured values to other soils, that are somehow characterized as being comparable. Such procedures would require a reasonable understanding of flow patterns of water through pores of soils. For this a detailed functional characterization of pore systems in soils is needed. One method is to estimate pore size distributions of non-swelling soil materials from moisture retention data and to use this derived pore-size distribution in a pore model to predict K values (Marshall, 1958). This method has also been applied to swelling soil materials by Green and Corey (1971) who reported reasonable agreement between calculated and measured K values, both for saturated and unsaturated soil. Because calculated and measured values did not agree directly, it was necessary to measure one K value (K_{sat}) experimentally to determine a "matching factor". This is the ratio between the measured and calculated value. All other calculated values, applying to unsaturated soil, had to be multiplied by this factor.

However, many pores in soil can be observed directly and their sizes measured by morphological techniques. Different types of pores, with supposedly different functions in the soil, can be distinguished (Brewer, 1964). In addition, physical theory describes relationships between pore size and conductivity for planar and tubular pores (Childs, 1969).

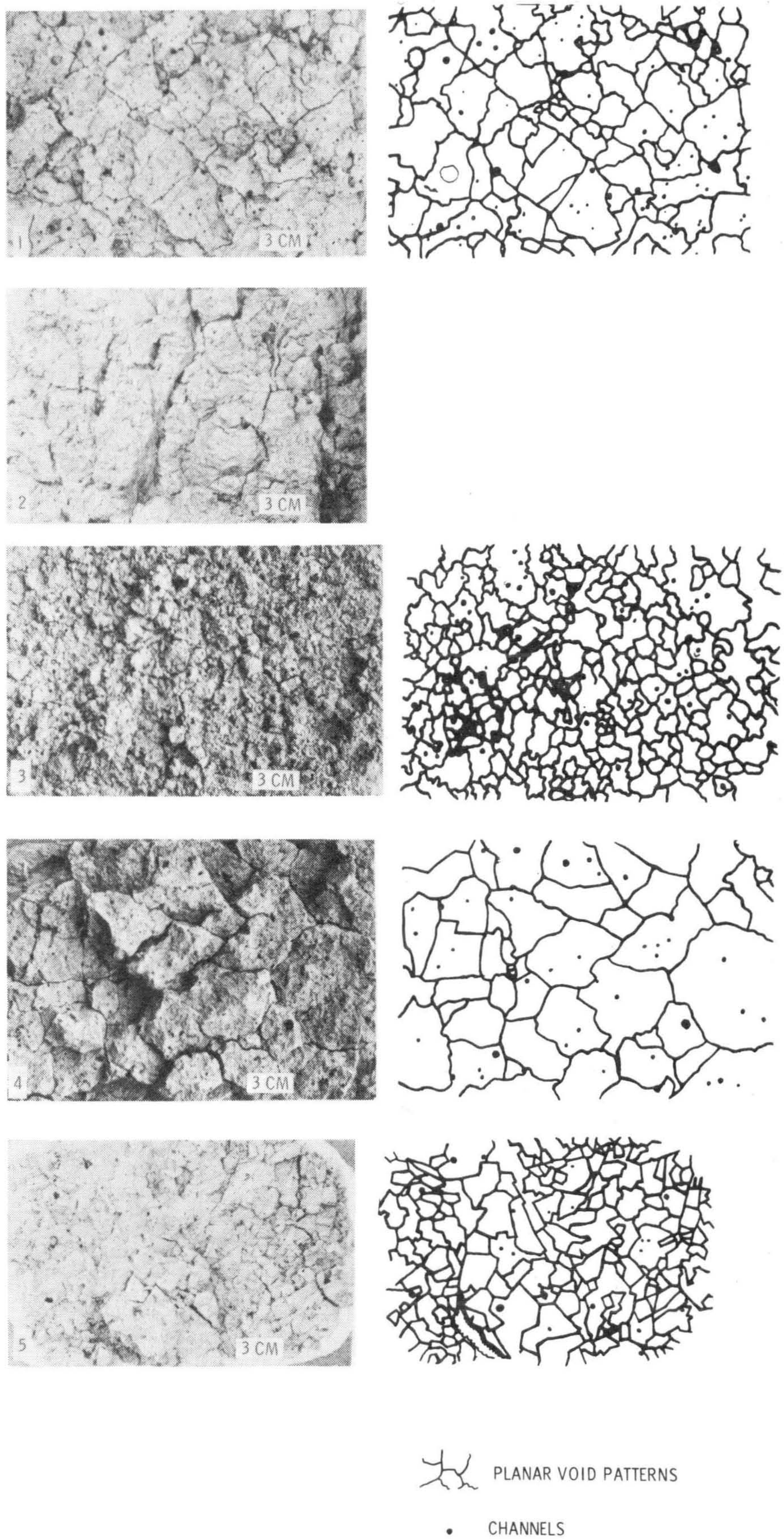

Fig.5.1 Secondary structures of four pedal soil materials.The numbers on the pictures correspond with those in tables 5.1 and 5.2.

In this investigation, relationships between soil structure and hydraulic conductivity were studied at the level of secondary structure. Secondary structures were observed in soil peels, prepared from undisturbed horizontal sections through selected soil horizons. Secondary structures were described in the field by noting sizes, shapes and arrangements of peds and abundance of channels (Table 5.1). Pictures of soil peels of the studied horizons are presented in Fig. 5.1. Sizes and shapes of peds were classified according to the Soil Survey Staff (1951) and Brewer (1964). Arrangement of peds was described by noting (1) accommodation (a measure of the degree to which adjacent faces are molds of each other), (2) packing (whether with some orderly arrangement or at random) and (3) inclination (orientation with reference to the vertical or horizontal) (Brewer, 1964, p. 345).

Description of grade of structure (Table 5.1) (Soil Survey Staff, 1951) is difficult. The (1) "degree of evidence in place" and (2) the durability of peds after an undefined procedure of "disturbance", result from processes of adhesion and cohesion which are mainly functions of variable moisture content. Ped durability may be expressed in terms of soil consistence (Soil Survey Staff, 1951). "Degree of evidence" of peds in place may be based on observation of arrangement of peds, including accommodation and packing.

Descriptive morphological classifications of secondary structures are becoming very complex, with increasing numbers of categories of size, shape and arrangement. The more detailed such vocabulary becomes, the more terms are needed to describe natural variability in a horizon. This development may be unfavorable for applied studies, insofar as one of the purposes of structure descriptions is to distinguish basic order in the overwhelming complexity of a pedal soil material. This points to the need for quantitative measurements of specific well defined structural features. Abundance and sizes of channels were measured on soil peels by Van der Plas et al. (1964) and Bouma and Hole (1965). Counts of large channels (> 1 mm dia.) on horizontal sections through soil horizons were made in the field by Slager (1966) and Baxter and Hole (1967). A technique is explored in this paper to quantify patterns of natural planar voids in soil peels.

In this study of relationships between void patterns and hydraulic conductivity the attempt has been made to represent natural structures by simplified morphological models, that use a few pore types (channels, planes and packing voids) for which physical expressions are available to relate pore size to conductivity. In such models much emphasis has to be given to continuity of pores in the soil, as this determines their effectiveness in transmitting water. Studies of pores in thin sections and in soil peels, yield data that applies two-dimensionally. Statistical procedures are necessary to use this data in predicting the behavior of a three-dimensional volume of soil.

5.1.2. Soil materials.

Soil peels (Bouma and Hole, 1965; Jager and vander Voort, 1965) were prepared from horizontal sections through selected soil horizons having well developed pedality. A block of soil was carefully carved out *in situ* from the level of the section downwards to fit into a rectangular metal

Table 5.1.

Morphological characteristics of soil horizons, sampled for studying K values of secondary structures (Fig. 3).

No.	Soil Classification	Field Structure: Soil Survey Manual	Brewer	Channels (counted in 625 cm^2 of exposed horizontal planes)
1&2	Typic Argiudoll (fine silty, mixed, mesic) Tama silt loam B_3-(silty clay loam).	(strong) medium prismatic parting to (moderate) medium subangular blocky.	Accomodated, faulted, medium tetracolumnar sec. peds, composed of accomodated, normal, medium, subrounded octablocky primary peds.	6 fine (1-2 mm diameter) 1 medium (2-4 mm diameter)
3	Typic Argiudoll (fine silty, mixed, mesic) Plano silt loam. B_2-(silty clay loam)	(weak) medium prismatic parting to (moderate) fine subangular blocky	Accomodated, faulted, medium tetracolumnar sec. peds, composed of accomodated, normal, fine subrounded pentablocky primary peds.	12 fine 10 medium 2 large (larger than 4 mm diameter)
4	Same as 3 B_3-(silty clay loam)	(moderate) coarse prismatic	Accomodated, bi-offset, medium pentacolumnar primary peds.	4 fine 4 medium 1 large
5	Typic Eutrochrept (very fine, mixed, mesic) Oshkosh clay B_3 (silty clay)	(moderate) medium prismatic parting to strong medium angular blocky	Accomodated, bi-offset, locally offset faulted, medium tetra-columnar sec. peds, composed of accomodated, normal, medium hexablocky primary peds.	4 fine 1 medium
6	Typic Udipsamment (sandy, mixed, mesic) Plainfield loamy sand B_2(loamy fine sand)	single grain	Apedal; basic fabric with intertextic related distribution pattern.	4 fine

Table 5.2.

Physical properties of soil horizons, used for studying K values of secondary structures. (Fig. 3).

No.	Type of soil and horizon		Bulk density (1/3b)	Particle density (gr/cm^3)	Porosity (%)	Organic matter (%)	pH
1 + 2	Tama silt loam	B_3	1.35	2.65	49.0	0.5	5.5
3	Plano silt loam	B_2	1.41	2.63	46.3	0.4	5.2
4	Plano silt loam	B_3	1.45	2.64	45.1	0.7	5.1
5	Oshkosh clay	B_2	1.43	2.62	45.5	0.8	7.7
6	Plainfield loamy sand	B_2	1.45	2.65	45.3	1.1	5.8

container. This was gently pushed down over the block of soil, which was then cut loose from below and removed with the container. The soil surface was smoothed, a peel was prepared from it and was mounted on masonite. General physical characteristics of the four studied horizons are reported in Table 5.2.

5.1.3. MEASUREMENT AND CALCULATION OF K

Physical methods.

Moisture retention curves were determined with standard procedures on large Saran coated fragments or field clods (Brasher et al., 1968). COLE values (Grossman et al., 1968), bulk density and porosity were calculated from these data, the latter after determining particle density (Blake, 1965). Hydraulic conductivity was measured in situ in the field with the double-tube method (Bouwer 1961, 1962; Bouwer et al., 1964, 1967; Baumgart, 1967) for measuring K_{sat} in soil well above the groundwater.

Morphological methods.

Pedality and occurrence of transpedal channels were described with methods, discussed in Sections 5.1.1 and 5.1.2. Here, a method will be explored to quantify patterns of interpedal planar voids, between accomodated peds. Flow through plane slits can be described by physical equations that relate pore size to moisture flow at defined hydraulic gradients. For a plane slit of unit length and width d,:

$$Q/t = \left[(\rho g d^3)/12\eta\right] \cdot \text{grad } \phi \qquad (1) \qquad \text{(Childs, 1969)}$$

where: Q/t is the amount of liquid, with viscosity η(g $cm^{-1}sec^{-1}$), conducted per unit time and length (cm^2sec^{-1}) and ρ = density of liquid (g cm^{-3}), g = gravitational constant (cm sec^{-2}) grad ϕ = hydraulic gradient (cm/cm). Assuming that only planar voids contribute to pore volume in a soil body, which has n parallel slits per unit area, each of width d, one finds: $K_{sat} = g\rho f d^2/12\eta$, in which f = total porosity occupied by these pores = n . d (Childs, 1969). In natural soil materials only very small fractions (1-2%) of total pore volume are occupied by planar voids. Fine voids in the basic fabric that contribute only negligibly to flow, account for a high percentage of total porosity.

Therefore this equation for K_{sat} was not used, and flow per unit area is described by:

$$v = \frac{n}{S}(Q/t) = \left(\frac{ng\rho d^3}{12\eta \cdot S}\right) \cdot \text{grad } \phi \qquad K = \frac{ng\rho d^3}{12\eta \cdot S} \qquad (2)$$

where: S = top surface area of measurement in a soil peel (cm^2) in which n cm of planar voids occur. K (cm/sec) is derived at grad ϕ = 1 cm/cm.

For tubular pores we find that flow rate and pore size are related as follows (Childs, 1969):

$$Q/t = \frac{\rho g \pi r^4}{8\eta} \cdot \text{grad } \phi \qquad (3)$$

where: Q/t is the amount of liquid, with viscosity η, conducted per unit time (cm^3/sec) and r is tube radius (cm). With n tubes per cm^2, it follows:

$$v = n(Q/t) = \frac{n\rho g \pi r^4}{8\pi} \cdot \text{grad } \phi$$

If these tubes are the only pores, $n\pi r^2 = f$, where f = total porosity. Then:

$$v = \frac{\rho g r^2 f}{8\eta} \cdot \text{grad } \phi \text{ and } K = \frac{\rho g r^2 f}{8\pi} \quad \text{(Childs, 1969)}$$

When scattered large channels occur in a porous soil mass, use of f may be confusing, since channels contribute only a small fraction (f) to total porosity (see Table 5.3). If a soil horizon has n channels of radius r per S cm^2 horizontal soil surface, the following relationship applies:

$$v = \frac{n}{S}(Q/t) = \frac{n\rho g \pi r^4}{S \cdot 8\eta} \cdot \text{grad } \phi. \text{ For grad } \phi = 1 \text{ cm/cm we find K: (cm/sec)}$$

$$K = \frac{n\rho g \pi r^4}{S \cdot 8\eta} \qquad (4)$$

where: v = the measured rate of infiltration into soil surface area S, at saturation and at a given hydraulic gradient.

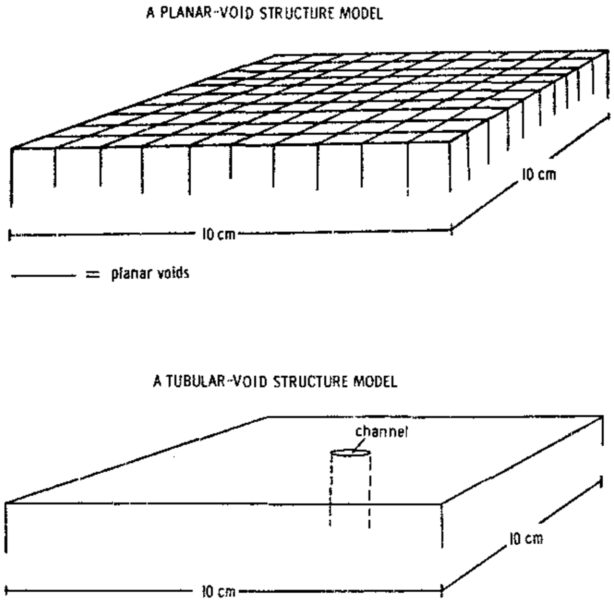

Fig. 5.2. Horizontal sections through a tubular and a planar void model of soil structure.

Hydraulic conductivities and porosities of planar and tubular pore models of soil structure (Fig. 11).

Planar void model Size of blocks	Width of planar voids	Porosity (%)	K (cm/day)
1 cm^2	10µ	0.2	1.5
	50µ	1.0	180
	100µ	2.0	1440
4 cm^2	10µ	0.1	0.7
	50µ	0.5	90
	100µ	1.0	720
	1000µ	10	719712
Tubular pore model:	**Diameter of channel**	**Porosity (%)**	**K (cm/day)**
	100µ	0.8×10^{-4}	0.02
	200µ	0.3×10^{-3}	0.34
	500µ	0.2×10^{-2}	14.6
	1000µ	0.8×10^{-2}	211.2
	4000µ	0.13	54130.5

This approach can be illustrated by calculating K_{sat} values, considering horizontal sections through abstract models of "soil" (Fig. 5.2). The upper figure shows a surface of 100 cm^2, occupied by square blocks, mutually separated by a distance d. The blocks are impermeable and water moves only along the planes. The lower figure shows the same surface with one tubular pore (channel). Water can only move through this pore. K values for these models were calculated for different sizes of pores [using equations (2) and (4), derived from (1) and (3) that were graphically represented in Fig. 3.9 in Chapter 3). assuming that planes and channels extend vertically downwards (see Table 5.3.) "Effective planar widths" (d^1) were calculated for the four secondary fabrics, following this procedure in reverse by measuring length of natural planar voids in soil peels and using a measured K_{sat} value.

It was assumed that movement of water occurs along planes only, that planar voids have one "effective width" and extend downwards into the soil for a distance of, in this case 12 cm (Bouma and Hole, 1971a).

$$d^1 = \sqrt[3]{(K \cdot 12\eta \cdot S)/(L \cdot \rho \cdot g)} \qquad (5)$$

where: S = top surface area of the soil peel and d^1 = effective planar width. L = total length of planar voids in soil peel. Other terms were explained earlier.

However, planar voids will usually not be vertically continuous in a soil sample, that is several times larger than the average ped size. The following procedure, using a method to estimate vertical plane continuity, was therefore applied to calculate K_{sat} of the four secondary structures with a planar void model.

The procedure had the following steps:

1. A picture was made of soil peels from horizontal and vertical sections of the horizon to be characterized. Peels were large enough to represent at least 25 primary peds.

2. Tracings were made of the pictures, showing patterns of natural planar voids (Fig. 5.1). Total lengths of planar voids were measured from pictures of horizontal peels with a map measurer and ped sizes were determined by estimating for every exposed ped the diameter of a circle with a similar surface. Then average ped size was determined.

3. Distribution of widths of planar voids was determined in air-dry horizontal soil peels, with a ribbon-count procedure (see Van der Plas, 1962, Brewer, 1964 p. 50). Line or point-count procedures were not suitable because the surface of planar voids was only a very small fraction of the total peel surface. The ribbon-count procedure implies measurement of numbers and sizes of individuals in the soil peel with a binocular microscope at a magnification of, in this case, 30x. The microscope was mounted so that the field of vision, including a measuring scale, could be moved over the peel surface. A small observational ribbon 60 microns wide, was thus projected on the peel. Every planar void that crossed the ribbon was counted, and the smallest observed dimension was recorded. In each peel at least 300 planar voids were counted, and grouped in size classes, corresponding to scale units.

4. A "representative plane length l_i" was calculated for each size class: $l_i = L(p_i/p_t)$ where L = total length of planar voids in an air-dry peel, p_i = number of planes in a certain size class i, i = 1,2,3...n, and p_t = total number of planes counted. Plane widths were measured in air-dry soil peels. COLE values (Grossman et al., 1968) were determined for primary peds to estimate volume changes of air-dry peds upon saturation, and resulting decreases in plane width. If average ped size is 10 mm, a COLE value of 3% will increase this to 10.3 mm. In a soil material with accomodated peds, the width of all

planar voids will then be 300 microns less. Planes smaller than 300 microns in the air-dry peel will close.

5. Calculated K values are to be compared with values measured in situ with the double-tube method. Simulation techniques have shown that measurement involves a soil sample with a height of about $2R_c$, which is 12 cm (Bouwer, 1961). In pedal soil materials with peds, much smaller than 12 cm, K_{sat} will be determined by the smallest voids in the interpedal void system. A model is necessary to predict sizes of such "planar necks" in the flow system. The hypothesis used is that interconnected open planar voids govern the flow process. With an average vertical ped size of v cm, there are 12/v layers of peds. Swelling resulted in a reduction of the number of classes from n to n-x, where x is the largest pore size class closed by swelling (all classes between 1 and x are closed too). Chances of a size class of planes to be vertically continuous, can be estimated as they are proportional to the l_i values for each open class, considering a structure model with 12/v layers of peds. For example: open planes, interconnected through the layers of peds according to the hypothesis, are of size class (n-x+1) or larger. Chances to be of class (n-x+2) or larger (excluding class n-x+1), are lower. Suppose l_i values for the classes are l_{n-x+1}, l_{n-x+2}, l_{n-x+3}... etc., with total length of open planes after swelling l_t. Considering the contact between the first and second layers of peds, probability of a plane of class (n-x+2) to be connected with a pore similar or larger in size than itself is proportional to the l_i values involved: $(l_t - l_{n-x+1})/l_t$. A similar expression can be derived for the first three layers of peds. Finally, probability that planes of size class (n-x+2) are connected throughout the 12 cm long sample, by planes either of its own size or larger is: $[(l_t - l_{n-x+1})/l_t]^{(12/v) - 1}$. A similar calculation is made for the class (n-x+3) etc. Only if such probabilities are higher than Z% are they considered statistically significant, and corresponding pore classes are included in the calculation of conductivity (Z was arbitrarily

chosen as 5%). Assume that class n-x+s represents the last class to have a probability higher than 2% of being continuous into a similarly sized or larger pore-class. Now only a fraction p of open pore-length (where $p = l_{n-x+1} + l_{n-x+2} + \ldots l_{n-x+s}$) contributes to conductivity. Flow into voids of size class n-x+s+1 or larger will, according to the model, have to pass voids of size class n-x+1 or larger, while moving through the 12 cm high sample. The probability that flow occurs through size class n-x+1 is highest. Therefore, l_i values of all pores larger than class n-x+s are assigned to class n-x+1. Two l_i values are therefore given in Table 5.4 for this class, one directly calculated for the class, and the second as a rest factor. The final equation for the calculation of K, using equation (5) for each of the size classes, becomes then:

$$K = 86400\left[\left(\sum_{i=n-x+1}^{i=n-x+s}\left(\frac{\rho g d_i^{3}}{12\eta}\right) \times \frac{l_i}{S}\right) + \frac{\rho g d^{3}_{n-x+1}}{12\eta} \times \frac{l_t - (l_{n-x+1} + l_{n-x+2} \cdots + l_{n-x+s})}{S}\right] \tag{6}$$

where: K is the hydraulic conductivity (cm/day) and d_i = is the average width (cm) of a planar void in a size class i. S = top surface area of the soil peel. The rest of the terms are explained in the text.

Table 5.4. Calculation of $K_{sat.}$ for four secondary soil structures (Fig. 5.1)

Soil type	Horizon	Average ped size (cm)		COLE	L (cm)	l_t (cm)	Open pores after swelling		K (cm/day) calc. planar model		K meas.	Effective planar width d' (μ)	Planar poros-ity (%)	K Calc. channel model (cm/day)
		Hor.	Vert.				Size# class (μ)	l_i (cm)	Per class	Total				
Tama silt loam (No. 1, Fig 5.1)	B_3	1.50	2.0	0.030	127	48.6	36 96	15.6 + 20 9	4.0 19.9	23.9	22	39	0.2	1500
Plano silt loam (No. 3)	B_2	.91	1.7	0.030	157	26.5	37 97	9.8 + 7.7 9.0	2 20.7	22.7	20	38	0.2	25000
Plano silt loam (No. 4)	B_3	1.90	2.5	0.028	86	18.4	18 78 138	3.4 + 8.1 5.1 1.8	0.1 6.8 11.8	18.7	12	36	0.1	21650
Oshkosh clay (No. 5)	B_2	0.76	1.5	0.029	107	23.0	32 92	5.9 +10.9 6.2	1.4 6.2	7.6	6	29	0.1	1390

#One microscopic scale unit corresponded here to 60 microns; larger magnifications are recommended for future work.

5.1.4. RESULTS AND DISCUSSION

Occurrence of planar voids and channels in soil materials can result in high K_{sat} values, even though they contribute minimal fractions to soil porosity (Table 5.3). Methods to estimate K_{sat} which are based on relative volumes of pore size classes, either determined micromorphologically with point counts or physically by moisture retention measurements tend therefore to be very unsensitive because of the experimental error involved.

An alternative is to count the number or length of specific pore types in a certain soil surface area, as discussed in this paper.

Calculated values of d' (effective planar width (equation 5), varied within a narrow range of 29 to 39 microns (Table 5.4). This could point to the feasibility of a method where total planar-void length L is measured in a certain soil surface area and K is calculated according to equation 5, after estimating an "effective planar width d'". The calculated values of K_{sat} for four secondary soil structures according to the plane-slit structure model (equation 6) were close to those, measured with the double tube method in the field (Table 5.4). This model applies to structures with accomodated, relatively large peds, that should have a small range in horizontal size, so as to make the corrections for swelling applicable. Flow in the model is supposed to be occurring only along planar voids, open after swelling, that constitute a system with interconnected planes. Since all basic structures of the four soil horizons had a porphyroskelic related distribution pattern (see Chapter 2), it can be assumed that water movement through these very fine basic structures is negligible. Relatively large but isolated and vertically discontinuous voids such as vughs and chambers will not contribute to the conductivity of a soil layer about 12 cm thick. However, channels may be vertically continuous for quite a distance. Worm or ant channels, for example, may extend from the soil surface downwards to a depth of 5 feet

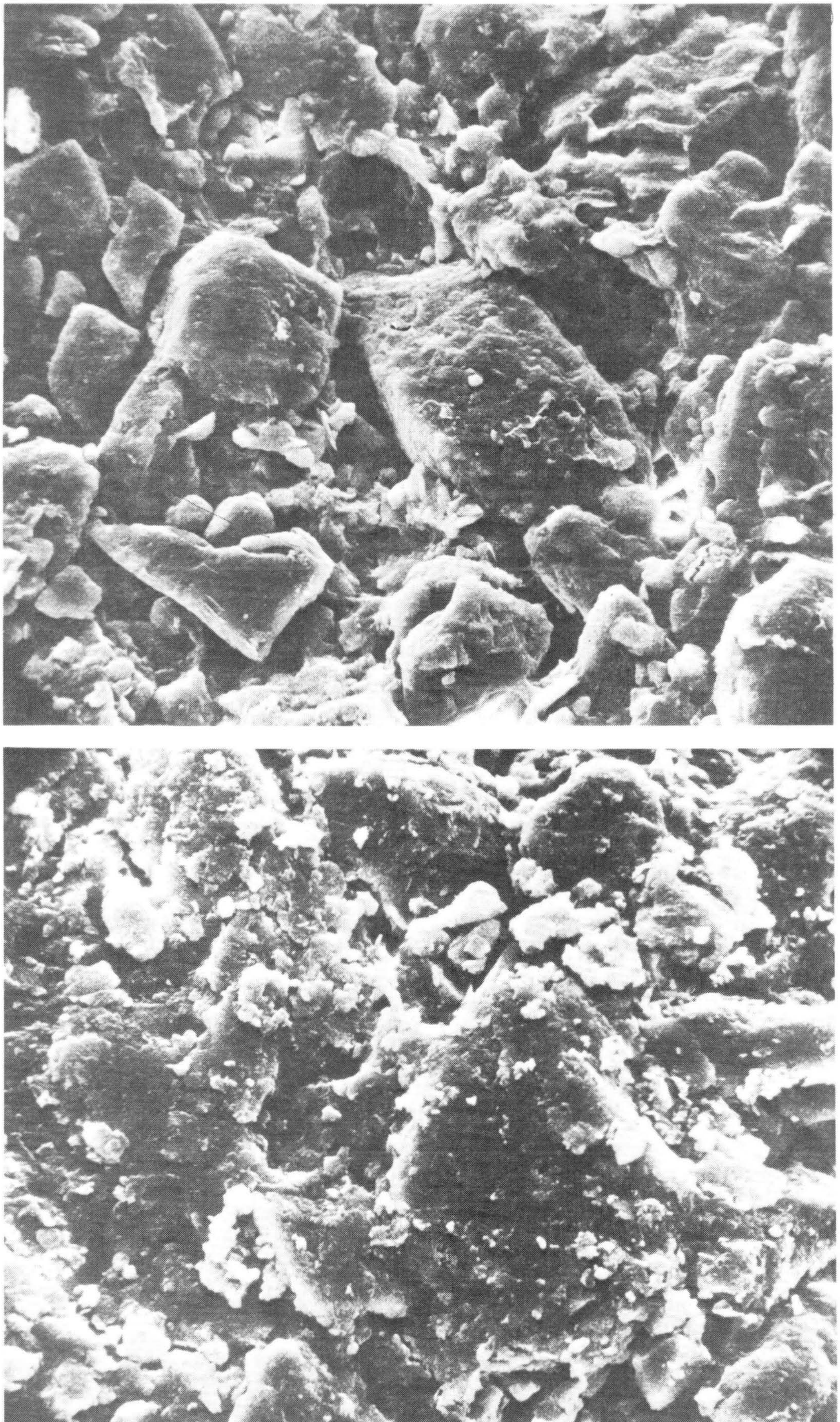

Fig 5.3 Ped interior (upper) and ped surface (lower) in a B2 horizon of a Plano silt loam. Picture was made with a scanning electron microscope (Photo courtesy of Dr.E.B.Sachs, USDA Forest Products Laboratory, Madison, Wis)

(Baxter and Hole, 1967). The planar structure model was nevertheless used as an hypothetical model because:

1. Illuviation and other cutans, and skeletans on ped faces strongly indicate movement of liquid through planar voids. A picture of a ped surface and a ped interior of the B_2 of a Plano silt loam (Fig. 5.3), taken with the Scanning Electron Microscope, shows that ped surfaces were partly sealed, in contrast to the open ped interior, although no ped-illuviation cutans were observed in thin section. Similar examples were given by Lynn and Grossman (1970). Moreover, ped faces in a freshly exposed soil are often wet, while interiors of peds are only slightly moist.

2. Flow rates were calculated for the four studied soil horizons, using the counted number of channels on exposed horizontal sections, in the field (table 4) and equation 4, applied to each size class, followed by summation.

Calculated K values for the four soil horizons, based on the occurrence of channels only, are in the last column of Table 5.4. Values are unrealistically high, particularly when channels larger than 2 mm are present. This is mainly caused by the lack of a suitable pore-continuity model (like the one used for interpedal planar voids) for channels occurring in natural soil. Very high K_{sat} values may be measured when large channels are vertically continuous throughout a relatively small soil core, that is used to determine K_{sat} in the laboratory (Klute, 1965). In a natural profile, however, chances are that such a large pore, if in contact with tension-free water will fill up, and drain through surrounding smaller, but more numerous planar or packing voids. Obviously, more research is needed to establish the hydraulic function of channels in the natural soil fabric.

3. The calculated values were compared with those determined by the double-tube method in the field. This measurement involves both horizontal and vertical flow components. Planar void patterns extend in all directions, whereas channels, notably the larger ones, tend to be more vertically oriented. Agreement between calculated and measured values is partly a result of the method used.

5.1.5. LITERATURE CITED

Anderson, D. M. and R. R. Binnie, 1961. Modal analysis of soils. Soil Sci. Soc. Amer. Proc. 25:499-503.

Baumgart, H. D., 1967. Die Bestimmung der Wasserleitfähigkeit k_f von Böden mit tief liegender Grundwasseroberfläche. Mitteilungen aus dem Institut für Wasserwirtschaft und Landwirtschaftlichen Wasserbau der Technischen Hochschule Hannover. 275 p.

Baxter, P. F. and F. D. Hole, 1967. Ant (Formica cinerea) pedoturbation in a prairie soil. Soil Sci. Soc. Am. Proc. 31:425-428.

Blake, G. R., 1965. Particle density. Amer. Soc. Agron. Monograph 9 :371-373.

Boersma, L., 1965. Field measurement of hydraulic conductivity above a water table. Amer. Soc. Agron. Monograph 9:235-252.

Bouma, J. and F. D. Hole, 1965. Soil peels and a method for estimating biopore size distribution in soil. Soil Sci. Soc. Am. Proc. 29:483-485.

Bouma, J., 1969. Microstructure and stability of two sandy loam soils with different soil management. Agricultural Research Report 724, p. 110. Pudoc Wageningen, The Netherlands.

Bouma, J. and F. D. Hole, 1971a. Soil morphology and hydraulic conductivity of adjacent virgin and cultivated pedons at two sites: A Typic Argiudoll (silt loam) and a Typic Eutrochrept (clay). Soil Sci. Soc. Amer. Proc. 35:316-319.

Bouma, J., D. I. Hillel, F. D. Hole and C. R. Amerman, 1971b. Field measurement of unsaturated hydraulic conductivity by infiltration through articicial crusts. Soil Sci. Soc. Amer. Proc. 35:362-364.

Bouwer, H., 1961. A double tube method for measuring hydraulic conductivity of soil in situ above a water table. Soil Sci. Soc. Amer. Proc. 25: 334-339.

Bouwer, H., 1962. Field determination of hydraulic conductivity above a water table with the double tube method. Soil Sci. Soc. Amer. Proc. 26:330-335.

Bouwer, H. and H. C. Rice, 1964. Simplified procedure for calculation of hydraulic conductivity with the double tube method. Soil Sci. Soc. Amer. Proc. 28:133-134.

Bouwer, H. and H. C. Rice, 1967. Modified tube diameters for the double tube apparatus. Soil Sci. Soc. Amer. Proc. 31:437-439.

Brasher, B. R., D. P. Fransmeier, V. Valassis and S. E. Davidson, 1966. Use of Saran resin to coat natural soil clods for bulk density and water retention measurements. Soil Sci. 101:108.

Brewer, R., 1964. Fabric and mineral analysis of soils. John Wiley and Sons Inc., New York. p. 470.

Buol, S. W., and D. M. Fadness, 1961. A new method of impregnating fragile materials for thin sectioning. Soil Sci. Soc. Amer. Proc. 25, 253.

Chayes, F., 1956. Petrographic Modal Analysis (John Wiley and Sons, New York).

Childs, E. C., 1969. The Physical Basis of Soil Water Phenomena. John Wiley. p. 493.

Gardner, W. R., 1970. Field measurement of soil water diffusivity. Soil Sci. Soc. Amer. Proc. 34:832-833.

Green, R. E. and J. C. Corey, 1971. Calculation of hydraulic conductivity: A further evaluation of some predictive methods. Soil Sci. Soc. Amer. Proc. 35:3-8.

Grossman, R. B., B. R. Brasher, D. P. Franzmeier and J. L. Walker, 1968. Linear extensibility as calculated from natural-clod bulk density measurements. Soil Sci. Soc. Amer. Proc. 32:570-573.

Hillel, D. I. and W. R. Gardner, 1970. Measurement of unsaturated conductivity and diffusivity by infiltration through an impeding layer. Soil Sci. 109, 149-153.

Jager, A. and Voort, W. J. M. van der, 1966. Collection and Preservation of Soil Monoliths. Soil Survey Papers No. 2, Soil Survey Institute, Wageningen, The Netherlands.

Jongerius, A., 1957. Morfologische onderzoekingen over de bodemstructuur. Thesis Wageningen, p. 93.

Klute, A., 1965. Laboratory measurement of hydraulic conductivity of saturated soil. Amer. Soc. Agron. Monograph 9:210-221.

Kubiena, W. L., 1938. Micropedology. Collegiate Press Inc., Ames, Iowa.

Kunze, R. J., G. Uehara, and K. Graham, 1968. Factors important in the calculation of hydraulic conductivity. Soil Sci. Soc. Amer. Proc. 32:760-765.

Lynn, W. C. and R. B. Grossman, 1970. Observations of certain soil fabrics with the scanning electron microscope. Soil Sci. Soc. Amer. Proc. 34: 645-648.

Marshall, T. J., 1958. A relation between permeability and size distribution of pores. Journal of Soil Sci., Vol. 9 (1):1-8.

Slager, S., 1966. Morphological studies of some cultivated soils. Agricultural Research Report 670 Pudoc Wageningen. The Netherlands.

Soil Survey Staff, 1951. Soil Survey Manual USDA Handbook 18, pp. 503.

Van der Plas, L., 1962. Preliminary note on the granulometric analysis of sedimentary rocks. Sedimentology 1, 145-157.

Van der Plas, L. and Slager, S., 1964. A method to study the distribution of biopores in soils. In Soil Micromorphology:411-419. Elsevier, Amsterdam.

Van der Plas, L., and A. C. Tobi, 1965. A chart for judging the reliability of point counting results. Am. Journ. Sci. 263:87-90.

5.2. RELATIONSHIPS BETWEEN SATURATED HYDRAULIC CONDUCTIVITY AND MORPHOMETRIC DATA OF AN ARGILLIC HORIZON [1]

Abstract

A method of calculating K_{sat} in pedal soil materials on the basis of morphometric data yielded reproducible results for seven soil peels sampled in the argillic horizon of a Batavia silt loam. Calculated values were reasonably close to those measured *in situ* with the double tube method. The method was also successfully applied to impregnated horizontal sections through soil cores. Dye studies demonstrated the validity of some of the underlying assumptions of the method, which predicts a strong relationship between core height and measured hydraulic conductivity in pedal soil materials. Experiments confirmed this relationship and a representative core size was defined for the studied horizon using the morphometric data.

Additional index words: double tube method, dye-tracing, pore interaction model.

5.2.1. Introduction

Relationships between soil morphology and saturated hydraulic conductivity (K_{sat}) are potentially useful tools for the soil surveyor in improving his ability of estimating soil permeabilities in the field. Estimates of K_{sat} may be quite general but still satisfactory when applied to relatively large soil areas such as mapping units (Klute, 1972; Nielsen, et al., 1972). Since water moves through the pores in the soil, morphometric techniques were developed to study sizes and patterns of soil voids in soil peels (Bouma and Hole, 1965; Bouma and Anderson, 1973).

Methods of calculating hydraulic conductivity (K) from moisture retention data have been widely used (Marshall, 1958; Green and Corey, 1971 and many others). The essential part in these methods is a pore-interaction model, that describes the dominant effect of small pores ("necks") on the conductivity of a three dimensional porous body having a wide variety of pore sizes. This concept was found to apply also to planar voids on soil peels of different horizons. K_{sat}, calculated with morphometric data using a newly developed planar-void pore-interaction model, agreed well with K_{sat} measured in situ with the double-tube method in four soil horizons (Bouma and Anderson, 1972). This paper examines the reproducibility of the K_{sat} calculations from morphometric data obtained from several peels of the same horizon.

Several techniques have been developed both for field and laboratory use to measure K_{sat} (Bouwer, 1962, Klute, 1965). Methods to measure K in situ are generally preferable to those using soil cores in the laboratory because field sampling of cores and associated transport may involve disturbance of the natural structure that could result in erroneous unrepresentative measurements. However, in situ methods may be quite elaborate and measurements on soil cores remain an efficient and therefore attractive procedure.

In this study measurements of K_{sat} on cores are compared with K_{sat}-computations from morphometric data, to investigate the often great variability among K_{sat} values derived from different cores in the same horizon. Part of that variability is due to the heterogeneous structure of the soil, and although it is generally agreed that core samples should be sufficiently large to be representative for the soil volume to be tested, the necessary volumes of such cores for different soil materials have never been clearly defined. Morphometric soil structure analysis, defining the size of the elementary structural units in the soil, can be used to illustrate differences in structure among soil horizons (Bouma and Anderson, 1973). The pore-interaction model used in that study predicted a relationship between core height and measured K which is further explored in this paper.

Studies are reported on the use of a dye to establish patterns of water movement in natural soil. The patterns, indicated by the dye, are used to interpret measurements and calculations of K_{sat} and also the relationship between the two.

5.2.2. Materials and Methods

The horizon under study is the B21t of a Batavia silt loam (Typic Argiudoll) at the Charmany University Experimental Farm in Madison, Wisconsin. Horizon boundaries were between 33 and 66 cm below the soil surface. Samples were taken downwards from the 40 cm level. The horizon description was as follows: Dark brown (7.5YR 3/3), brown to dark brown when broken and rubbed (7.5YR 4/3); silty clay loam; weak coarse prismatic parting into strong medium subangular blocky;

slightly firm; ped surfaces smooth, root channels abundant inside peds but not reaching the ped surface; ped cutans common; gradual and smooth upper (with A2) and lower (with B22) boundaries.

The number and sizes of channels were determined in horizontal sections of 625 cm^2 (25 x 25 cm) each throughout the profile (Bouma and Hole, 1965). Results for the B21t, averaged from three observations, are as follows: 3 channels larger than 4 mm; 14 channels with sizes between 2 and 4 mm and 11 channels between 1 and 2 mm.

K_{sat} was determined _in situ_ by the double tube method (Bouwer, 1962).

During the fall of 1971 and the spring of 1972, three 30 cm high columns (Bouma, _et al._, 1971) were carved out of the horizon at 40 cm depth and dye experiments performed in them to demonstrate patterns of liquid movement. The top of two of the columns was exposed and cleaned with a hole cleaner (Bouwer, 1962) to permit saturated flow. Rhodamine B dye was mixed with water in a ratio of 1:10 and was ponded on top of the column for a period of two days. Afterwards, three soil peels (Bouma and Hole, 1965) were sampled from each column at 7 cm intervals. A morphometric counting technique was then applied to each of these peels to calculate K_{sat} for the purpose of investigating the reproducibility of the counting technique. Color patterns in these peels were used to discuss differences between calculated and measured K_{sat} values.

The remaining column was prepared to demonstrate flow patterns associated with unsaturated flow induced by a gypsum crust (Bouma and Denning, 1972). Rhodamine B was again added to water infiltrating through the crust and soil peels were taken of the subcrust soil. The equation to calculate the K_{sat} is based on the physical relationship between the width of a planar void and its capacity to transmit liquid at a given gradient and includes a pore interaction model (Bouma and Anderson, 1973).

$$K_{sat} = \left[\sum_{i=n-x+1}^{i=n-x+s} \left(\frac{\rho g d_i^3}{12\eta} \right) \cdot \frac{\ell_i}{S} \right] + \left(\frac{\rho g d_{n-x+1}^3}{12\eta} \cdot \frac{\ell_t - (\ell_{n-x+1} + \ell_{n-x+2} + \cdots \ell_{n-x+s})}{S} \right) \quad (1)$$

where: ρ = density of water, g = gravitational constant, η = viscosity of water, d_i = average width of a planar void in size class i, ℓ_i = representative plane length for size class i: $\ell_i = L(\frac{p_i}{p_t})$ where L = total length of planar voids in an air-dry peel and p_i = number of planes in a certain size class i, i = 1, 2, 3... n and p_t = total number of planes counted in air-dry peels in the ribbon count procedure. Plane widths are counted in air-dry peels and are corrected for swelling by using COLE data (Grossman, et al., 1968). S = top surface area of peel. Size class n-x is the largest class to be closed by swelling. Class n-x+s is the largest class to have a sufficient probability of being continuous throughout the sample through planes of similar or larger size. It is assumed that flow occurs through all planes open after swelling. The second term of the equation gives the contribution to flow of all planes larger than n-x+s, which are assumed to lead into "necks" of size n-x+1, the smallest open size class.

Soil cores 10 cm high with a diameter of 7.5 cm were taken in the field in the fall of 1971 and the spring of 1972 to measure K_{sat} in the laboratory (Klute, 1965). Rhodamine B dye, mixed in a ratio of 1:1 with water, was run through the cores after the measurement to make visible the patterns of liquid movement inside the cores. The cores were then oven dried, completely impregnated with plastic (Buol and Fadness, 1961) and cut into 3 cm thick horizontal slices, the faces of which were polished. A counting technique similar to the one used for the soil-peels was employed and K_{sat} was calculated from the morphometric data.

To investigate the effect of different core heights on measured K_{sat} values, series of ten cores with a diameter of 7.5 cm but with heights of 5, 7.5, 10 and 17 cm were taken, and K_{sat} was measured in the laboratory (Klute, 1965). The first three sizes were sampled with metal rings using a core sampling device. The 17 cm cores were obtained with a hydraulic probe by cutting the proper length from the probe borings. This 17 cm sample was then placed inside a cylindrical metal container of such height as to allow both ends of the core to be free from obstruction. Then a viscous gypsum mixture (Bouma and Denning, 1972) was applied inside the container around the outside of the core encasing the sample. Good contact between the sample and the hardened gypsum avoided boundary flow during the K measurement.

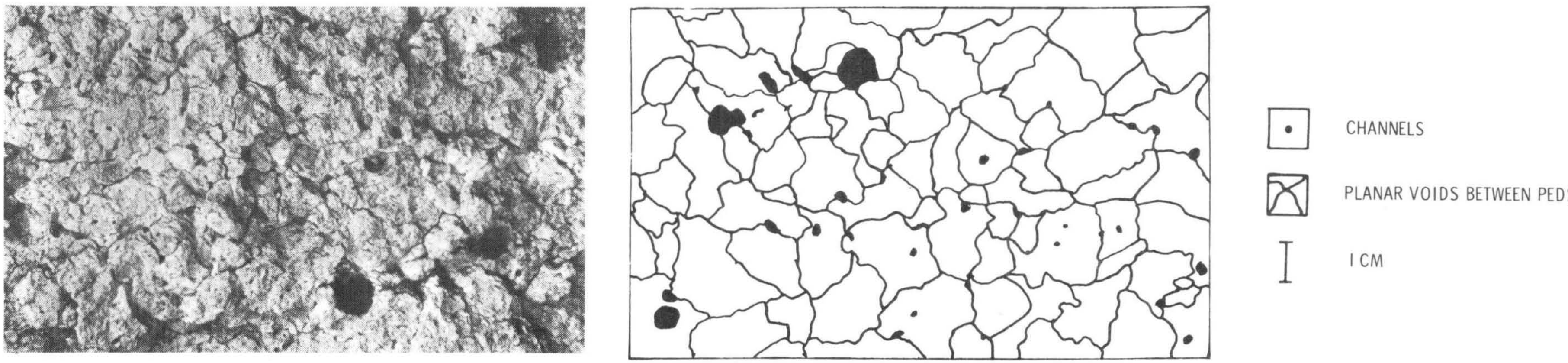

Figure 1. Representative picture of a soil peel surface sampled from a horizontal section through the B21t horizon in a Batavia silt loam.

5.2.3. Results and Discussion

5.2.3.1. Reproducibility of K-calculations with morphometric data

Results of K-calculations using morphometric data were reported earlier for four soil horizons from four different pedons, each horizon being represented by one soil peel (Bouma and Anderson, 1973). This paper describes results of the method as applied to seven soil peels sampled in one horizon in a Batavia silt loam pedon. A representative picture of a soil peel surface is in Fig. 1. Average ped height, as measured in a soil peel taken from a vertical cut through the horizon, was 2.0 cm.

The calculated K values for the seven soil peels were very close, even though there was some variation among peels in average ped size, total length of planar voids in the air-dry peel (L) and the total length of planar voids after swelling (ℓ_t) (Table 1). These results demonstrate the effect of the planar-void pore-interaction model, as applied in this calculation, which describes the dominant effect on permeability of the smaller pores in a heterogeneous pore system (Bouma and Anderson, 1972). The unrealistically high K_{sat} of 60,000 $\pm$ 3,000 cm/day would result if all open planes were used in the K-calculation (according to equation 2), including the larger ones exposed in a two-dimensional soil peel surface, thereby neglecting the "neck" effect introduced by underlying smaller planar voids.

$$K_{\text{all planes}} = \sum_{i=n-x+1}^{i=n} \left(\frac{\rho g d_i^{\,3}}{12\eta} \right) \cdot \frac{\ell_i}{S} \qquad (2)$$

Table 1. Results of K calculations using morphometric data from seven soil peels sampled in the B2t of a Batavia silt loam.

Soil Peel No.	Average Ped Size (cm)	COLE	L (cm)	l_t (cm)	Pore Size Class (μ)	l_i (cm)	K (cm/day) Per Size Class	K calc. Total	K Measured Double Tube
1	0.94	0.03	132	18.2	15 48 81	1.6+7.6 5.6 3.2	0.2 4.4 12.2	16.8	
2	1.05	0.03	105	17.6	15 48 81	2.4+8.2 3.6 3.4	0.3 2.9 12.6	15.8	27
3	1.02	0.03	105	20.1	24 57 90	3.7+9.4 4.3 2.7	1.1 5.4 13.8	20.3	50
4	0.96	0.03	116	18.1	9 42 75	2.1+7.6 4.7 3.7	0.5 2.5 19.1	21.1	43
5	0.72	0.03	121	24.0	15 48 81	1.9+13.7 5.4 3.0	0.5 4.2 11.3	16.0	57
6	0.79	0.03	168	59	28 61	7.8+43.7 7.5	9.0 11.9	20.9	
7	0.90	0.03	268	19	6 39	4.8+9.4 4.6	6.2 11.0	17.2	

Table 2. Results of K-calculations using morphometric data from thirteen polished sections through three soil cores sampled in the B2t of a Batavia silt loam. Asterisks in core B refer to polished faces in Fig. 2.

Distance of Face From Top of Core (cm)	Average Ped Size	COLE	L (cm)	l_t (cm)	$l_{col.}$	Pore Size Class (μ)	l_i (cm)	K (cm/day) Per Size Class	K calc. Total	K measured lab
CORE A										
3 cm	0.89	0.03	62	18.6	51	27 60 93	2.5+12.3 2.5 1.3	5.8 .6 16.8	23.2	
3.3 cm	0.89	0.03	67	22.0	48	27 60 93	2.7+15.4 2.2 1.7	6.8 7.4 20.0	34.2	15
7.5 cm	0.89	0.03	74	11.9	12	27 60 93	3.2+4.1 3.0 1.6	2.3 1.0 20.8	24.1	
7.8 cm	0.89	0.03	72	16.5	7	27 60 93	2.9+9.4 2.7 1.5	5.1 9.2 18.5	32.8	
CORE B										
3.5 cm*	0.9	0.03	51	8.2	46	27 60 93	1.2+5.1 1.3 .65	2.1 4.4 12.3	18.8	
3.8 cm	0.9	0.03	58	9.3	48	27 60 93	1.5+5.9 1.2 0.7	2.9 4.2 8.7	15.8	
6.5 cm*	0.9	0.03	67	11.4	23	27 60 93	6.7 1.7 1.0	3.0 5.0 12.2	20.2	16
6.8 cm*	0.9	0.03	56	7.3	15	27 60 93	1.4+3.3 1.4 1.2	2.2 4.8 15.6	22.6	
7.2 cm	0.9	0.03	56	12.9	13	27 60 93	1.4+9.2 1.4 0.9	3.9 5.0 11.6	19.5	
CORE C										
3.3 cm	0.9	0.03	56	17.9	43	27 60 93	2.3+12.1 2.4 2.1	5.9 8.2 13.9	28.0	
3.6 cm	0.9	0.03	52	16.0	41	27 60 93	2.1+10.5 2.9 1.5	4.9 6.7 19.7	31.3	
7.3 cm	0.9	0.03	54	9.2	15	27 60 93	2.2+5.1 1.8 1.1	2.7 6.4 13.9	23.0	75
7.6 cm	0.9	0.03	52	11.4	18	27 60 93	2.6+6.1 1.9 0.80	3.4 6.7 10.0	20.1	

The K-values calculated with the pore-interaction model were lower, though of the same order of magnitude, than the double-tube values measured in situ (Table 1). This could be due to flow through tubular or elongated pores other than planar voids, that may interconnect planes in the soil, thereby bypassing planar "necks". The dye studies made in excavated columns in the field, confirmed flow through some channels to a depth of 14 cm below the infiltrating surface, as evidenced by staining of channel walls. However, many channels were found to be uncolored at the same depth, indicating that these channels did not contribute to flow, presumably because they were not connected with voids containing tension-free water. For the same reason all channels were left uncolored under conditions of unsaturated flow into a column capped with a gypsum crust, that created a subcrust tension of 20 mbars. In any case, larger channels, though colored, were never completely filled with water and continuous through the sample. This follows from calculations of K_{sat} based solely on the occurrence of channels (according to equation (7) in Bouma and Anderson, 1973), using morphological counts made in the field of channels exposed on horizontal sections in the pedon, and assuming that all channels are filled and conduct water. These calculated K_{sat} values were unrealistically high (K_{sat} = 32,000 $\pm$ 5000 cm/day). In conclusion, the figures in Table 1 show that the morphometric method of calculating K_{sat}, including a planar-void pore interaction model, yields reproducible results in this horizon that are of the same order of magnitude as values measured in situ with the double tube method.

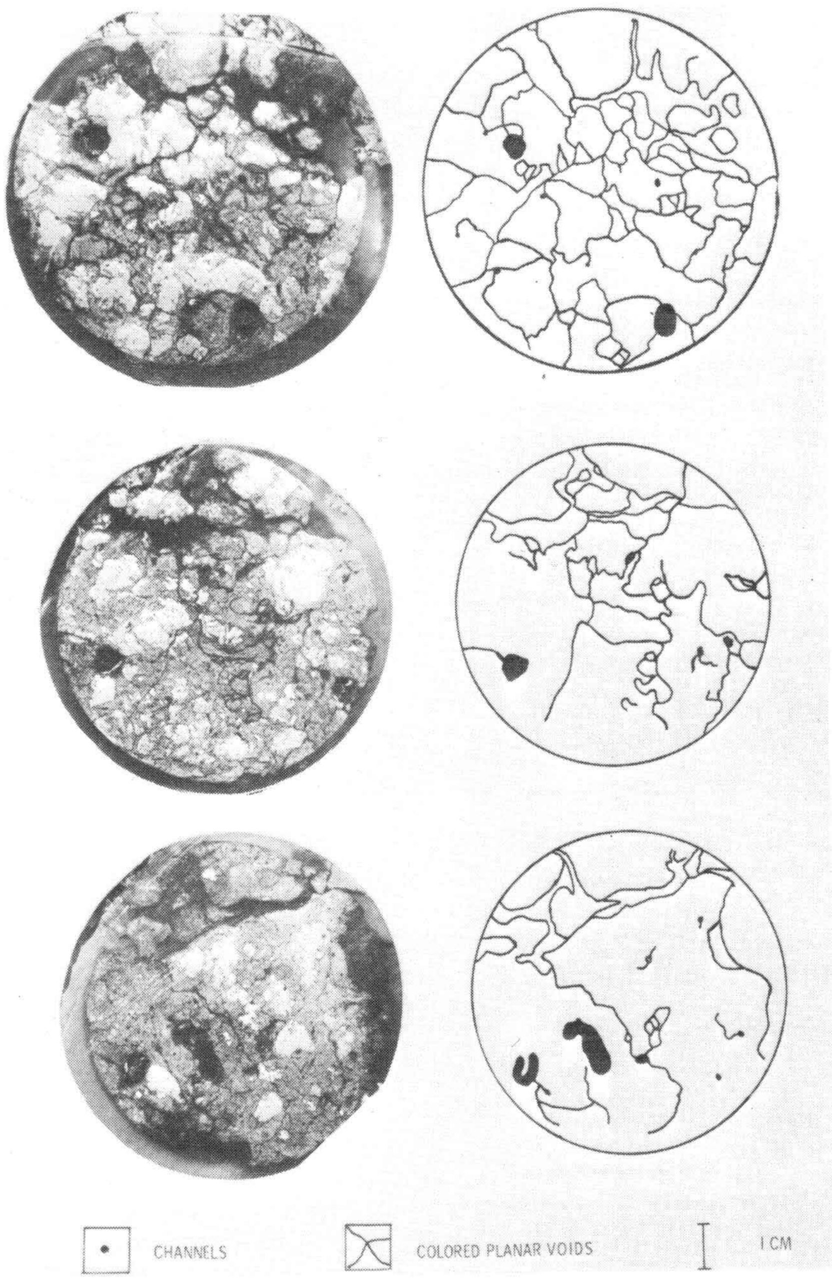

Figure 2. Pictures of impregnated horizontal sections through soil cores with drawings showing the decrease in length of colored planar voids with depth. The sections were 3.5 cm (upper), 6.5 cm (middle) and 6.8 cm (lower) below the top of the core (see asterisks in Table 2). Note the many uncolored planar voids in the sections.

5.2.3.2.

Calculation of K-sat from morphometric soil core data

K_{sat} was calculated from morphometric measurements for thirteen faces, of three different cores (Table 2). Each face had a surface area of 45.4 cm^2. Fig. 2 (left part) shows three faces obtained at increasing distances from the top in core B. Sizes of all planar voids, as measured on these faces, were used for the K-calculation. The calculated K_{sat} values were close to those measured experimentally in two cores and of the same order of magnitude in the third. Each face yielded an estimate of K_{sat} for the complete core after use of the planar-void pore-interaction model in the calculations because each face was sufficiently large to represent the fine pedal structure in this horizon. The large number of about 50 peds were present per face in each core. However, soil structures with larger peds, such as occur in some B3 or C horizons, would require much larger face areas to be representative. For such horizons, counts made on relatively small faces of 45 cm^2 would be inadequate for calculating K_{sat} for the horizon as a whole.

Dye studies were made to trace patterns of water movement during the measurement of K_{sat}. Use of dyes offers many problems since coloring substances may be absorbed by the soil during percolation, thereby losing their function as tracers (Reynolds, 1966; Corey, 1968). However, in these experiments conductivities were measured in the relatively small cores before and after application of the dye solution, showing that rates were only insignificantly lower afterwards and that the solution leaving the core had an unchanged very red color. The assumption is made, therefore, that only voids with colored walls, as observed in the polished faces and represented in the drawings of Fig. 2, conducted liquid. The total length of colored planar voids was measured in each polished face (ℓ_{col} in Table 2). According to the assumption made in the calculation procedure that flow follows all open pores, this length of colored planes should be similar to the calculated ℓ_t values, which represent the total length of all open pores after swelling. Agreement was good for the lower slices in the cores, considering the much larger total length of all planes (L). The length of the colored planes in the top slices of the cores was much higher than the corresponding ℓ_t values. Liquid apparently moves into planes here that are supposedly closed after swelling. This phenomenon can be explained by considering that faces of adjacent subangular blocky peds will not completely seal off interpedal planar voids upon swelling due to their curved and not strict planar morphology (see Fig. 1). Even though subangular blocky structure is present throughout the samples, effects of partial sealing apparently become insignificant within a few centimeters depth, where conditions prevail corresponding to those of the model.

In conclusion, these data demonstrate that only a few pores, contributing an insignificant small fraction to the total pore volume, determine K_{sat} of the entire core.

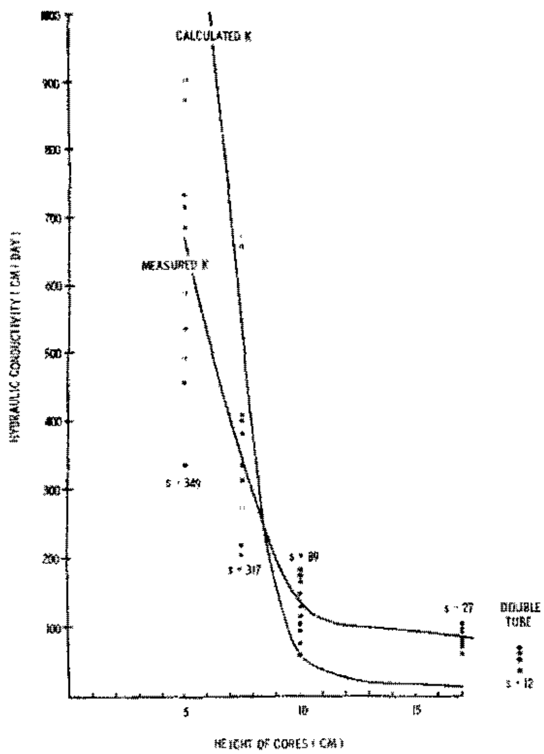

Figure 3. Measured and calculated hydraulic conductivities and standard deviations (s) for series of cores with different heights. K values measured with the double-tube method are included as a reference.

5.2.3.3.

Relationships between dimensions of soil cores and measured K-sat

Although it is generally realized that soil cores should be sufficiently large to represent the soil material to be characterized, minimum lengths of cores from different soil materials have never been defined. The dominant effect of smaller pores on the hydraulic conductivity of a soil material has important implications for this problem. The probability of a small plane forming a "planar neck" in the flow system increases as a core becomes longer and the probability of a large plane being continuous decreases. This was expressed in the pore-interaction-model where probabilities were calculated for certain sizes of planes to be continuous throughout a sample (Bouma and Anderson, 1973). This can for example be illustrated for the second largest plane-size open after swelling, with $\ell_i = \ell_{n-x+2}$. Considering the contact between the first and the second layer of peds, the probability (P) of a plane of class (n-x+2) to be connected with a plane similar or larger than itself is proportional to the ℓ_i values involved:

$$P = \frac{(\ell_t - \ell_{n-x+1})}{\ell_t}$$

where ℓ_t is the total length of open planes after swelling and where ℓ_{n-x+1} is the length of the smallest plane-size-class open after swelling. The probability P of a plane of size class (n-x+2) to be connected throughout a sample with height H by planes either of its own size or larger can be expressed as:

$$P = \left[(\ell_t - \ell_{n-x+1})/\ell_t\right]^{(H/v)-1} \qquad (3)$$

where v = average ped height to be measured on soil peels taken from vertical sections through the horizon. Equation (3) indicates the effect of sample height because P will strongly decrease with increasing H, all other factors being constant. This implies that larger pores tend to become discontinuous throughout higher cores, which would result in a considerable drop in the hydraulic conductivity. Equation (1) was used to calculate K_{sat} values for cores of the studied horizon that were 5, 7.5, 10 and 17 cm high, all with a diameter of 7.5 cm. Calculated K values were 2000, 500, 60 and 4 cm/day respectively (Fig. 3). The experimentally measured K values showed similar trends, although somewhat less extreme. Soil structure is considered as a constant in these experiments, whether a core is 5 centimeters or 17 centimeters high. The subangular blocky peds increase somewhat in size with depth but this increase is sufficiently small from 40 to 57 centimeters depth in the horizon to be neglected. Standard deviations, indicated in Fig. 3 for each set of measurements, decreased strongly as sample height increased. The 17 cm high samples were closest to the values measured *in situ* with the double tube which is considered as the reference level, although the real reference would be a core with the height of the horizon to be tested. The data indicate that in this horizon, which is representative for pedal horizons in silty soils, K_{sat} values measured in cores are an inverse function of the height of the core. Cores from this horizon to be used for K_{sat} measurements should be at least 17 cm high to be representative.

Acknowledgement

The authors are indebted to C. R. Amerman for valuable suggestions.

5.2.4. Literature Cited

Bouma, J. and F. D. Hole, 1965. Soil peels and a method for estimating biopore size distribution in soil. Soil Sci. Soc. Amer. Proc. 29:483-485.

Bouma, J., D. I. Hillel, F. D. Hole and C. R. Amerman, 1971. Field measurement of unsaturated hydraulic conductivity by infiltration through artificial crusts. Soil Sci. Soc. Amer. Proc. 35:362-364.

Bouma, J. and J. L. Denning, 1972. Field measurement of unsaturated hydraulic conductivity by infiltration through gypsum crusts. Soil Sci. Soc. Amer. Proc., 36:846-848.

Bouma, J. and J. L. Anderson, 1973. Relationships between soil structure characteristics and hydraulic conductivity. Proceedings of the symposium on the field moisture regime. New York. 1971 (in press).

Bouwer, H., 1962. Field determination of hydraulic conductivity above a water table with the double-tube method. Soil Sci. Soc. Amer. Proc. 26:330-335.

Buol, S. W. and D. M. Fadness, 1961. A new method of impregnating fragile materials for thin sectioning. Soil Sci. Soc. Amer. Proc. 25, 253.

Corey, J. C., 1968. Evaluation of dyes for tracing water movement in acid soils. Soil Sci. 106:181-187.

Green, R. E. and J. C. Corey, 1971. Calculation of hydraulic conductivity: A further evaluation of some predictive methods. Soil Sci. Soc. Amer. Proc. 35:3-8.

Grossman, R. B., B. R. Brasher, D. P. Franzmeier and J. L. Walker, 1968. Linear extensibility as calculated from natural-clod bulk density measurements. Soil Sci. Soc. Amer. Proc. 32:570-573.

Klute, A., 1965. Laboratory measurement of hydraulic conductivity of saturated soil. Amer. Soc. Agron. Mono. 9:210-221.

Klute, A., 1972. The determination of the hydraulic conductivity and diffusivity of unsaturated soils. Soil Sci. 113:264-277.

Marshall, T. J., 1958. A relation between permeability and size distribution of pores. J. Soil Sci. 9:1-8.

Nielson, D. R., J. W. Biggar, and J. C. Corey, 1972. Application of flow theory to field situations. Soil Sci. 113:254-264.

Reynolds, E. R. C., 1966. The percolation of rainwater through soil demonstrated by fluorescent dyes. J. Soil Sci. 17:127-132.

5.3. A comparison of hydraulic conductivities calculated with morphometric and physical methods

Abstract

Hydraulic conductivity of coarse porous media with packing pores could be calculated not only with accepted physical, but also with morphometric techniques if matching factors were used. Morphometric K curves were closest to physical curves derived from moisture adsorption characteristics. The morphometric technique can be applied exclusively to small or fragile homogeneous soil materials that cannot be sampled for moisture retention determinations in the laboratory. The pore interaction model of Marshall overestimated K_{sat} when measured r-values were used. Moisture retention curves, calculated with morphometric data, agreed well in coarse porous media with physical adsorption curves.

Additional Index Words: moisture retention, adsorption, desorption.

5.3.1. INTRODUCTION

Calculation methods to derive hydraulic conductivity (K) from moisture retention data are increasingly used because of their attractive simplicity, as compared with elaborate direct K-measurements (see review by Klute, 1972). Good results have been obtained by the methods of Marshall (1958) and Millington and Quirk (1961, 1964) if matching factors are used (Green and Corey, 1971; Jackson, 1972 and Bruce, 1972). These methods use a pore-interaction model to express the dominant effect of smaller pores ("necks") on the overall permeability of a three-dimensional soil sample with pores of many sizes (Marshall, 1958).

Total porosity is divided into n small classes, each class being represented by a pore size $r_n (r_1 > r_2 > r_3 > . . . r_n)$. The radius of the circular "neck" area r_t, considering all pores, is then defined by:

$$r_t = \frac{e}{n^2} \; (r_1^{\;2} + 3r_2^{\;2} + 5r_3^{\;2} + \ldots (2n-1)r_n^{\;2} \qquad (1)$$

where: e = porosity. This "neck" model also applies to unsaturated soil where larger pores are filled with air. Then, larger size classes are omitted and, for example, the following equation would apply for the "neck" if size class r_1 is filled with air:

$$r_{t-1} = \frac{e'}{(n-1)^2} \; (r_2^{\;2} + 3r_3^{\;2} + 5r_4^{\;2} + \ldots (2n-3)r_n^{\;2} \qquad (2)$$

where: e' = total porosity minus the porosity contributed by size r, and (n-1) is the total number of pore classes considered. Conductivities are calculated, using the dimensions of the thus defined "necks," by substitution in Poisseuille's equation that relates the flow rate in tubular pores to their diameter at a given hydraulic gradient (Marshall, 1958). The resulting equation relates K to pore sizes as follows:

$$k(\theta)_i = (\frac{K_s}{K_{sc}}) \cdot \frac{e^P}{8n^2} \times \sum_{j=1}^{m} (2j + 1 - 2i)r_j^2 \qquad (3)$$

$$i = 1, 2, \ldots m$$

(Equation 3 is similar to equation 5 of Marshall (1958) but is given in the notation of Green and Corey (1971) and includes a matching factor (K_s/K_{sc}) which is the ratio between the measured and the calculated K_{sat}).

$k(\theta)_i$ is the calculated k (intrinsic permeability in cm^2) for a specified water content θ_v. (Numerically hydraulic conductivity K = 1 cm/day ≈ $k_i = 10^{-10} cm^2$), e and n were defined previously; p = coefficient varying in different calculation procedures between 0 and 2 (Marshall, 1958; p = 2); m = number of pore-size classes (each of which of the same size as an n-class) for which r values are available. Pore size distributions can be estimated from moisture retention data, if a directly measured pore size distribution is not available. Bouma and Anderson (1973) applied equation (3) directly to results of point counts made in thin sections of basic fabrics of soil materials and reported fair agreement for some samples between K curves calculated with morphometric data and those calculated with moisture retention characteristics obtained by desorption. Agreement between these curves and experimentally determined curves was reasonable for some samples. This finding could have a practical application for calculating K values of small samples, such as crusts or thin layers in sediments, that are too small or fragile for individual sampling and moisture retention determinations to be followed by K-calculations. Thin sections can be made of such samples, however, and point-count procedures can be applied to obtain a pore size distribution which, in turn, can then be used to calculate the K-curve. A K_{sat} value can usually be measured in situ for curve matching purposes even in small samples.

The purpose of this study was to: (i) further investigate the potential of the morphometric method by comparing results with those obtained by accepted physical methods. Moisture retention data in this study were derived by desorption and adsorption processes. Morphometric data was also used to calculate moisture retention curves. (ii) test the validity of the pore interaction model, which is based on r values, by comparing calculated K_{sat} values using morphometric data, and measured K_{sat} values. The methods were applied to a sand and three homogeneous gypsum-sand mixtures, the latter used in the crust test procedure for measuring hydraulic conductivity in situ between saturation and a moisture tension of approximately 100 cm water (Bouma et al., 1971, 1972).

5.3.2. Materials and Methods

Four porous media were investigated in this study. The sand was obtained from the coarse-sandy C horizon of the Plainfield loamy sand. Dry mixing with various quantities of gypsum-powder was followed by wetting and stirring of the mixture to a viscous paste as described by Bouma and Denning (1972). Hardening of the paste was allowed for a period of at least 48 hours. Quantities of gypsum in the mixture are expressed as a percentage of total volume in the dry mixture. Moisture desorption and adsorption characteristics were obtained with standard procedures (Richards, 1965).

A microscopic point-count technique was applied to obtain estimates of total volumes and size distributions of visible pores in a thin section (Chayes, 1956, Anderson and Binnie, 1961). One thousand two hundred points were counted per section in 240 fields with each 5 points at a linear magnification of 80x. Resulting percentages are to be read as $\pm$ 2% (95% probability). To obtain optimal counting efficiency, distances between adjacent points in the counting ocular were made larger than the largest dimensions of simple packing voids as present in thin sections of the basic fabrics (Van der Plas, and Toby, 1965). The size of a counted pore, below one of the points in the ocular, was determined by measuring the smallest possible intergranular distance in the pore through the point, because shortest dimensions in pore systems, their "necks", are most significant in determining resistance to watermovement.

Calculations of K were made with the method of Marshall (1958) as applied to both the morphological and physical data (Bouma and Anderson, 1973). K values of the samples were determined in the laboratory with the crust test using long cylinders of the different materials capped with gypsum crusts of increasing resistance (Bouma and Denning, 1972). The obtained K versus P curves were translated into K versus θ curves by using adsorption data obtained with physical techniques, (Fig. 3). Morphometric point-count data was also used to calculate moisture retention curves by relating measured r values, and their relative volumes determined by point count, to corresponding h values by: $h = \frac{2\sigma}{r}$, where h = soil moisture pressure (dyne cm^{-2}) σ = surface tension of water (dyne cm^{-1}).

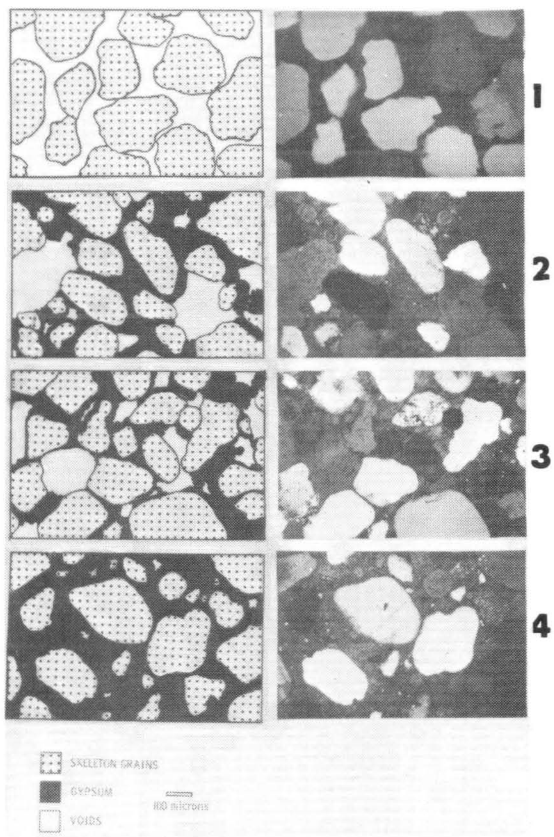

Figure 1. Pictures and corresponding drawings of four thin sections of porous media used in this study to calculate K from morphometric and physical data. Sample 1 is a sand; Sample 2 is a 12%; Sample 3 is a 20% and Sample 4 a 50% gypsum-sand mixture.

5.3.3. Results and Discussion

Pictures of thin sections of the four studied porous media are presented in Fig. 1. The results of the morphometric point counts are in Fig. 2. Adsorption and desorption curves for the four porous media are presented in Fig. 3. Total porosities determined with the point count were somewhat lower than those calculated with physical methods using bulk densities and particle densities (Fig. 3). This difference was most pronounced at higher contents of gypsum because only larger pores can be observed microscopically in a thin section with a thickness of approximately 20 microns, whereas small packing pores as occurring between small gypsum particles are invisible in transmitted light (Bouma and Anderson, 1973). Results of K calculations and K measurements are presented in Fig. 4. The calculated curves for the sand (sample 1) were close together and close to the measured curve. The curve calculated with the physical method using adsorption data was closer to the morphometric curve than the one calculated with desorption data. This was found to be true in all samples studied. The desorption process leaves relatively large pores filled with water at tensions where these pores would be air-filled if an adsorption process were used (Fig. 3). This phenomenon is known as "hysteresis". For example, at a tension of 20 mbar the sand has 35 vol% moisture after a desorption process and 27 vol% after adsorption; implying that more relatively large pores are filled with water after desorption. The physical calculation method is based on exclusion of water-filled pores upon increasing tension and different K curves result, therefore, if both types of data are used (Fig. 4).

Agreement between the curves calculated with morphometric and adsorption data was excellent for the 12% gypsum-sand sample (Sample 2) and fair for the 20% mixture (Sample 3). Measured K curves were closest to the curves

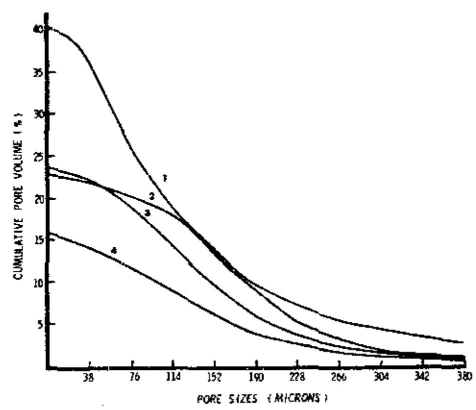

Figure 2. Results of morphometric point-counts made on thin sections of four porous media, expressed as the cumulative porosity as a function of pore size. The numbers of the curves correspond to those of the porous media in Figure 1.

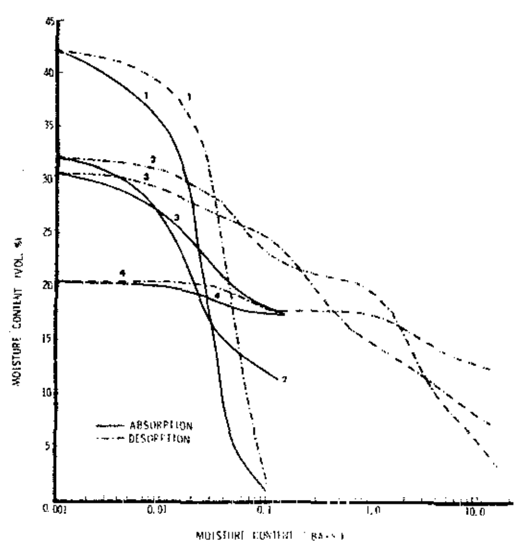

Figure 3. Moisture retention characteristics of four porous media, defined by adsorption and desorption processes.

calculated with morphometric data. The 50% gypsum-sand mixture (Sample 4) had only a few relatively large pores inside a fine-grained matrix that governs the hydraulic behavior of the whole sample (Fig. 1). The morphometric method overemphasizes the function of these larger pores and agreement with the physical curves was poor. Application of the morphometric technique should therefore be restricted to porous media with packing pores as illustrated in Fig. 1 for Samples 1, 2 and 3 with K_{sat} values exceeding 1 cm/day. Many crust materials and thin layers in stratified sediments have such properties

Both physical and morphometric procedures needed very large matching factors (Table 1) indicating that calculated K_{sat} values were much higher than the measured ones. The pore-interaction model of Marshall (1958) was derived using r values and the unrealistically high K values, obtained in this paper with directly measured r values, seem to indicate that this pore interaction model is inaccurate as it apparently overemphasizes the larger pores. However, the slope of the K versus θ_v curve is predicted quite accurately for coarse porous soil materials with packing pores, and use of a matching factor can thus result in satisfactory calculation results.

The calculated moisture retention curves are presented in figure 5. Agreement between the morphometric curves and those physically determined by adsorption is only good for samples 1 and 2, while desorption curves are significantly different for samples 2 and 3. Differences are due to hysteresis phenomena, as discussed in the context of K-calculations. Good agreement in samples 1 and 2 shows that the relationship between pore size and moisture tension as used, which is based on a capillary model, is realistic for sands with only a few or no fine particles. However, the model proves to be unrealistic as the content of fines (soil plasma) increases.

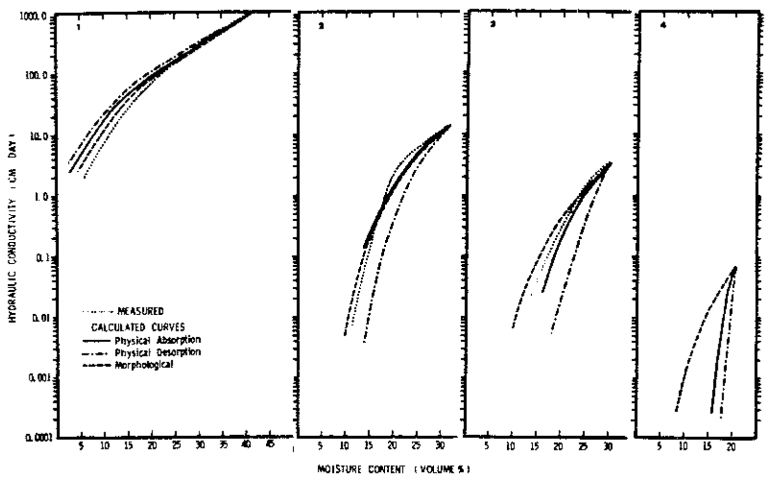

Figure 4. Hydraulic conductivity (K) calculated with morphometric and physical methods for four porous media and measured K curves for three porous media.

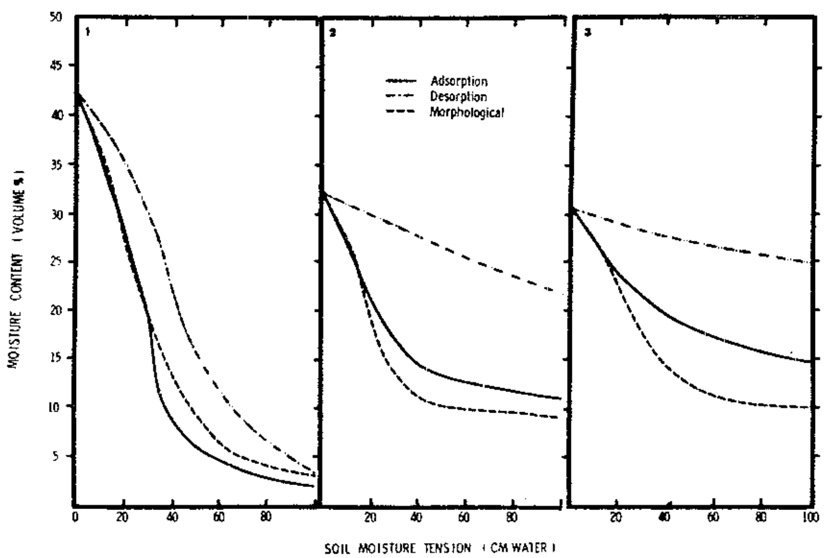

Figure 5. Moisture retention curves for three porous media calculated with morphometric data and measured with physical desorption and adsorption techniques.

Table 1. Matching factors ($K_{sat-measured}/K_{sat-calculated}$) for calculations of K with morphometric and physical techniques applied to four porous media.

Porous medium	Morphometric	Physical (absorption)	Physical (desorption)
sand	0.33	0.095	0.30
sand - 12% gypsum	0.004	0.045	0.133
sand - 20% gypsum	0.0002	0.011	0.027
sand - 50% gypsum	0.0001	0.0013	0.009

5.3.4. Literature Cited

Bouma, J., D. I. Hillel, F. D. Hole, and C. R. Amerman. 1971. Field Measurement of Unsaturated Hydraulic Conductivity by Infiltration Through Artificial Crusts. Soil Sci. Soc. Amer. Proc. 35:362-364.

Bouma, J., W. A. Ziebell, W. G. Walker, P. G. Olcott, E. McCoy, and F. D. Hole. 1972. Soil absorption of septic tank effluent. A field study of some major soils in Wisconsin. University of Wisconsin-Extension, Geol. and Nat. Hist. Surv., Information Circular No. 20.

Bouma, J. and J. L. Denning. 1972. Field Measurement of Unsaturated Hydraulic Conductivity by Infiltration Through Gypsum Crusts. Soil Sci. Soc. Amer. Proc. 36:846-847.

Bouma, J. and J. L. Anderson. 1973. Relationships between soil structure characteristics and hydraulic conductivity. Proceedings of Symposium on the Field Moisture Regime. New York. 1971. ASA Special Publication (In press).

Bruce, R. R. 1972. Hydraulic Conductivity Evaluation of the Soil Profile from Soil Water Retention Relationships. Soil Sci. Soc. Amer. Proc. 36:555-561.

Green, R. E. and J. C. Corey. 1971. Calculation of Hydraulic Conductivity: A Further Evaluation of Some Predictive Methods. Soil Sci. Soc. Amer. Proc. 35:3-8.

Jackson, R. D. 1972. On the Calculation of Hydraulic Conductivity. Soil Sci. Soc. Amer. Proc. 36:380-382.

Anderson, D. M. and R. R. Binnie, 1961. Modal analysis of soils. Soil Sci. Soc. Amer. Proc. 25:499-503.

Chayes, F., 1956. Petrographic Modal Analysis (John Wiley and Sons, New York).

Klute, A. 1972. The determination of the hydraulic conductivity and diffusivity of unsaturated soils. Soil Sci. 113:264-275.

Marshall, T. J. 1958. A Relation Between Permeability and Size Distribution of Pores. Soil Sci. 9:1-8.

Millington, R. J., and J. P. Quirk. 1961. Permeability of porous solids. Trans. Faraday Soc. 57:1200-1206.

Millington, R. J. and J. P. Quirk. 1964. Formation factor and permeability equations. Nature. 202:143-145.

Richards, L. A. 1965. Physical condition of water in soil. In <u>Methods of Soil Analysis</u>. Amer. Soc. Agron. Monograph 9:128-152.

Van der Plas, L., and A. C. Tobi, 1965. A chart for judging the reliability of point counting results. Am. Journ. Sci. 263:87-90.

5.4. CONCLUSIONS

1. The purpose of using morphometric techniques should not be to reproduce results that can more easily be obtained by physical methods, but to use specific advantages inherent to such techniques, such as distinction and measurement of different types of pores. Planar voids and channels, though contributing only small fractions to total pore volume, strongly affect the conductivity of soil materials. Morphometry can be used to construct simple but relevant models of soil structure with planar-voids, channels or packing voids, from which K may be estimated using basic physical equations relating pore size to conductivity. In a pore system with varying sizes, conductivity is governed by the smallest pores in the system. Hypothetical models are therefore necessary to predict pore continuity in soil materials from pore measurements that are necessarily made in two-dimensional sections. A continuity model for interpedal planar voids was introduced.

2. A recent method to calculate K_{sat} in pedal soil materials using morphometric data yielded reproducible results for soil peels and soil cores sampled in one argillic horizon. Calculated values were reasonably close to those measured experimentally. These results indicate that morphometric soil structure characteristics can be used to predict K_{sat} of pedal soil materials. Qualitative descriptions of soil structure, noting sizes and shapes of peds and their degree of development have been a part of the standard profile description in soil survey practices for many years. Interpretations of these data and correlations with physical properties of the soil are rather difficult to make because of the general nature of these data. More quantitative and reproducible approaches, as for example the one discussed in this paper, yield data that may be more useful for predicting soil physical behaviour.

3. The planar-void-pore-interaction model of flow as introduced by the calculation method predicts a pronounced relationship between core height and measured K_{sat} in pedal soil materials. This was confirmed by experiments. These results suggest that morphological soil structure data should play an important role in defining representative sizes of soil samples to be used for physical determinations in different soil materials.

4. Hydraulic conductivity of homogeneous coarse porous media with packing pores can be calculated with both physical and morphometric techniques if matching factors are used. Morphometric K-curves and moisture retention curves calculated with morphometric data are closest to physical curves derived from moisture adsorption characteristics.

5. The pore-interaction model of Marshall overemphasizes the hydraulic function of large packing pores in sandy soil materials.

6. The concept of soil structure should apply not only to aggregated, but also to unaggregated soil materials because they have characteristic basic structures that strongly affect their hydraulic behaviour.

7. Morphological study of soil materials, with the purpose of relating soil structure to hydraulic conductivity, involves observation of basic, matric, secondary and tertiary soil structures in sufficient detail to obtain an informative, yet readable and reproducible description. Relationships between this type of data and hydraulic conductivity characteristics, as explored in this paper, can be used to improve field estimates of K.

6. USE OF PHYSICAL METHODS TO EXPAND SOIL SURVEY INTERPRETATIONS OF SOIL DRAINAGE CONDITIONS

As use of soil maps for planning purposes increases, questions become more specific concerning the physical behavior of the different units of soil depicted on the maps. One of the more important physical properties of a soil is its capacity to retain and transmit water, which is reflected by the water content at a given time. Soil drainage classes, as defined in the Soil Survey Manual (1951), are used in the Soil Survey program to classify natural soil pedons on the basis of dynamic hydrological properties. Reliance in this procedure is placed mainly on empirical judgements and observed soil-morphological features. This method has proven its value as a broad qualitative indicator.

The new taxonomic soil classification system (Soil Survey Staff, 1970) defines soil moisture regimes on the basis of frequent _in situ_ measurements of the changes in soil moisture content in the course of a year.

Predictions of soil behavior are difficult to make solely on the basis of these two kinds of data namely, those derived from morphological observations and those from _in situ_ moisture measurements made, by necessity, over a limited period of time. This is particularly true when environmental conditions deviate periodically from the average or when they change permanently. Soil physical techniques describing flow of water in soil materials under specified conditions are increasingly available in recent years. The purpose of this exploratory paper, therefore, is: 1. To review some of the concepts underlying the distinction of different soil drainage regimes in soil survey practices; 2. To explore the feasibility of using soil physical characteristics and methods to quantify these concepts; and 3. To demonstrate the potential of some recently developed relatively simple approximate physical methods for predicting hydrological behavior of soils under simplified conditions.

6.1. The soil survey concept of soil drainage

Soil drainage (Soil Survey Manual, 1951) is defined as a function of the natural hydrologic regime through time. It refers to the rapidity and extent of the removal of water from the soil in relation to additions. This relation determines when the soil is dry or completely saturated and poorly aerated. The frequency and duration of periods of saturation form the basic criteria for distinguishing seven drainage classes, ranging from very poorly drained to excessively drained. In the course of mapping, a soil surveyor is usually able to make only a few direct observations of individual pedons in a landscape, but the drainage classification that he assigns to the polypedons purports to describe their hydrodynamics throughout four seasons. Therefore, he needs as many indicators as possible from which to make inferences. The indicators listed in the Manual, include: climatic data, soil color patterns, nature of organic surface layers, soil slope, and texture and structure of the horizons that will affect the permeability of the soil. However, relationships between such indicators and the very complex hydrodynamics of the soil tend to be speculative, and so are the resulting estimates of runoff, soil permeability and internal soil drainage. For example, although morphological soil structure data can be used to calculate hydraulic characteristics of some soil horizons, the description of soil structure as defined in the Soil Survey Manual does not provide an adequate basis for such calculations (Bouma and Anderson, 1973). Soil color patterns, such as iron oxide mottling, may indicate periodic water saturation but redox processes may have different effects in different soils as will be illustrated later in this paper for the Almena silt loam and the Hibbing silt loam. Estimates of drainage conditions based on descriptions of structure and mottling are therefore bound to be somewhat speculative. More basically, pedogenic soil features and the entire pedons and polypedons themselves are seen as records of past environments, viz., as products of specific combinations of soil forming factors and processes functioning over many years (Marbut, 1935). In turn, the nature of some of these processes can be inferred from observing such features in the soil and if these processes are not expected to change with time, future soil behavior can be predicted. But soil survey results are intended for making predictions of future behavior of the soil which will be very difficult to make if the former combination of processes of soil formation change as it will, for example when a "well drained" soil is used as a porous medium for liquid waste disposal (Bouma, 1971c).

Changing soil-use patterns tend to be the rule rather than the exception in our urbanizing society. So in addition to using a classification of soil drainage, which is mainly based on evidences of processes that occurred in the past, or on in situ measurements made over a limited period of time, the investigator needs procedures that will provide data adequate for predicting soil behavior more precisely as a function of a wide range of man-induced as well as of natural environmental conditions.

Current activity in the study of moisture regimes in soil above the ground water, as discussed here, relates to recent attention to fluctuations in the water table itself. For many years, observations of soil mottling and gleying have been used to estimate fluctuating ground-water levels. This was found to yield somewhat inconsistent results (Schelling, 1960; van Heesen, 1970; Simonson and Boersma, 1972). More emphasis was therefore placed on direct measurement of ground-water levels in wells, and the use of the data in defining ground-water regimes (van Heesen, 1970). More recently, models have been developed using physical and statistical techniques for predicting ground-water fluctuations as a function of environmental conditions (Boersma, et al., 1972). This paper explores a similar approach to the moisture regimes of soil above the ground water. The soil survey concept of soil drainage in terms of permeability (which is more or less characteristic for a soil) and internal drainage (which is governed by environmental factors) is similar, in principle, to the soil physical concept in which characteristic constants (hydraulic conductivity and moisture retention) are used in mathematical or numerical procedures to calculate moisture conditions at any time as a function of selected boundary conditions. Discussions of the relevant soil physical concepts are available in the literature (see Childs, 1969; Hillel, 1971). A brief review, relating these concepts to those used in the soil survey program, follows.

6.2. Soil permeability

Soil permeability (Soil Survey Manual, 1951, p. 167) is defined as "that quality of the soil that enables it to transmit water or air". Darcy's law states that the amount of flow in a saturated soil is proportionate to the gradient of the soil water potential in that soil. The proportionality factor K is generally designated as the hydraulic conductivity (ℓ/t) which is a characteristic value for a soil material. Percolation and infiltration rates are more variable and not characteristic, because they may result from varying potential gradients (Bouma, et al., 1972). More importantly, liquid above the ground-water table commonly occurs in soil whose pore volume is only partially filled with water. In this case, water movement still occurs, though at a much slower rate. Darcy's law also applies to unsaturated flow (Richards, 1931).

Soil moisture tension increases as the moisture content decreases. Since larger pores drain first with increasing tension, the hydraulic conductivity drops sharply. This is because the flow of liquid through a (tubular) pore is proportionate to its radius to the fourth power. In summary, a soil material is not characterized by one specific "permeability", but by an infinite number of hydraulic conductivities (a K-curve) corresponding with as many moisture contents ranging downwards from saturation. Hydraulic conductivity curves are specific for a soil material, since they are largely a function of the pore size distribution. Physical models of flow use only K-values to characterize flow processes. Therefore, application of these models to soils requires K-measurements. Measurements are preferably made *in situ*, to avoid the deviant results that come from disturbances of the soil through sampling, transportation and storage. Methods are available to measure *in situ* K_{sat} (Bouwer, 1962) and K_{unsat} (Rose, 1965; Watson, 1966; Bouma, *et al.*, 1971, 1972). Laboratory methods are also available (Klute, 1965, 1972).

6.3. Internal soil drainage

Internal soil drainage (Soil Survey Manual, 1951) was defined as "that quality of a soil that permits the downward flow of excess water through it", which is reflected in the frequency and duration of periods of saturation. This differs from soil permeability in the inclusion of the climatic factor: A soil of "medium" internal drainage may be similar in permeability to one of "slow" internal drainage occurring in a more moist climate. Different classes of internal drainage, ranging from none to very rapid, are essentially based on the estimated length of the period in the year during which the soil is saturated. This also includes the occurrence of ground water. A soil with a constantly high ground-water table may have no internal drainage. Many factors, besides permeability of soil horizons, determine the amount of water present in the soil at any given time. These include the level of the ground water, precipitation patterns, interception by vegetation, crusts on the soil surface and associated run-off, occurrence and depths of soil horizons and their initial moisture content, and extraction of liquid from the soil by evapotranspiration. Quantitative physical techniques have been developed in the last decade describing flow in simplified soil systems (usually aggregates packed in a soil column) under simplified physical conditions. These techniques can be mathematical (for example: Raats and Gardner, 1972) or numerical.

For example, numerical techniques, using high-speed digital computers, were applied to calculate: 1. Moisture profiles in stratified porous media under transient-flow conditions (Hanks and Bowers, 1962; Whisler and Klute, 1967); 2. Infiltration and redistribution of water in homogeneous soil materials (Staple, 1966, 1969; Rubin, 1967); 3. Intermittent infiltration and redistribution in homogeneous soil materials (Ibrahim and Brutsaert, 1968). Generally good agreement was reported between calculated and measured values. Numerical techniques use saturated and unsaturated hydraulic conductivity values for every layer in the flow system and moisture retention data, that show soil moisture content as a function of soil moisture tension. Infiltration and redistribution of liquid in soil is influenced by hysteresis, which is the phenomenon that the moisture content in a soil sample at a given tension is partly determined by whether water was absorbed by initially drier soil or water was desorbed from an initially wetter sample. Moisture retention data, therefore, has to be defined in terms of a desorption and an absorption curve for use in numerical analyses. At this time numerical analyses have not been reported for real complex field situations, where only a fraction of the water from intermittent irregular rains enters a heterogeneous soil profile, in which water is redistributing and from which it is being extracted by plants. Future flow models will most probably become more sophisticated and more realistic. At this time it appears advisable to collect basic data, as discussed, for major soil types in anticipation of such future developments. Practical disadvantages of numerical procedures for calculating simplified moisture flow patterns are their complexity and need for highspeed computors and computor programming expertise. Some approximate physical methods have been developed also to calculate some hydrodynamic properties of soil (Bybordi, 1968; Davidson, et al., 1969; Gardner, et al., 1970; Peck, 1971; Raats, 1973). These methods, that assume the availability of K values and moisture retention data, are simple and quick, and therefore very attractive for use in approximate analysis of hydrodynamics of soils under simplified conditions. This paper reports results of the application of two of these techniques to four Wisconsin soils with ground-water tables standing more than 6 m below the soil surface: 1. A "somewhat poorly drained" Almena silt loam; 2. A "well to moderately well drained" Hibbing silt loam; 3. A "well drained" Batavia silt loam; and 4. A "somewhat excessively drained" Plainfield loamy sand. Drainage-class classifications are according to Hole (1973).

6.4. Soils and methods

The Almena silt loam (Aeric Glossaqualf) had the following soil horizons: (a) A1: 0-20 cm. Dark brown (10YR 3/3) silt loam, platy structure, gradual and smooth boundary (b) A2: 20-33 cm. Grayish yellow brown (10YR 5/2) silt loam, platy structure, few iron mottles, clear and smooth boundary; (c) B21g: 33-68 cm. Brown (7.5YR 4/6) inside peds, dull brown (7.5YR 5/3) on walls of cracks tonguing into B, iron mottles inside peds, silt loam, medium prismatic structure,diffuse and smooth boundary, (d) B22g: 68-110 cm. Bright brown (7.5YR 5/6) inside peds with common fine bright brown (7.8YR 5/8) iron mottles; dull orange (7.5YR 7/3) on walls of cracks, silt loam, medium and coarse prismatic structure, clear and wavy boundary, (e) IIB3: 110-126 cm. Brown (7.5YR 4/6) inside peds with common bright brown (7.5YR 5/8) iron mottles; light brownish gray (7.5YR 7/2) on walls of cracks, loam; coarse prismatic in upper part of horizons massive in lower part, gradual and wavy boundary, (f) IIC: 126-180 cm. Dull brown (7.5YR 5/4) coarse sandy loam with many large boulders, massive structure.

The Hibbing silt loam (Typic Eutroboralf) had the following soil horizons: (a) Ap: 0-25 cm. Reddish brown (2.5YR 5/4) silt loam; fine and medium subangular blocky structure; skeletans on ped faces, clear and smooth boundary, (b) B2t: 25-50 cm. Red (2.5YR 4/6) clay; very coarse prismatic parting to medium angular blocky structure; $CaCO_3$-glaebules; gradual and smooth boundary, (c) B3: 50-120 cm. Red (2.5YR 4/6) clay; prisms as B2. Pockets of weak-red (10R 5/4) clay, very rich in $CaCO_3$, gradual and smooth boundary, (d) C: 120-180 cm. Red (2.5YR 4/6) clay; prisms as in B2. The Batavia silt loam (Typic Argiudoll) had the following horizons: (a) Ap: 0-30 cm. Very dark brown (10YR 2/2) silt loam; medium subangular blocky structure; abrupt and smooth boundary, (b) B2t: 30-78 cm. Dark brown (7.5YR 3/3) silty clay loam; medium prismatic parting to medium subangular blocky structure, (c) B3: 78-100 cm. Dark brown (7.5YR 3/4) inside peds with few bright brown (7.5YR 5/8) iron mottles, silty clay loam, coarse prismatic parting to medium prismatic and medium subangular blocky structure; gradual and broken boundary, (d) IIC: 100-180 cm. Dark yellowish brown (10YR 4/4) sandy loam with pebbles and boulders; single grain (intertextic S-matrix). The Plainfield loamy sand (Typic Udipsamment) had the following horizons: (a) Ap: 0-25 cm. Very dark grayish brown (10YR 3/2) loamy sand; fine subangular blocky structure; abrupt and smooth boundary, (b) B2: 25-50 cm. Strong brown (7.5YR 4/6) sand; single grain; gradual and smooth boundary, (c) B3: 50-70 cm. Strong brown (7.5YR 5/8) sand; single grain; gradual and smooth boundary, (d) C: 70 cm+. Brownish yellow (10YR 6/6) coarse sand, single grain.

Measurements of hydraulic conductivity of the major horizons in these four pedons were made in situ with the double tube method (Bouwer, 1962) and the crust-test (Bouma, et al., 1971b, 1972). Undisturbed samples were taken for measurement of moisture retention characteristics in the laboratory. Detailed descriptions of these methods are given by Bouma, et al. (1972).

The approximate method of Bybordi (1968) was applied to the three soils for calculating moisture profiles during steady-state infiltration. This simple method uses K-values graphically derived from a measured hydraulic conductivity curve. The basic equation, given here for a two layer system, is as follows:

$$Z_n = - \left[\int_{h_o}^{h_1} \frac{dh}{1-\frac{v}{K_1}} + \int_{h_1}^{h_2} \frac{dh}{1-\frac{v}{K_2}} \right]$$

where K_1 and K_2 are the moisture dependent hydraulic conductivities of the two layers, h = moisture tension (cm) and Z = height (cm) above reference plane. The integral limit h_1 is not known initially. Starting at h_o, integration is continued through the bottom layer until Z_n assumes the value of Z_1, which is the thickness of this layer. The corresponding h is found to be h_1. This tension is continuous across the boundary and is therefore the lower limit of the second term of the integration, which is continued using the K_2 values, that apply to the second layer, until Z_n assumes the value Z_2 at a pressure of h_2.

In his paper, Bybordi described flow to a water table. In this application only the lower horizon boundaries are considered. Ground water may occur in the soil but is not essential to the analysis. The tensions in each horizon at a certain flow rate can be derived from the K-curve, since the flow rate is equal to the hydraulic conductivity under steady-state conditions with only gravity-flow occurring. Such tensions are sometimes not reached, however, due to interferences of underlying horizons that have different K-curves. This calculation method is used to calculate the tension profiles resulting from these interferences. Moisture contents in the profiles were derived from the calculated tension profiles by using moisture retention data.

A second approximate method (Peck, 1971) was used for calculating redistribution after infiltration into an initially uniform profile. This method was applied to major soil horizons of the four soils discussed: The B21g of the Almena silt loam (silt loam), the B2t of the Hibbing silt loam (clay), the B2t of the Batavia silt loam (silty clay loam) and the C of the Plainfield loamy sand (coarse sand). At each depth in a horizon the moisture content θ and water potential Ψ increase during redistribution to maximum values (θ_* and Ψ_*, respectively) and then decrease. As time advances, the maxima occur at greater depths. At the time when the maxima are at a depth $z = z_*$ the soil is drying in the zone above z_* and wetting in the region below z_*. The plane $z = z_*$, which moves downwards into the profile, is referred to as the transition plane. The basic equation is as follows:

$$\frac{d\theta}{dt} \approx - \frac{(\theta_* - \theta_o)}{\alpha Q}\left[D\frac{(\theta_* - \theta_o)^2}{\alpha Q} + K\right]$$

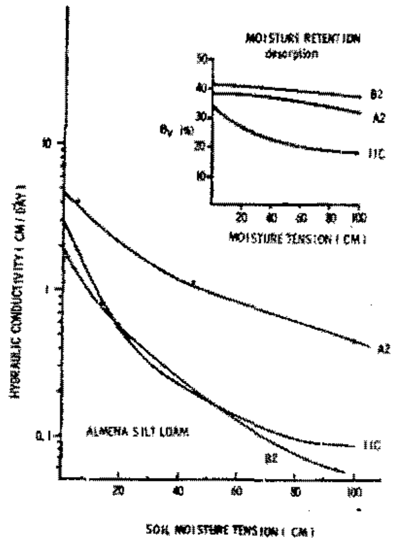

Figure 1. Hydraulic conductivity and moisture retention data for soil horizons in an Almena silt loam.

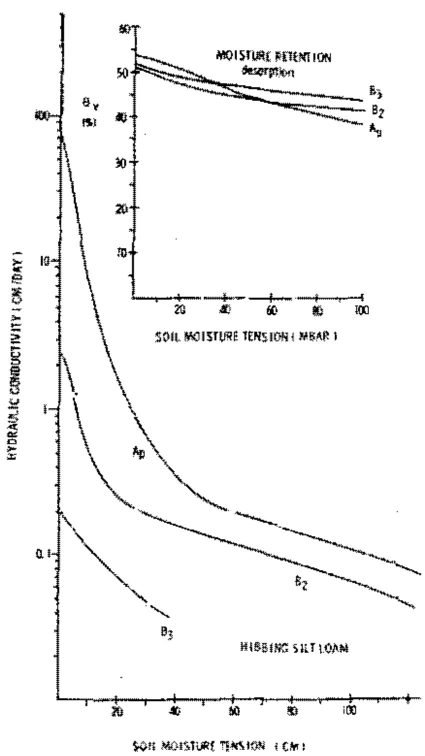

Figure 2. Hydraulic conductivity and moisture retention data for soil horizons in a Hibbing silt loam.

where Q = amount of infiltrated water. θ_o = original moisture content in the soil. D = diffusivity = $K\frac{d\Psi}{d\theta}$. The latter term is the slope of the moisture retention curve. K = hydraulic conductivity and α and β are constants (α = 0.70 and β = 0.78, Peck, 1971). Two expressions for α and β are used to calculate values for $\bar{\theta}$, the average moisture content in the transmission zone of thickness Z_*, as a function of time:

$$\alpha Q = (\theta_* - \theta_o) \cdot Z$$

$$\beta = \frac{(\theta_* - \theta_o)}{(\bar{\theta} - \theta_o)}$$

6.5. Results and discussion

Results of hydraulic conductivity and moisture retention measurements for major horizons of the three soils are in Figs. 1, 2, 3 and 4. Results of the Bybordi calculations are in Figs. 5, 6, 7 and 8.

The hydraulic conductivity and moisture retention data are a function of the pore-size distributions in the different studied horizons. For example, the C horizon of the Plainfield loamy sand with a coarse-sand texture, has many relatively large and few fine pores. The K_{sat} value is therefore relatively high at 450 cm/day (Fig. 4). The compact B2 horizon of the Almena silt loam, with a silt loam texture, has many fine and few large pores. K_{sat} is relatively low at 2 cm/day (Fig. 1). The water in unsaturated soil has a negative pressure which is expressed as the soil moisture tension (cm). The moisture content in the soil decreases and

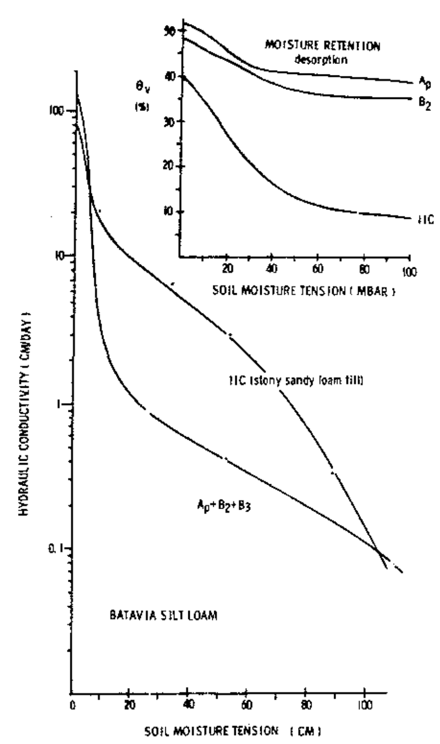

Figure 3. Hydraulic conductivity and moisture retention data for soil horizons in a Batavia silt loam.

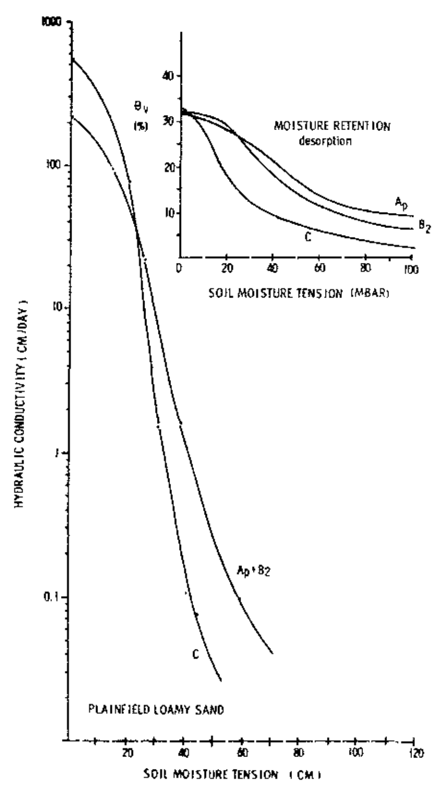

Figure 4. Hydraulic conductivity and moisture retention data for soil horizons in a Plainfield loamy sand.

progressively larger pores will empty as moisture tensions increase. This is reflected in the slopes of the conductivity curves which are plotted as a function of the moisture tension. For example, the curve for the Plainfield-C has a steeper slope than the curve for the Almena-B2, while the slope of the curves for the Plainfield-B2 (loamy sand, Fig. 4) and the Batavia-IIC (sandy loam, Fig. 3) are intermediate. These differences are also reflected in the moisture retention curves. The Plainfield-C looses 23 vol % moisture between saturation and 40 cm pressure (Fig. 4) and the Almena-B2 only 2 vol % (Fig. 1). Of particular interest are curves for the Batavia-B2 (silt loam, Fig. 3) and the Hibbing-B2 (clay, Fig. 2). These horizons have well developed structural elements (peds) with relatively large interpedal cracks (planar voids) and worm-and root channels. These large pores are filled at saturation, resulting in relatively high K_{sat} values (140 cm/day and 70 cm/day, respectively). Conductivities in these horizons drop sharply between saturation and low tensions of approximately 20 mbars, because these large pores are emptied in this tension range leaving only the relatively small pores inside the peds available for flow. Finally, the data show, for example, that the Plainfield-C is much more permeable than the Almena-B2 at saturation, but that the opposite is true at a low tension of 40 cm, which corresponds with steady flow rates of respectively 1 mm/day and 2.5 mm/day.

Fig. 5 shows calculated moisture tensions in the Almena silt loam at three low flow rates. The corresponding phase distributions show that the mottled B2 horizon is close to saturation (air content 4 vol %) even at a very low flow rate of 1 mm/day. Moisture tensions in the A horizons would

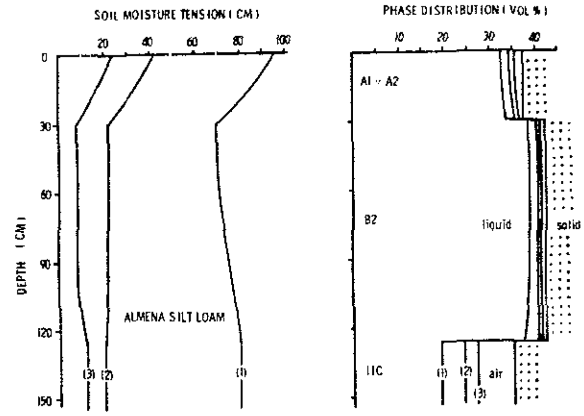

Figure 5. Moisture tensions and corresponding phase distributions in soil horizons of an Almena silt loam at three steady flow rates: (1) = 1 mm/day, (2) = 5 mm/day; (3) = 1 cm/day.

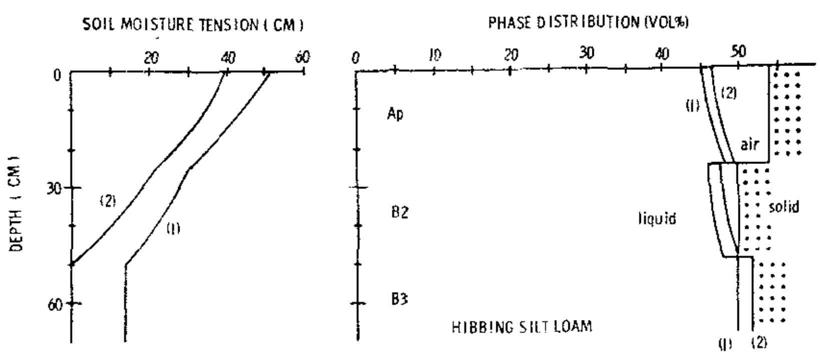

Figure 6. Moisture tensions and corresponding phase distributions in soil horizons of a Hibbing silt loam at two steady flow rates: (1) = 1 mm/day; (2) = 2 mm/day.

have been 46 cm at 1 cm/day, 90 cm at 5 mm/day and 220 cm at 1 mm/day (see K curve in Fig. 1) if this horizon would have extended much deeper. The lower calculated tensions in the topsoil illustrate therefore the ponding effect of the underlying B2. The glacial till has a conductivity curve which is virtually identical to that of the overlying B2. Different moisture retention data resulted in somewhat higher air contents in the till at the flow rates considered. Fig. 6 shows calculated moisture tensions in the Hibbing silt loam at two very low flow rates. The K_{sat} of the B3 horizon was only 2 mm/day and higher flow rates into the overlying horizon would lead to ponding of water in the overlying horizons. The phase distribution in Fig. 6 shows that only 7% of the pore volume in the topsoil is occupied by air at a flow rate of 2 mm/day, indicating a virtually saturated soil condition. Moisture tensions in the Ap horizon would have been 110 cm at 1 mm/day and 60 cm at 2 mm/day if this horizon would have extended much deeper (see K-curve in Fig. 2). The data for this soil are quite comparable to those for the Almena silt loam, as both illustrate the ponding effect of a very slowly permeable B horizon below a relatively permeable A.

The Almena silt loam has a higher capacity than the Hibbing silt loam to transmit water and moisture contents at comparable flow rates are lower. But differences are relatively small and both soils offer many practical problems because of their slow permeability. This contradicts the current placement of these two soils in different drainage classes (Hole, 1973). The Hibbing silt loam has no mottles and has been classified as well to moderately well drained; the highly mottled Almena silt loam has been

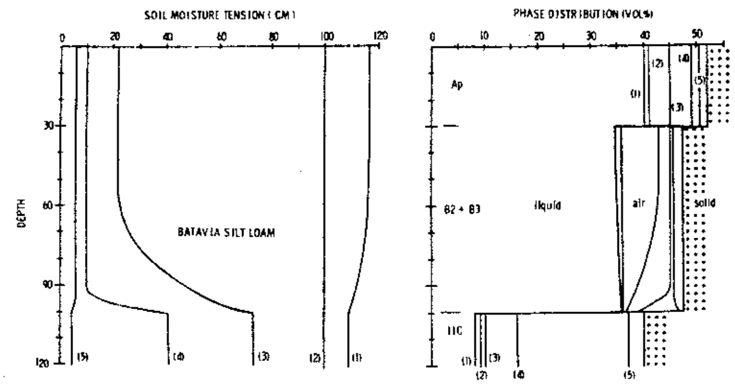

Figure 7. Moisture tensions and corresponding phase distributions in soil horizons of a Batavia silt loam at five steady flow rates: (1) = 0.5 mm/day; (2) = 1 mm/day; (3) = 1 cm/day; (4) = 5 cm/day; (5) = 50 cm/day.

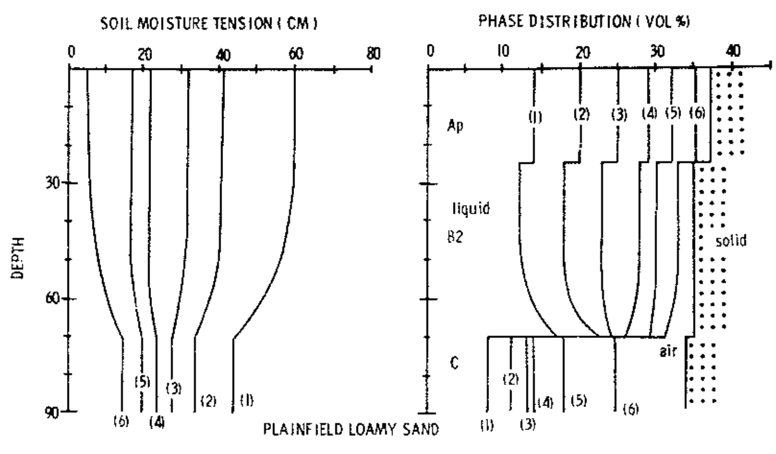

Figure 8. Moisture tensions and corresponding phase distributions in soil horizons of a Plainfield loamy sand at six steady flow rates: (1) = 1 mm/day; (2) = 1 cm/day; (3) = 5 cm/day; (4) = 50 cm/day; (5) = 100 cm/day; (6) = 200 cm/day.

classified as somewhat poorly drained. Lack of visible mottling in the Hibbing silt loam is probably due to the red color in this soil that was formed in red clay sediments. The physical data for both soils illustrate that morphological criteria for soil drainage, such as occurrence of mottling, have to be used with care because unrestricted application may lead to misleading conclusions.

Fig. 7 shows the calculated tensions in horizons of the Batavia silt loam at five flow rates varying between 0.5 mm/day and 50 cm/day. The effect of the sandy loam till below the silty cover is obvious. Both soil materials have a conductivity of 1 mm/day at 100 mbar. However, moisture retention characteristics of the two materials are quite different, which results in a much higher volumetric moisture content in the B2 as compared with the IIC (Fig. 7). The water content in the silty clay loam B horizon in the boundary zone with the sandy loam IIC increases only at the very high flow rate of 50 cm/day and at the very low rate of 0.5 mm/day. This zone is drier at the intermediate rates than it would have been if the silt had extended to greater depth. The conductivity curves for these soils (Fig. 3) can be used to illustrate that a soil horizon has not just one but an infinite number of permeabilities. At tensions between zero (saturation) and 8 cm, the silt cap is more permeable than the underlying till. This is most probably due to the occurrence of large root- and worm channels and cracks. Between tensions of 8 and 100 cm, the till is more permeable than the silt. The silt is again more permeable at tensions higher than 100 cm. The differences result from the different pore size distributions of both materials and are reflected in the curves of Fig. 7. Field soil scientists are often puzzled by the occurrence of mottling in the lower parts of the B horizon in such a soil, because permeabilities should be sufficiently high to avoid periodic saturation with water. The phase distributions in Fig. 7 show that moisture contents in the B horizon are relatively high, even at low flow rates. The horizon is composed of large peds and water movement occurs mainly along interpedal voids (Bouma and Anderson, 1973). Reducing conditions may therefore occur inside peds, resulting in mottling, while water moves freely through the horizon. This particular type of mottling is currently being investigated.

Fig. 8 shows the calculated tensions in the Plainfield loamy sand at six flow rates, ranging from 1 mm/day to 200 cm/day. The Ap and B2 are more permeable than the C horizon at flow rates lower than 37 cm/day, corresponding with a tension of 22 cm. At higher flow rates the opposite is true (Fig. 4). At flow rates lower than 37 cm/day water tends therefore to accumulate in the lower part of the B, near the boundary with the C horizon, whereas tensions increase in this zone (with a corresponding decrease in moisture content) at higher than 37 cm/day. The effects are comparable to those discussed for the Batavia silt loam. The differences in physical behavior between the B2, (with 1% clay, 10% silt and a medium-size sand fraction) and the C (coarse sand, no clay and 1% silt) is rather pronounced due to the different pore size distribution. In all cases, the shape of the K-curve determines tensions and derived moisture contents as a function of rate of flow.

Horizon boundaries in these examples are pictured as straight lines whereas they are more gradual in reality. Therefore, changes in tensions and moisture contents are actually less abrupt than shown. In these examples boundaries of genetic soil horizons are considered to be of physical significance as well, separating layers with distinctly different physical characteristics. Though this assumption appears to be reasonable, there is as yet hardly any data in the literature correlating dimensions of morphologic and "hydraulic" soil horizons. It has been shown that genetically identical soil horizons may physically behave quite differently (Bouma, 1969; Bouma and Hole, 1971a). Relationships between soil structure characteristics and hydraulic characteristics (Bouma and Anderson, 1973) may prove to be useful in defining "hydraulic" soil horizons. Even more important is the question whether or not the investigated soil is representative of the cartographic unit or the classification unit to be characterized. The soil surveyor uses pedological criteria in establishing his mapping units, which are presumably relatively homogeneous, and in determining the soil classification of "representative" pedons. The assumption that such pedological individuals would also have a characteristic physical behavior is rather hypothetical at this time. Nielsen, et al. (1972) studied the variability of soil physical characteristics in an 150-acre field. More work of this type is very much needed.

Steady-state flow in a soil profile, as calculated in this paper for four pedons, will not be common in the upper soil horizons due to the intermittent character of rains. However, such processes may be quite realistic for deeper horizons (Raats and Gardner, 1972) and for extended infiltration into crusted soil (Bouma, 1971c).

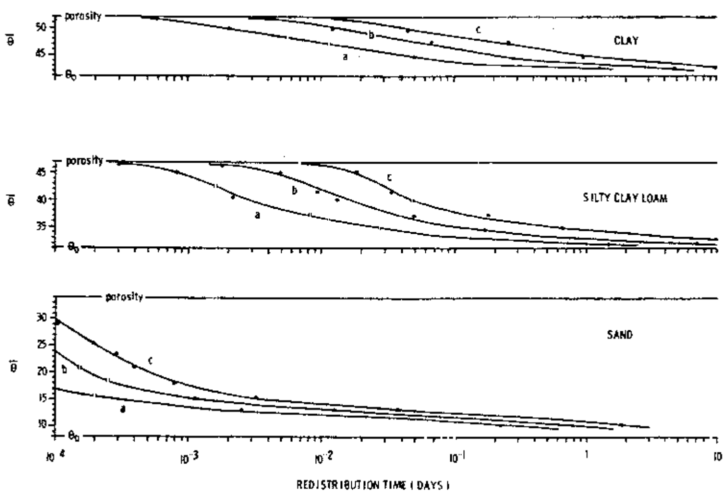

Figure 9. The average moisture content in the transmission zone as a function of time, calculated for three infiltrated quantities of water: (a) = 2 mm; (b) = 5 mm; (c) = 10 mm. The three soil horizons considered were: B2 of Hibbing (clay); B2 of Batavia (silty clay loam) and C of Plainfield (sand). Curves for the B2 of the Almena had a similar slope as those for the B2 of the Hibbing.

The average moisture content in the transmission zone $\bar{\theta}$, as calculated with the Peck approximation for three infiltrated quantities of water is plotted in Fig. 9 as a function of time to show that these data can be used to define the drainage rate. The horizons are considered here as separate entities because the Peck calculation cannot be applied to a series of different layers. After waiting 144 minutes (1/10 day) following the infiltration of 5 mm of water (curves b) the clay has 47% moisture and 5% air; the silty clay loam has 35% moisture and 12% air and the sand has 12% moisture and 22% air. After waiting one day the moisture contents would be 43%, 33% and 10%, respectively. Original moisture contents of the three horizons (θ_o) were chosen to be corresponding with a very low K-value of approximately 0.2 mm/day, which describes a near static condition, that might be called the "field capacity". The derived θ_o values were 41% for the clay, 31% for the silty clay loam and 8% for the sand. The shape of curves calculated for the B2 of the Almena silt loam were essentially identical to those of the B2 of the Hibbing silt loam ("clay" in Fig. 9) and were not separately plotted in Fig. 9.

Calculations can be made varying Q and θ_o as needed to make estimates for particular soil horizons.

6.6. The role of physical methods in soil survey interpretations

This application of physical methods is intended to expand soil survey interpretations. Its function is not to replace any of the current classifications of soil drainage or soil moisture regimes, but, rather, to supplement them. The broadly defined drainage classes or moisture regimes are sufficiently detailed for many general interpretations of soil maps and quantitative physical data may then not be needed. The physical data are essential for some engineering purposes, such as, for example, selection and design of systems for on-site liquid waste disposal (Bouma, et al., 1972). The preparation of specific engineering designs is beyond the scope of soil map interpretations, but a basic physical characterization of soil-map units in terms of K values and moisture retention data, including an analysis of variability, should be available for major soils to satisfy increasing professional demand of engineers and research soil scientists. They will use this basic data in their specific flow-models or calculation schemes. A third category of users of soil information need more specific data than provided by broad qualitative descriptions but these users do not have the opportunity or training to process basic physical data in computer programs or calculation schemes describing their specific problems. In this case, the best solution would seem to be to apply relatively simple approximate physical methods, as discussed, as part of soil survey interpretations.

5.7. Conclusions

Future interpretations of soil maps will increasingly require that quantitative assessments be made of the hydrodynamic behavior of soils under different uses. Traditional classifications of soil drainage commonly used in soil survey interpretations are very useful as broad indicators of current conditions, although exclusive use of morphological criteria may result in erroneous conclusions. In order to expand soil survey interpretations, procedures are needed for predicting moisture conditions in a soil at any time as a function of varying environmental conditions.

Elaborate calculation methods predicting hydrodynamic behavior of soil materials with numerical or mathematical procedures are at present available to analyze simplified flow conditions and flow geometries. Use of these methods for soils in the field will become more attractive as they become more closely correlated with actual, variable conditions in the field. Approximate calculation methods are very attractive at present in that they are simple and rapid, once K values and moisture retention data are available, in providing a better understanding of, admittedly simplified, flow conditions in soils. K values and moisture retention data are needed for both elaborate and approximate methods. In any case, physically poorly defined measurements of "percolation rates" or "field capacity" will not suffice. Application of physical techniques in the soil survey program assumes that cartographic units depicted on soil maps and associated representative pedons not only act as relatively homogeneous pedological individuals but also as individuals with a characteristic physical behavior. This assumption is hypothetical and research is needed to test it.

Acknowledgements

The author is indebted to P. A. C. Raats and F. D. Hole for helpful suggestions.

6.8. Literature Cited

Boersma, L., G. H. Simonson and D. G. Watts. 1972. Soil Morphology and Water Table Relations: I. Annual Water Table Fluctuations. Soil Sci. Soc. Amer. Proc. 36:644-649.

Bouma, J. 1969. Microstructure and stability of two sandy loam soils with different soil management. Agr. Res. Rep. 724, Pudoc, Wageningen, Netherlands. 110 p.

Bouma, J. and F. D. Hole. 1971a. Soil structure and hydraulic conductivity of adjacent virgin and cultivated pedons at two sites: A Typic Argiudoll (silt loam) and a Typic Eutrochrept (clay). Soil Sci. Soc. Amer. Proc. 35:316-319.

Bouma, J., D. I. Hillel, F. D. Hole, and C. R. Amerman. 1971b. Field measurement of unsaturated hydraulic conductivity by infiltration through artificial crusts. Soil Sci. Soc. Amer. Proc. 35:362-364.

Bouma, J. 1971c. Evaluation of the field percolation test and an alternative procedure to test soil potential for disposal of septic tank effluent. Soil Sci. Soc. Amer. Proc. 35:871-875.

Bouma, J., W. A. Ziebell, W. G. Walker, P. G. Olcott, E. McCoy and F. D. Hole. 1972. Soil absorption of septic tank effluent, a field study of some major soils in Wisconsin. Information circular No. 20. Geol. and Nat. Hist. Surv., Univ. Ext., Madison, Wisconsin.

Bouma, J. and J. L. Denning. 1972. Field measurement of unsaturated hydraulic conductivity by infiltration through gypsum crusts. Soil Sci. Soc. Amer. Proc. 36:846-848.

Bouma, J. and J. L. Anderson. 1973. Relationships between soil structure characteristics and hydraulic conductivity. Proceedings of the Symposium on the Field Moisture Regime. ASA special publication.

Bouwer, H. 1962. Field determination of hydraulic conductivity above a water table with the double tube method. Soil Sci. Soc. Amer. Proc. 26:330-335.

Bybordi, M. 1968. Moisture profiles in layered porous materials during steady-state infiltration. Soil Sci. 105:379-383.

Childs, E. C. 1969. The Physical Basis of Soil Water Phenomena. John Wiley. p. 493.

Davidson, J. M., Stone, L. R., Nielsen, D. R., and Larue, M. E. 1969. Field measurement and use of soil properties. Water Resources Research 5:1312-1321.

Gardner, W. R., D. I. Hillel and Y. Benyamini. 1970. Post-irrigation movement of soil water. I. Redistribution. Water Resources Research 7 (4). 851.

Hanks, R. J. and S. A. Bowers. 1962. Numerical solution of the moisture flow equation for infiltration into layered soils. Soil Sci. Soc. Amer. Proc. 26:530-534.

Hillel, D. I. 1971. Soil and water, physical principles and processes. Academic Press. p. 288.

Hole, F. D. 1973. Wisconsin Soils. Information Circular No. 22 Wisconsin Geological Natural History Survey, University of Wisconsin, Madison.

Ibrahim, H. A. and W. Brutsaert. 1968. Intermittent infiltration into soils with hysteresis. Journ. of the Hydr. Div. Proc. Am. Soc. of Div. Eng. 113-137.

Klute, A. 1965. Laboratory measurement of hydraulic conductivity of saturated soil. Amer. Soc. Agron. Monograph 9:210-221.

Klute, A. 1972. The Determination of the Hydraulic Conductivity and Diffusivity of Unsaturated Soils. Soil Science. Vol. 113. 264-277.

Marbut, C. F. 1935. Soils of the United States. In: U.S. Dept. Agr. Atlas of American Agriculture. 98 pp.

Nielsen, D. R., J. W. Biggar and J. C. Corey. 1972. Application of Flow Theory to Field Situations. Soil Science 113:254-264.

Peck, A. J. 1971. Redistribution of soil water after infiltration. Aust. J. Soil Sci. 9:59-71.

Raats, P. A. C. 1973 (in press). Steady upward and downward flows in a class of unsaturated soils. Soil Sci.

Raats, P. A. C. and W. R. Gardner. 1972. Movement of water in the unsaturated zone near a water table. Monograph of soil drainage. Amer. Soc. of Agronomy , J. V. Schilfgaarde, Ed.

Richards, L. A. 1931. Capillary conduction of liquids in porous mediums. Physics I., 318-33.

Rose, C. W., Stern, W. R. and Drummond, J. E. 1965. Determination of hydraulic conductivity as a function of depth and water content for soil in situ. Aust. J. Soil Sci. 3, 1.

Rubin, J. 1967. Numerical method for analyzing hysteresis-affected, post-infiltration redistribution of soil moisture. Soil Sci. Soc. Amer. Proc. 31:13-20.

Schelling, J. 1960. New aspects of soil classification with particular reference to reclaimed hydromorphic soils. Trans. Intern. Congr. Soil Sci. Madison 4:218-224.

Simonson, G. H. and L. Boersma. 1972. Soil Morphology and Water Table Relations: II. Correlation Between Annual Water Table Fluctuations and Profile Features. Soil Sci. Soc. Amer. Proc. 36:649-653.

Soil Survey Manual. 1951. USDA Handbook No. 18. p. 503.

Soil Survey Staff. 1970. SCS. U.S. Dept. Agr. Selected Chapters from Soil Taxonomy of the National Cooperative Soil Survey. Washington, D.C.

Staple, W. J. 1966. Infiltration and redistribution of water in vertical columns of loess soil. Soil Sci. Soc. Amer. Proc. 30:553-558.

Staple, W. J. 1969. Comparison of computed and measured moisture redistribution following infiltration. Soil Sci. Soc. Amer. Proc. 33:840-847.

van Heesen, H. C. 1970. Presentation of the seasonal fluctuation of the water table on soil maps. Geoderma. 4:257-279.

Watson, K. K. 1966. An instantaneous profile method for determining the hydraulic conductivity of unsaturated porous materials. Water Resources Research 2:709-715.

Whisler, F. D. and A. Klute. 1967. Analysis of infiltration into stratified soil columns. Proceedings of symposium on water in the unsaturated zone. Wageningen, Netherlands.

7. APPENDICES

The following subchapters will discuss procedures and methods which were used in the previous chapters to study soil morphology and processes of water movement through soil.

7.1. The preparation of soil peels.

7.2. Soil moisture retention characteristics.

7.3. *In situ* measurement of saturated hydraulic conductivity: The Bouwer double tube method.

7.4. Field measurement of unsaturated hydraulic conductivity by infiltration through artificial gypsum crusts.

7.5. Field measurement of unsaturated hydraulic conductivity with the instantaneous profile method.

7.6. Calculation of hydraulic conductivities from moisture retention data.

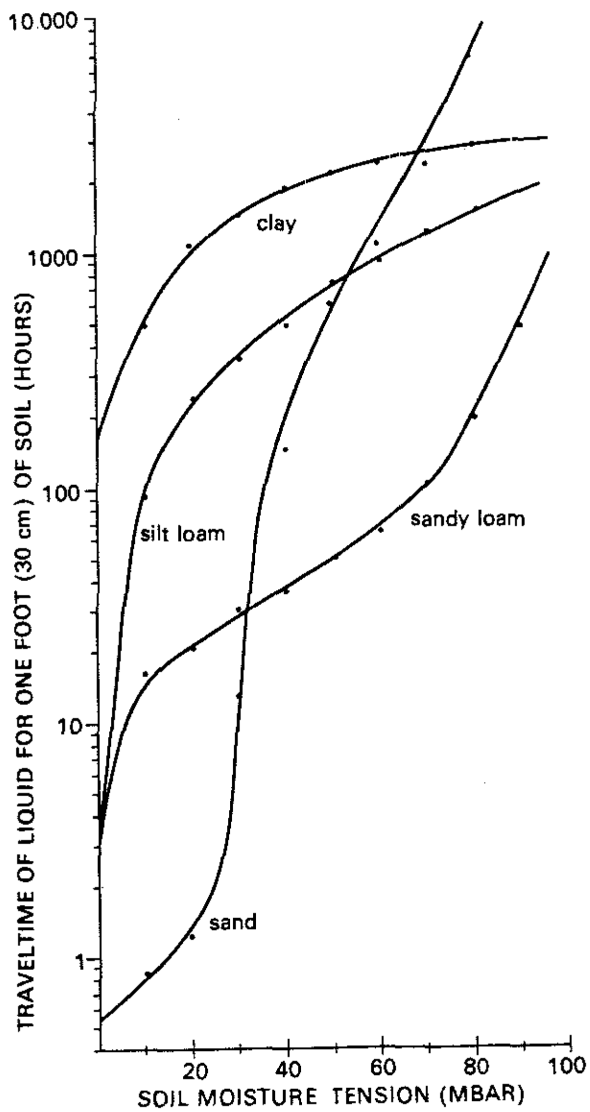

Fig. 6.7. Traveltime of liquid for one foot of soil at different soil moisture tensions, calculated for four soil materials.

gradient of 1 cm/cm equal to K) in a hypothetical one-dimensional flow system below the gravel bed. K_{sat} (P = 0) would represent the infiltration rate into an uncrusted soil surface, and K decreases in characteristic patterns with increasing soil crusting, and increasing soil moisture tension. A lower limit of allowable infiltration rate, based on practical and economical criteria was tentatively defined as approximately 2 cm/day (see lower horizontal lines in the curves of Fig. 6.8) based on a seepage bed area of 1000

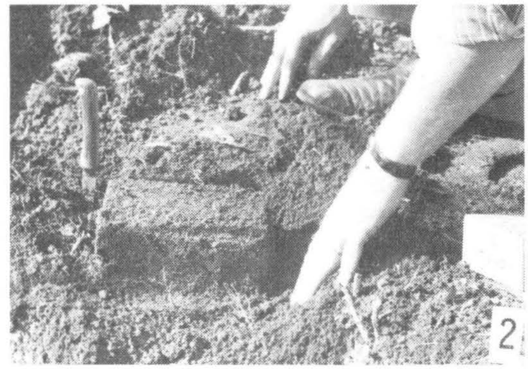

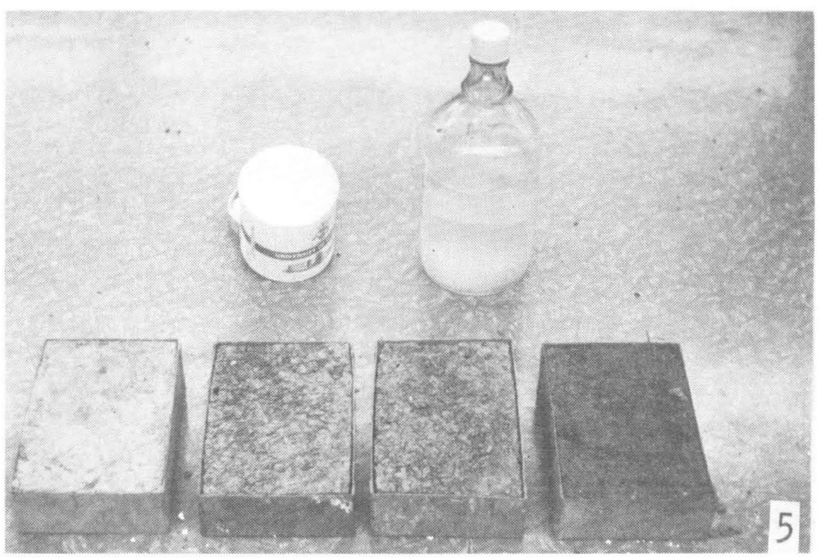

Fig 7.1

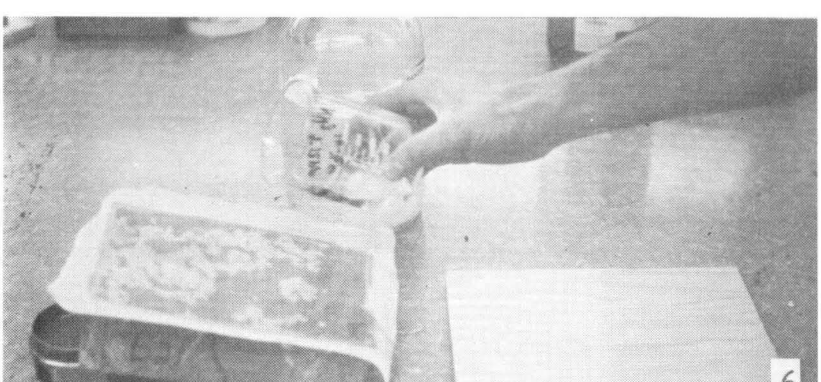

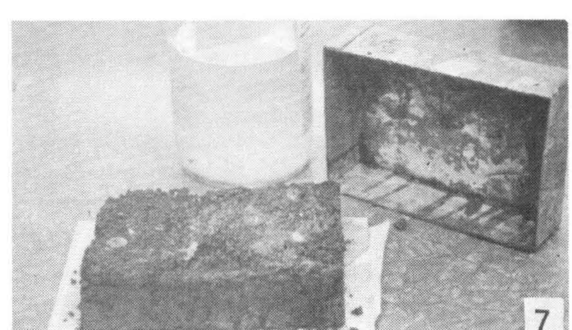

Appendix 7.1.

The preparation of soil peels

Several publications have described this procedure in detail (Bouma and Hole, 1965; Soil Sci Soc. Amer. Proc. 29:483-485; Jager et al., 1966 (Section 5.1.5). The pictures in Fig. 7.1 illustrate the procedure as applied to pedal soil materials. A horizontal plane is prepared at the desired depth in the profile (Picture 1) if a horizontal soil peel is to be taken. Vertical peels are obtained from flattened vertical profile walls. A metal box, which size of bottom area will determine the surface area of the future soil peel, is filled with undisturbed soil. This is achieved by carving out a volume of soil corresponding to that of the box (Picture 2) and by gently pushing the box on top of it (Picture 3). Box and excess soil are cut loose with a spade (Picture 3) and next excess soil in the box is removed with a knife (Picture 4). The flattened exposed soil in the box is the future bottom area of the soil peel that is to be attached to a supporting board. It is important to make this surface smooth so as to facilitate contact between soil and board. The soil in the box is slowly air-dried for about a week. Fast drying is not recommended because unnatural cracking patterns may result. Once air-dried (Picture 5: showing several filled boxes of major horizons in a Batavia silt loam), liquid plastic is applied to the soil surface, which has been covered with a piece of cheesecloth to increase soil cohesion and to facilitate attachment to the supporting board later (Picture 6). The plastic solution consists of polyvinyl-acetate, dissolved in acetone (1:8 solution). The box is slightly tilted during pouring to create downward flow of plastic over the soil surface (Picture 6). The box is immediately turned around on top of a piece of wood or masonite as soon as the exposed soil surface is covered with plastic (Picture 7). This is to avoid deep percolation of plastic into the block of soil through larger crevices. A thin layer of liquid plastic should also be applied to the board to aid the cementing process. The exposed soil surface on the board (Picture 7) does not show natural ped surfaces. The top part of the block of soil has therefore to be removed, leaving only those peds on the peel that are attached to the board by plastic or by interpedal binding forces. Excess soil can be removed by gently knocking on the back of the board. Slow wetting of the block of soil with a slightly moist sponge may be helpful to facilitate removal of excess soil. The soil surface to be exposed on the future soil peel should show natural cleavage faces occurring in the soil. It is imperative therefore that this surface should not be touched with knives, needles or fingers. If this procedure is carefully executed, natural ped surfaces can be shown in soil peels, pictures of which were shown in Fig. 2.2 in Chapter 2.

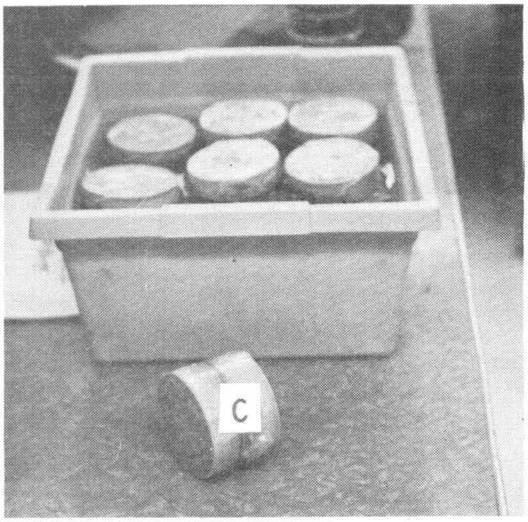

Fig. 7.2. Slow saturation of undisturbed field samples, sampled with the double cylinder hammer driven core sampler. The open ends of the cores (c) are covered with cheesecloth and are taped into place with water-resistant tape. Saturation of the samples occurs in the plastic container (see text).

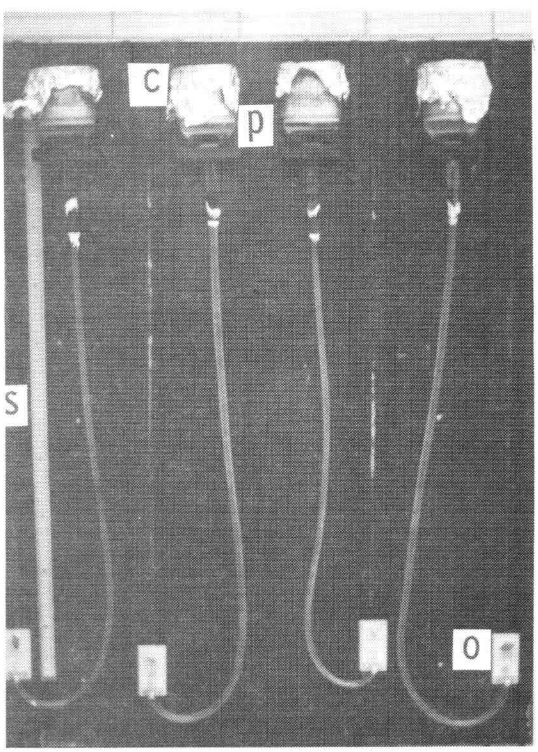

Fig. 7.3. Moisture retention determinations in the range from saturation to 100 cm tension. Glass cups (c), with a porous dish (p) inside, contain a soil sample inside a ring which is placed on a thin layer of sand. Flexible plastic tubing, which is filled with water up to the porous dish, is attached to a dish that can be moved up and down a scale (s), thus creating points of outflow (o) at different distances from the cup. The cores and the cups are covered with aluminum foil to avoid evaporation.

Appendix 7.2.

Soil moisture retention characteristics (References in Section 5.1.5)

Moisture retention characteristics (desorption) can be determined from samples obtained in the field with the double cylinder hammer driven core sampler (Blake, 1965, p. 376) in small cylindrical rings (5 cm high with a diameter of 7.5 cm, see Fig. 7.2). The soil in the ring is slowly saturated by first absorbing water in the field-moist sample at a tension of approximately 20 cm for at least one day. This is achieved by placing the cores on moist sponges in a plastic container which has about 1 cm of water at the bottom (Fig. 7.2). Then, the soil is completely saturated by raising the water level to the upper brim of the core. Moisture contents at 20, 40, 60, 80 and 100 cm tension are determined by placing the cores inside porous cups (p) (Fig. 7.3) in which a thin layer of fine sand was placed to insure good contact between the soil in the ring and the porous disk in the cup. Different tensions can be created at the level of the disk by lowering or raising the point of outflow (o) of the water-filled flexible tube below the cup. The tension is equal to the vertical distance (cm) between the bottom of the porous plate and the point of outflow (o). A vertical scale is mounted next to the tube to measure the tension. Use of a 5 cm high sample requires that distances are measured from the middle of the sample (2.5 cm above the porous plate) downwards rather than from the porous plate itself. Equilibrium is reached at each measurement when water stops flowing from the tube at point (O). The cores are weighed at each point of measurements. An alternative procedure would be to measure the amount of outflow at point (o) between successive applied tensions Aluminum foil should be wrapped around the core and the cup to avoid evaporation (Fig. 7.3). Moisture contents corresponding with tensions exceeding 100 cm are measured by applying air-pressures to cores that are placed on a porous plate inside a metal container, following standard techniques (Richards, 1965). After determining the whole range of moisture contents, corresponding with tensions ranging from zero (saturation) to 15 bar (wetting point) the cores are dried at 105° C. It is essential that soil is never lost from the cylinder during successive measurements, as this would result in erroneous calculation results. To avoid this problem, the cylinder can be wrapped with cheesecloth which is to be taped with water-resistant tape (Fig. 7.2). Moisture contents can also be determined by processes of adsorption (see Chapter 3). Then, the original moisture content of the core should be low (for example, corresponding with 300 cm tension). The core is placed on the cup to which a tension of 100 cm is applied. Water is absorbed then until equilibrium is reached, as evidenced by the constant level of the water in the plastic tube at point O. Successive measurements can be made at 100, 80, 60, 40 and 20 cm tension. Calculations of moisture contents at different tensions and soil porosity can be made for each sample. This calculation is relatively simple when samples in cylinders (with a constant volume) are used. To illustrate the calculation procedure, an example will be presented based on the Saran-clod method, where the volume of the sample is not constant.

The method to determine soil physical characteristics from large clods obtained from pedal swelling soil materials and using saran resin as a coating material, was introduced by Brasher et al., 1966. Clods should have a volume of at least 100 cm^3, but preferably more than that. They should represent the soil strucutre from the sampled horizon. In general about 20 elementary units of structure should be represented in any clod sample. A medium sized blocky structure, with ped volume of 1 cm^3 should be represented by a clod volume of at least 20 cm^3. This guide does not work in coarse prismatic structures, since individual peds may have volumes of 150 cm^3 or more. It should be clearly stated when values are determined for such single peds. The method consists of the following steps:

1. A weighed air-dry clod is coated with saran; and slowly saturated with water through one flattened side of the clod where the coating has been temporarily removed.

2. After saturation, the open side of the clod is coated again with saran and weight and volume of the clod are determined.

3. The coating on the flattened side is removed again, and the clod is placed in a pressure apparatus to determine water contents and soil volume at different pressures. After equilibrium has been reached at a given pressure, the clod is coated again at the flattened side, and weight and volume are determined. It is essential not to loose any soil from the clod during this procedure, since this would lead to erroneous results. After determining moisture contents and volumes of clods for a range of pressures (usually 0.03b, 0.1b, 0.3b, 1b, and 15b), the clod is dried at 105°C. Then all values are available to calculate bulk densities, porosities at different suctions, and the moisture retention curve. Non-swelling soil materaals, such as sands, can be sampled directly in cylinders of known volumes.

Example of clod method calculation: Clod from C-horizon of Mexico silt loam, calculations for 1 bar suction only.

Basic data: Air dry weight of clod: 55.30 gr. Coated with saran: 57.90 gr. Weight of coats: 2.60 gr. = 1.73 cc (Spec. dens. saran = 1.50). At 1 bar equilibrium: 57.10 gr. Volume of clod (+ plastic): 30.50 cc (difference between weight of beaker with water and total weight when clod is suspended in the beaker). After drying clod + plastic at 105°C for one day: weight = 47.40 gr. Volume = 27.9 cc.

Calculation 1:

Determine bulk density (bulk density = gr/cm^3 of natural soil). Since B.D. of soil is required, the plastic has to be excluded. Volume of soil at 1 b = 30.50 - 1.73 = 28.77 cc. The weight of 57.10 gr. is composed of water, plastic and soil. After drying at 105°C, weight = 47.40 gr. (= soil + plastic). From a separate experiment it was learned that the saran plastic looses 25% of its weight when heated for 24 hrs. at 105°C. Soil weight only, therefore, is 47.40 - (0.75 x 2.60) = 45.45 gr. This is an important value, from which dry bulk densities at different moisture contents are derived. B.D. at 1 bar is:

$$\frac{45.45}{28.77} = 1.58.$$

Calculation 2:

Determine percentage of moisture (in % of dry weight and volume) at 1 bar. Stovedry soil weight was 45.45 gr. We need to know now the weight of the moisture only at 1 bar. Soil + plastic + water = 57.10 gr. Soil + water = 57.10 - 2.60 = 54.50 gr. Moisture % of dry weight =

$$\left(\frac{54.50 - 45.45}{45.45}\right) \times 100\% = 19.9\%.$$

Moisture % by volume = % of dry weight x B.D. = 19.9 x 1.58 = 31.4%.

Calculation 3:

Determine porosity (= vol. % of soil occupied by the non-solid soil phase). Calc. 2 showed that 31.4% of the soil volume is occupied by water at 1 bar suction. What about the remaining 68.6%? For this we need to know one additional soil characteristic: the particle density (= gr/cm^3 of the solid soil phase only). This can be determined by a separate procedure, using pyknometers (see appendix at the end of this section and Blake, 1965). Presuming we have a particle density of 2.60, the 45.45 gr of soil represents 17.45 cc. Total volume of clod was 28.77. Pores form 28.77 - 17.45 = 11.29 cc which is (11.29/28.77) x 100% = 39.2% of soil volume (this means that 7.8% of the pores in the soil are filled with air). In formula:

$$\text{Porosity} = \left(1.0 - \frac{\text{Bulk density}}{\text{Particle density}}\right) \times 100\%.$$

Calculation 4:

Determine coefficient of linear extensibility (COLE) as:

$$\sqrt[3]{(V_m/V_d)} - 1$$

where V_m = volume of moist whole soil fabric and V_d = volume of dry whole soil fabric (Grossman, et al., 1968). Here: COLE = (28.77/26.60) - 1 = 0.081.

Moisture retention characteristics for non-swelling soil materials, such as sands, were determined from samples obtained in the field with the double cylinder hammer driven core sampler (Blake, 1965, p. 376) in small cylindrical rings (5 cm high, with a diameter of 7.5 cm). These rings were placed in the pressure apparatus, and later calculations, which are basically the same as the ones for saran coated clods, were relatively simple since the bulk density was constant at different moisture contents and since there was no plastic coating involved. Bulk densities of these materials were determined separately (after using the same sampling device) from larger cores with a diameter and height of 7.5 cm.

Appendix:

Summary of pyknometer test to determine particle density of soil (see Methods of Soil Analysis).

Pyknometer (dry, empty) = W_1 gr. Pyknometer + about 5 gr. stove soil = W_2 gr. Pyknometer filled with de-aired water = W_3 gr. Pyknometer with water + soil = W_4.

$$\text{Particle density} = \frac{W_2 - W_1}{W_3 + W_2 - W_1 - W_4} \quad gr/cm^3$$

The principle on which the method is based is the same as that for the clod tests: a body suspended in water will be subjected to an upward force that is equal to the weight of the volume of the displaced liquid.

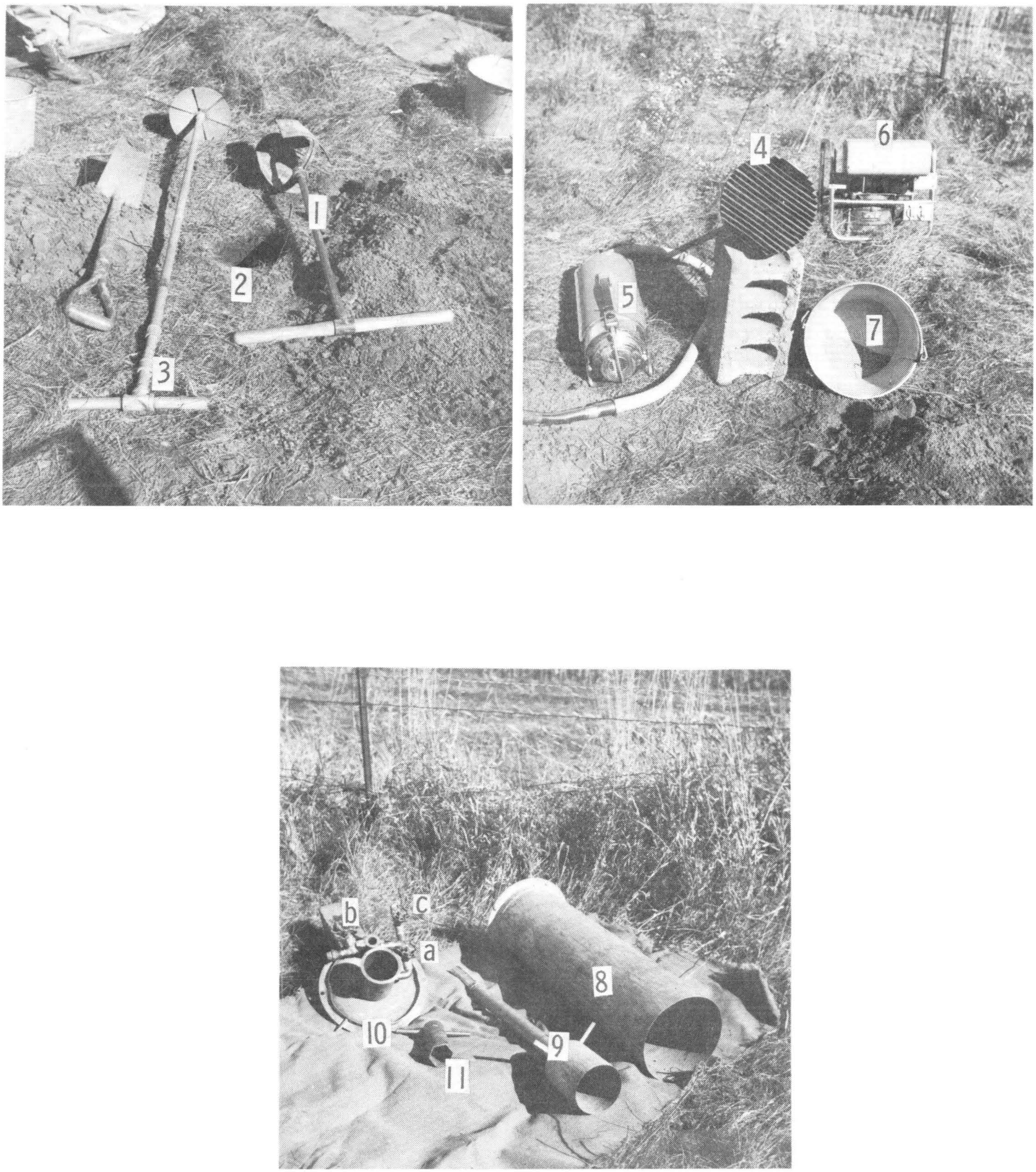

Fig. 7.4. Measurement of the hydraulic conductivity with the Bouwer Double tube apparatus.

Appendix 7.3 (References in Section 5.1.5)

3.2.3. In situ measurement of saturated hydraulic conductivity: The Bouwer double tube method

This method is a standard procedure for measuring hydraulic conductivity of saturated soil, well above the ground water table (Boersma, 1965, in: Methods of Soil Analysis, Part 1, p. 234). With the double tube method, two concentric tubes are inserted into an auger hole and covered by a lid with a standpipe for each tube (Fig. 7.5). Water levels are maintained at the top of the standpipes to create a zone of positive water pressures in the soil below the bottom of the hole. The hydraulic conductivity (K) of this zone is evaluated from the reduction in the rate of flow from the inner tube into the soil when the water pressure inside the inner tube is allowed to become less than that in the outer tube. This is done by stopping the water supply to the inner tube (closing valve a) and measuring the rate of fall of the water level in the standpipe on the inner tube while keeping the standpipe on the outer tube full to the top. This rate of fall is less than that obtained in a subsequent measurement in which the water level in the outer tube standpipe is allowed to fall at the same rate (by manipulating valve b) as that in the inner tube standpipe. The difference between the two rates of fall is the basis of the calculation of K.

Procedure:

The different stages of the method will now be explained in more detail with reference to the numbers on the included pictures (Fig. 7.4). A large auger, with a diameter of 10 inches (1) is used to make a cylindrical hole (2) to the desired depth. A bottom scraper (3) is used to obtain a flat surface at the bottom. Loose soil is removed from the hole. Before using the hole cleaner (4) the outer tube (8) is forced down in the hole. It is often necessary to widen the hole locally to make this possible. This is done with a scraper, not pictured here. When the outer tube is found to fit well it is temporarily removed again. The hole cleaner (4) is gently forced into the soil at the bottom of the hole. If the soil is dry, premoistening of it may be necessary. The thin metal fins of the hole cleaner should penetrate about 2 cm into the soil. Next, the hole cleaner is pulled out of the hole with an upward cork-screw movement that prevents smearing the soil surface, as would happen if the cleaner were turned without being pulled up at the same time. The detached mass of soil is up-ended for observation of the natural broken surface of soil held between the fins. A corresponding natural broken soil surface is left at the bottom of the hole.

The outer tube (8) is forced down as evenly as possible about 5 cm into the soil at the bottom of the hole (13). This may require careful blows of a sledge hammer on a wooded cross-piece. Control of the distance is by measurement from a fixed horizontal reference rod (15). With a vacuum cleaner (5), powered by a portable electric generator (6), loose soil fragments are removed from the bottom of the hole. This bottom surface is then covered with a thin (1 cm) layer of coarse sand (7) on top of which a baffle is laid (12), with attached strings looped over the top

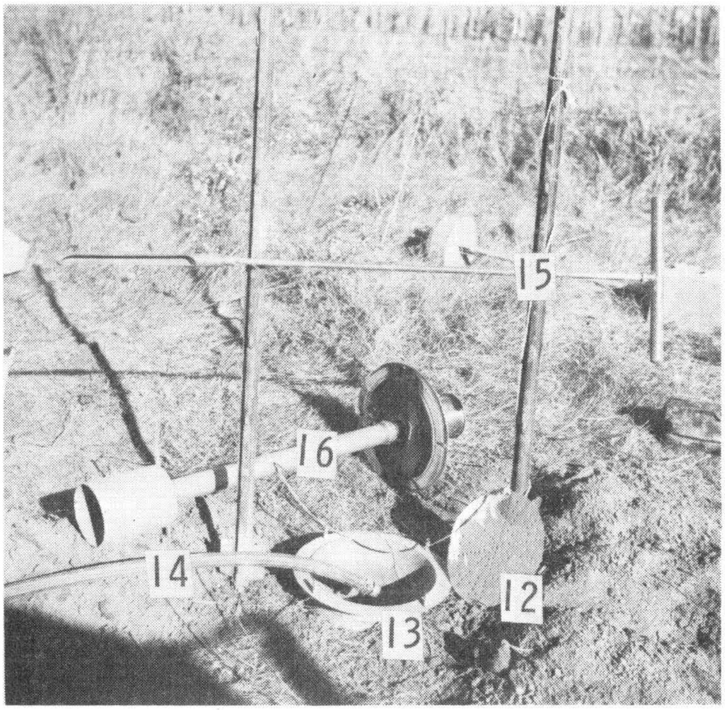

<u>Abbreviated explanation of numbers:</u>

1 = soil auger, 2 = test hole, 3 = bottom scraper, 4 = hole cleaner, 5 = vacuum cleaner, 6 = generator, 7 = bucket with sand, 8 = outer tube, 9 = inner tube, 10 = top plate, 11 = wrench to attach top plate to inner tube, 12 = energy breaker, 13 = outer tube in test hole, 14 = water-hose, 15 = reference rod, 16 = assembled inner tube - top plate, 17 = OTS-full measurement, 18 = equal level measurement.

of the tube. The outer tube is slowly filled with water (14). The energy breaker and sand layer protect the natural soil surface from erosion by the turbulent water. Then the inner tube (9) and the top plate (10) which has two basal standpipes leading to the inner tube and outer tube, respectively, and three valves (a, b and c)* are assembled into one fixed unit (16). A special wrench (11) is used to tighten a ring with washer inside the inner well of the top plate (10). This binds the inner tube to its standpipe.

The distance of the bottom of the inner tube from the top plate should be so spaced that the bottom of the inner tube will be only a few cm above the sand when the assembly (16) is set into and attached to the outer tube. The hose (14) is then attached adjacent to valve c on the top plate (1). When the outer tube is brim full and water starts streaming between the loose top plate and the upper rim of the outer tube, the bolts are tightly screwed, closing down on the gasket. This procedure flushes out air, avoiding its entrapment on the under side of the top plate. Valve a is now opened to admit water to the inner tube basal standpipe. Then the connection between the top plate and the inner tube is loosened again. The inner tube slides downwards to the soil surface. The sliding distance should not exceed a few cm in order to avoid turbulence that might disturb the soil surface. The inner tube is pushed down about 2 cm into the soil. In the meantime water is continuously entering the system in such a quantity as to keep both tubes filled all the time. Overflow water that spills onto the top plate from the outer tube basal standpipe (near valve b) is drained off the top plate through a brass tube and hose extension into a bucket nearby. The depth of penetration of the inner tube is accurately measured using the reference level (15). Next, the plastic standpipes for the inner and outer tubes are fastened to the two openings in the top plate. For slow infiltrations, a smaller inner tube standpipe (ITS) is used ($R = 0.6$ cm); for larger infiltrations a larger one is used ($R = 1.85$ cm). Valve c is then opened enough to ensure a slight overflow at the top of the standpipes.

Two types of readings are made, usually starting one hour after application of the water: 1. The outer tube standpipe (OTS) - full measurement (17). Valve a is kept closed, as is, of course, valve b. 2. The equal-level measurement (18). Valve a is closed and valve b is opened, but with obstruction by the fingers at the open end of the pipe, in such a way as to synchronize the drop of the water level in the OTS with that in the ITS. Eight stop watches are started simultaneously at the beginning of a reading. One watch at a time is stopped as the water level in the ITS reaches a mark on the tube. The marks are spaced 5 cm apart over a total distance of 60 cm. Elapsed time is recorded in tenths of a second.

---

*The functions of the three valves are explained as follows: Starting with the valves closed, they can be manipulated in the course of the experiment to control the flow of water. Opening valve c allows water to flow into the outer tube basal standpipe which is situated between valve c and valve b. Opening valve b bleeds water from the outer tube standpipe, which can be isolated from the water supply by closing valve c, and from inner tube standpipe by closing valve a.

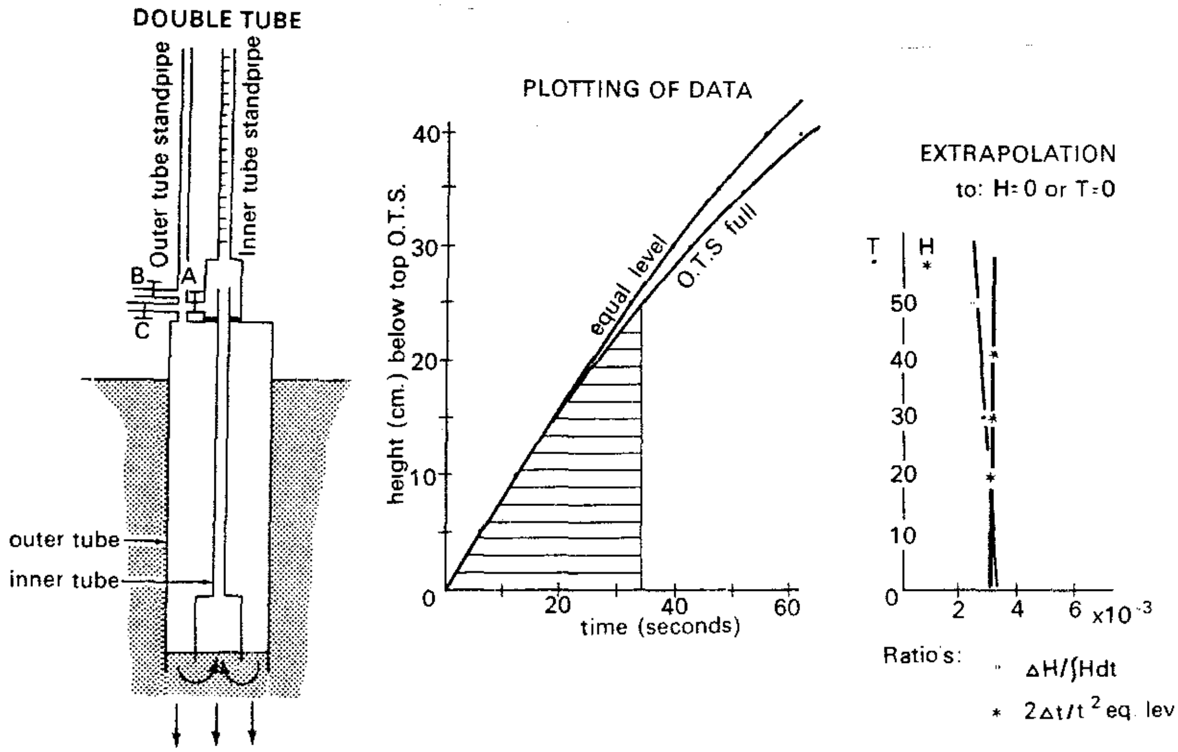

Fig. 7.5. The double tube method for measurement of K_{sat} in situ: cross section of the apparatus and plotting of experimental data.

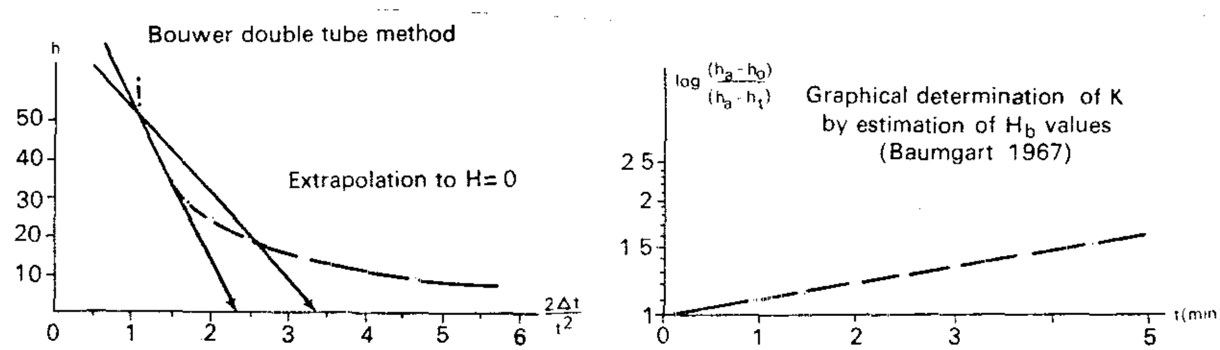

Fig. 7.6. Extrapolation procedure and graphical determination of K_{sat} using field data of the double-tube method (after Baumgart, 1967).

The readings over a distance of 40 cm should yield a difference of at least 6 seconds between two measurements; that is, between one OTS-full measurement and the average value of the preceeding and the next equal-level measurements. If the time difference is less than 6 seconds, measurement should be extended to, say, 60 cm and readings made within the lower 40 cm interval thereof. The measurements are to be repeated at regular time intervals until the ratio $\Delta t/t^2$ eq. level becomes constant (Bouwer, 1962). Here, Δt is the time difference between the OTS-full and the average value of equal level measurements before and after this OTS-full measurement.

A constant ratio may occur after a period varying from one to four hours. The constant ratio is supposed to indicate sufficient saturation of the soil below the tubes. The intervals between successive measurements should be approximately ten times as long as the time required for each separate reading, or 15 minutes (Baumgart, 1967), which is the shorter, to allow reëstablishment of equilibrium. The two final curves obtained (Fig. 7.5) differ because of flow of water from the outer tube into the inner, during the OTS-full measurement.

K is calculated according to the equation:

$$K = [R_v^2/(F_f \cdot R_c)] \cdot (\Delta H/\int H dt)$$

where: H = difference in hydraulic head H between both curves at any time t.

Hdt = surface below OTS curve (to be determined graphically)

F_f = flow factor, to be read from tables, expressing the influences of the dimensions of the system and the depth D to a layer with a much smaller or higher permeability. When D is several times larger than the diameter of the inner tube (R_c) a general set of curves may be used to estimate F_f (see Bouwer, 1961). The flow factor deviates usually only slightly from unity.

A more convenient method of calculation was suggested by Bouwer (1962) using the ratio: $2\Delta t/t^2$ eq. level instead of $\Delta H\int Hdt$.

The ratios obtained for the final set of data are extrapolated to zero, to correct for the decrease in infiltration that occurs during the equal level reading, due to the gradual decrease of hydraulic head (see example of data sheet and calculation in Table 3.2.3). The calculation of K values, according to this procedure may be difficult sometimes because of the rather inaccurate procedure of extrapolation (see left part of Fig. 7.6). Problems can be reduced when the total drop H of the water level in the inner tube standpipe (ITS) is varied for different measurements, so as to create a difference between the equal level and OTS-full times of approximately 8 sec. For example, in soils with a high infiltration, it may be necessary to extend the measurement to H = 80 cm, instead of the usual 40 cm. Baumgart (1967) made a study of the Bouwer method and suggests a somewhat modified procedure of calculation, that is based on the Bouwer calculation with an available H_b value.

Table 7.1. Calculations of the double-tube method for determining K_{sat} in situ.

General data:
Date: Aug. 5, 1969. Soil profile: Plano silt loam, B_2 55 cm depth. Time water started: noon.
Temp. water: 20°C. Tube radii: outer tube = 12.5 cm, inner tube (R_c) = 6.2 cm, R_v = 0.6 cm · d = 2.6 cm.

Measurements:

t H	1:45 PM OTS	1:55 Eq.1	2:05 OTS	2:15 Eq.	2:25 OTS	2:35 Eq.	2:45 OTS	2:55 Eq.	3:05 OTS	3:15 Eq.	3:25 OTS	3:35 Eq.	3:45 OTS	3:55 Eq.
0														
5	3.9	4.4	4.3	4.6	4.2	4.7	4.2	5.2	5.4	5.6	6.2	6.2	6.0	6.2
10	7.7	7.9	8.8	9.0	8.9	10.0	9.2	9.8	10.4	11.0	11.8	12.2	12.4	12.0
15	12.0	11.6	13.0	13.0	13.4	14.7	13.8	15.0	16.2	16.8	18.2	18.4	19.0	18.2
20	16.6	15.5	18.2	17.7	18.6	20.0	19.0	20.4	22.0	23.0	24.8	25.6	26.2	25.0
25	20.8	20.0	23.9	23.0	24.0	26.0	24.5	26.0	28.4	28.9	32.5	32.2	33.8	31.9
30	25.8	24.2	28.8	27.6	29.8	31.6	30.0	31.8	35.2	35.2	39.8	39.4	41.8	39.2
35	31.7	28.8	34.4	33.0	35.9	37.4	37.0	37.6	42.6	42.0	48.4	47.0	50.8	47.0
40	37.0	34.2	41.2	38.6	42.6	44.2	45.0	44.4	50.0	49.4	58.0	55.0	61.0	55.1

Ratio's $\frac{\Delta t}{t^2 \text{ eq.lev.}}$: 0.00305 (1:55-2:15); 0.0007 (2:15-2:35); 0.00032 (2:35-2:55); 0.00014 (2:55-3:15); 0.00020 (3:15-3:35) and 0.00020 (3:35-3:55). (constant!)

Calculation of K based on:

OTS: 3:45 PM
Eq.: level: average of 3:35 and 3:55

t	ΔH	Hdt	Ratio
30	1.0	352.5	$2.84\text{x}10^{-3}$
40	1.8	610.0	$2.95\text{x}10^{-3}$
50	2.2	975.0	$2.25\text{x}10^{-3}$

H	2Δt	t^2 eq. lev.	Ratio
20	1.8	625	$2.9\text{x}10^{-3}$
30	5.0	1544	$3.2\text{x}10^{-3}$
40	12	3025	$3.9\text{x}10^{-3}$

Ratio extrapolated to t = o : $3.0\text{x}10^{-3}$ (Fig. 3.2.3.3.) Ratio extrapolated to H = o; $3.0\text{x}10^{-3}$ (Fig. 3.2.3.3.)

The ratio $\frac{R_c}{d}$ (=2.38) was used to determine the flow factor F_f from a diagram of Bouwer (1961).

F_f = 1.1 Then:

$$K = \frac{R_v^2}{F_f \cdot R_c} \cdot \frac{\Delta H}{Hdt} = 13\text{cm/day, or } K = \frac{R_v^2}{F_f \cdot R_c} \cdot \frac{2\Delta t}{t^2 \text{ eq. lev.}} = 13\text{cm/day.}$$

H_b is the difference in cm between the top of the outer tube standpipe (OTS) and the water level at balanced flow conditions, when $Q_I = Q_H$, where Q_I is the flow leaving through the bottom of the inner tube due to intake and Q_H = flow, entering through the bottom of the inner tube due to a difference H between the water levels in inner and outer tube. Then:

$$K = \frac{2 \cdot 3R_v^{\;2}}{R_c F_f t} \cdot \log\frac{H_o - H_b}{H_t - H_b} \text{ (Bouwer, 1961)}$$

where R_v = radius of inner tube standpipe, R_c = radius of inner tube, F_f = flow factor, t = elapsed time, H = distance of water level in the inner tube below water level in the outer tube H_b = H at balanced flow. This equation can only be applied when H_b can be measured. Mostly this is not the case and then the OTS-full and equal-level measurements are made as discussed in the previous part. Baumgart (1967) suggests that this formula be used in all cases, and to estimate H_b values until the plotted values of t and log H_o-H_b/H_t-H_b are on a straight line. With some practice this can be done rather easily and quickly (see right part of Fig. 7.6., from: Baumgart, 1967). K values calculated by this procedure compared well, with those, obtained with the OTS-full equal level procedure. Application of this calculation method is recommended, because it saves time and is applicable to any type of test result.

Appendix 7.4 Field measurement of unsaturated hydraulic conductivity by infiltration through artificial gypsum crusts* (References in Section 5.2.4.)

7.4.1. Introduction

The solution of many problems associated with soil water flow depends upon knowledge of the hydraulic conductivity, K. As yet there appears to be no universally reliable way to obtain K from more fundamental physical measurements such as particle-size or pore-size distribution. Hence K is usually measured experimentally.

Of the numerous methods which have been proposed for this measurement (Klute, 1965a, b; Boersma, 1965a, b), the *in situ* methods must be regarded as inherently preferable as they are more directly applicable to the solution of field problems. Satisfactory procedures are now available for the *in situ* measurement of hydraulic conductivity under saturated conditions (K_{sat}), both below and above the water table (Bouwer, 1962). However, in many cases the flow regimen is such that the soil is unsaturated. In the presence of an impeding layer at the surface or in the presence of very low precipitation rates, the soil profile may never become saturated during infiltration, and the flow rate will be governed by the soil's unsaturated hydraulic conductivity which is, itself, a function of the matric suction prevalent in the soil.

*The type of gypsum used was ultracal-30, provided by the United States Gypsum Company. The authors wish to express their sincere thanks to Dr. R. B. Grossman for his helpful suggestion and to Mr. J. Needham (U.S. Gypsum Co.) for providing the gypsum sample.

Processes of infiltration into crust-capped profiles were recently studied by Hillel and Gardner (1969, 1970a). They reported that an impeding layer or crust at the top of an infiltrating profile causes a potential head loss at that point. Thus, if water head over the crust is kept small, it is possible to maintain infiltration into an unsaturated column yet retain the experimental advantages of easily measured inflow rate afforded by a flood infiltrometer. This finding formed the basis of a proposed method for measuring the unsaturated hydraulic conductivity at different suction and water-content values, which Hillel and Gardner (1970b) checked with artificially-packed laboratory columns, but not in the field.

7.4.2. Methods

The method described by Hillel and Gardner for measuring the hydraulic transmission properties of a profile, as a function of water content or suction, involves a series of infiltration trials through capping plates (or crusts) of different hydraulic resistances. The effect of this resistance is to prevent saturation at the subcrust boundary even though the crust itself is subject to a small positive head. Though estimates of K and D (the diffusivity) can be obtained during the transient stage of infiltration, the most reliable measurements are obtained by allowing the infiltration process to proceed to a steady state, when the flux becomes equal to the conductivity. The use of a series of crusts of progressively lower resistance can give progressively higher K-values corresponding to higher water contents up to saturation. Such a series of tests can be carried out if the soil is initially fairly dry, either successively in the same location or concurrently on adjacent locations.

The surface impedance can be applied either by means of a porous plate (e.g., ceramic) or by forming a continuous layer of puddled (slaked or compacted) soil material over the soil surface. Once the crust is established, water is applied (e.g., in a ring infiltrometer) and a small, constant head is maintained over the soil surface long enough for the inflow rate to become steady. This flow rate is equal to the conductivity in a one-dimensional flow system where the suction gradient below the crust is negligibly small (i.e. the hydraulic gradient tends to unity).

Tensiometric measurements on columns of different depth showed that in order to obtain a one-dimensional vertical flow system it was necessary to create an impervious boundary around a column at least 30 cm deep. A steel cylinder was used at the top of the column to support the small head of water over the crust, to provide a rigid sealing surface for the edges of the crust and to provide a guide for positioning tensiometers below the crust. Below the cylinder an aluminum foil moisture barrier sufficed, since saturated flow would not occur. Use of the foil also made the method applicable to stony soil. Hydraulic conductivity values were calculated from infiltration rates into capped columns and soil suction gradients below the crusts, if any.

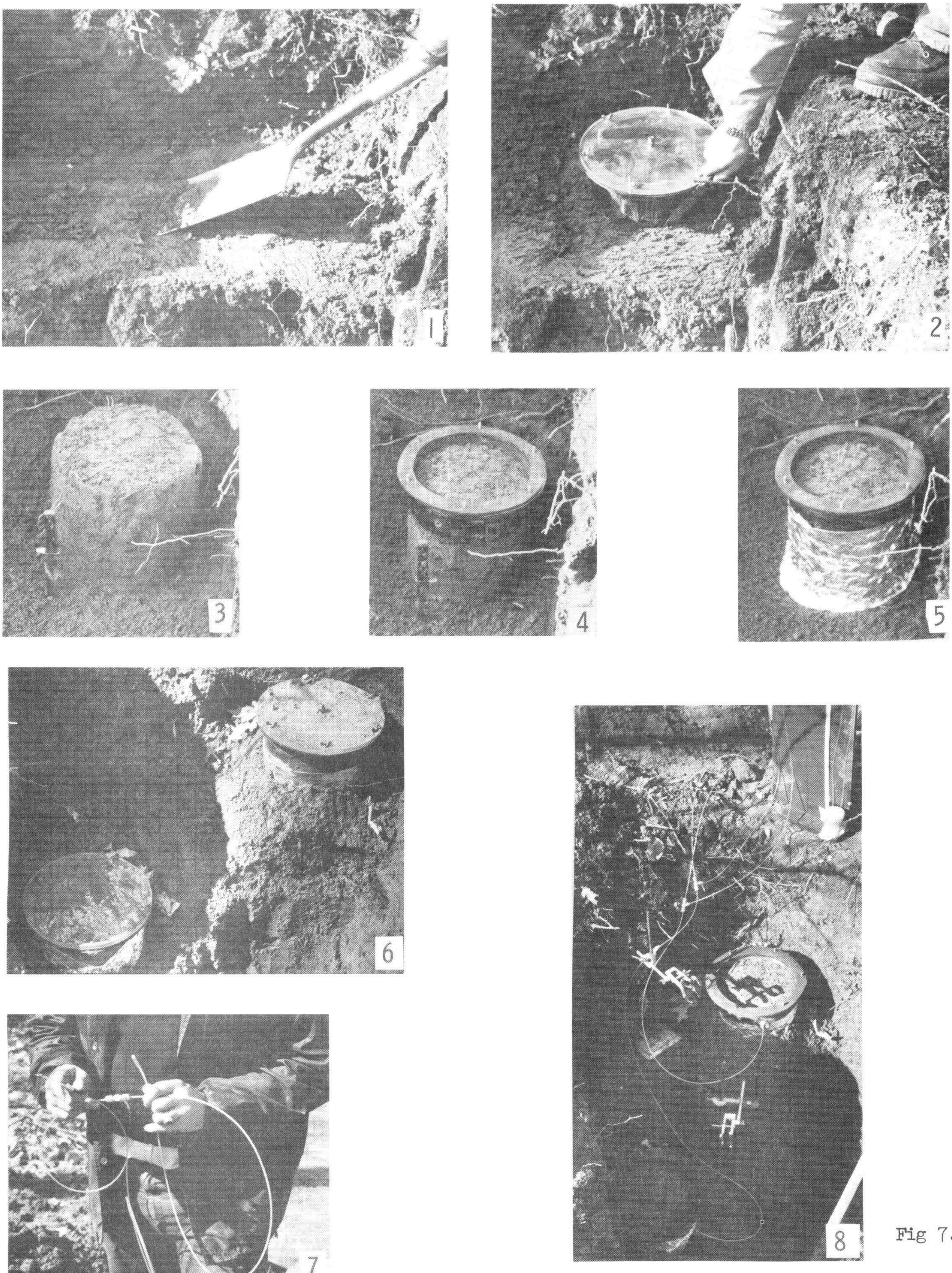

Fig 7.7

7.4.3. Procedures (see photo series, Fig. 7.7)

Tests were made at several sites in Wisconsin. The soils ranged in texture from sand to clay. At each site, a horizontal plane was prepared by using a putty knife and a carpenter's level (Picture 1). A cylindrical column of soil, at least 30 cm high, with a diameter of 25 cm, was carved out from the test level downward, taking care to chip or pick the soil away from the column as the desired boundary was approached, so as to prevent undue disturbance of the column itself (Pictures 2 and 3). A ring infiltrometer, 25 cm in diameter and 10 cm high with a 2.5 cm wide brim at the top was fitted onto the column (Picture 4). The sides of the column were then sealed with aluminum foil and soil was packed around it (Picture 5). A half-inch thick acrylic plastic cover with a diameter of 12" (30 cm) and with a thin rubber gasket glued to it was bolted to the top of the infiltrometer (Picture 6). An intake port and bleeder valve were provided in the cover.

Thin pencil-size mercury-type tensiometers (Pictures 7 and 8) were placed just below the crust in the center of the column and 3 cm deeper. Carefully positioned holes in the steel infiltrometer ring and external installation guides aided in positioning the tensiometers. Stony soils present some difficulties, but successful insertion of tensiometers is usually possible after probing at several points. Recent test results have indicated that one tensiometer 3 cm below the crust may suffice.

In the first experiments with the crust-test procedure, various puddled soil materials were used for crusts (Bouma et al., 1971b). Additional field experience, however, showed that some of these crusts (in particular the ones with a relatively low resistance) were rather unstable and easily disturbed due to continuous swelling of the clay particles. A different procedure was developed therefore in later experiments using dry gypsum powder, thoroughly mixed with varying quantities of a medium sand. After sufficient wetting, and continuous mixing, a thick paste was obtained. Then, this material was quickly transferred to the prepared column and applied on top with a carpenter's knife as a continuous crust with constant thickness. Special care was taken to seal the crust to the wall of the cylinder to avoid boundary flow. Within about 30 minutes, crusts of this type would harden, thereby providing a stable porous medium with a fixed conductivity value. Crust resistance could be varied by changing the relative quantities of gypsum and sand. Crusts composed of gypsum only had the highest resistance. For example: A subcrust tension of 52 mbar was induced in a sand column capped with a 5 mm thick gypsum crust with 3 mm water on top. This crust had a K_{sat} value of 0.007 mm/day. The microfabric of this crust consisted of very fine gypsum crystals. Some microfabrics of other crusts were pictured in Fig. 5.7 in Chapter 5. The upper picture shows relatively large pores occurring between sand grains, while fine gypsum crystals are concentrated around the grains, cementing them together. This crust was formed from a pre-wetted mixture composed of 14% gypsum and 86% sand by volume, as measured in the field using a graduated cylinder. As a crust on top of a column in sand, this mixture induced a subcrust tension of 11 mbar. K_{sat} of the crust was 8.3 cm/day. The middle picture shows a crust formed from a pre-wetted mixture with 30% gypsum by volume (70% sand). Pores are smaller and K_{sat} was 2.9 cm/day.

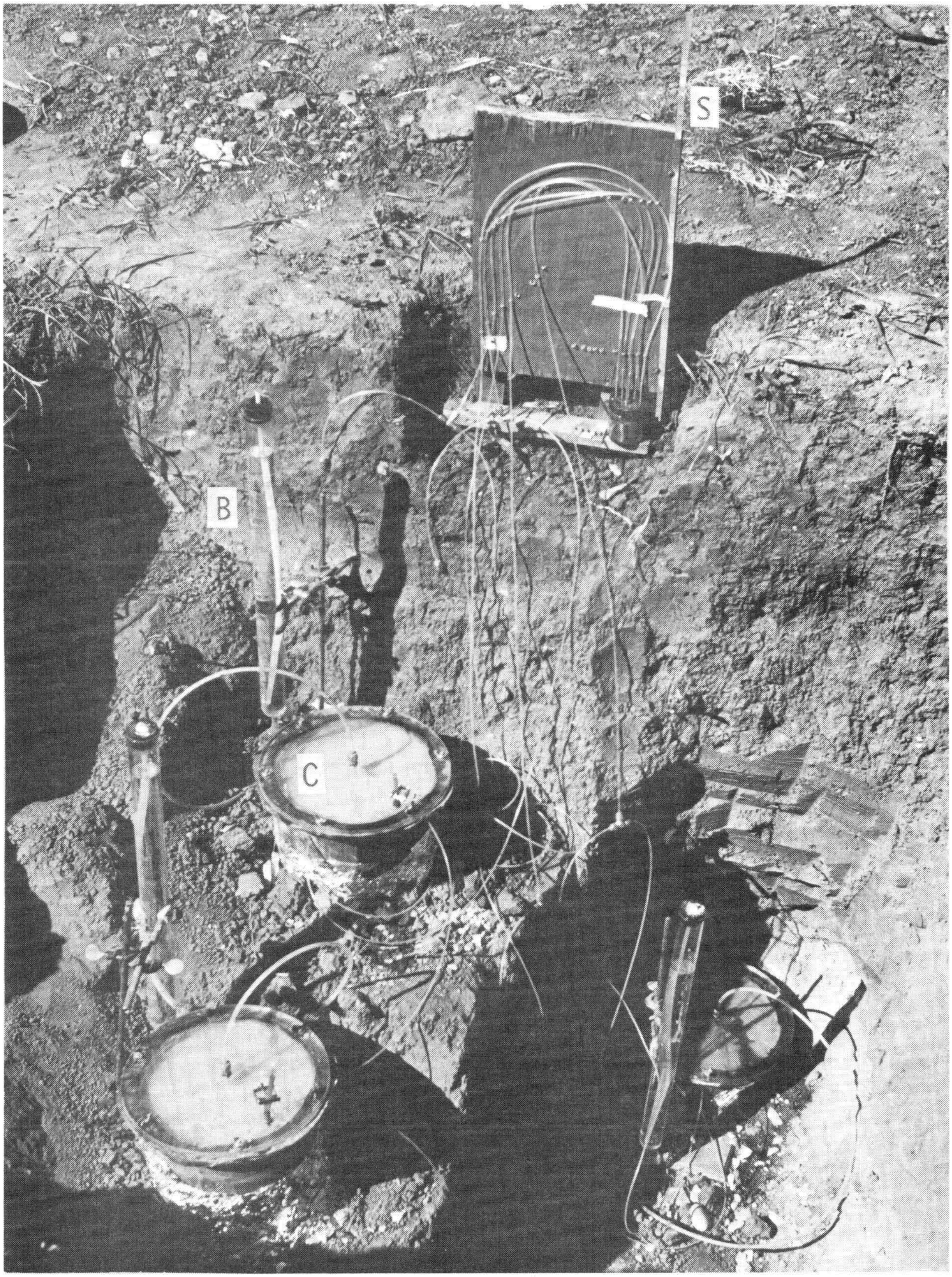

Fig. 7.8. Field measurement of unsaturated hydraulic conductivity in situ with the crust test procedure. Inflow into the soil through the crust on top of the column is measured with a burette (B) discharging into the water filled space between the crust and the acrylic plastic cover (C). Soil moisture tensions derived from the mercury rise in 1/8-inch plastic tubes along calibrated scales (S) are measured in the columns.

The induced subcrust tension in sand was 18 mbar. The third picture shows a crust formed from a dry mixture with 50% gypsum (50% sand). Virtually no larger pores are visible in the crust, indicating that pore sizes between the fine grained gypsum crystals are smaller than the thickness of the thin section (20 microns). K_{sat} of this crust was 0.8 mm/day and the induced tension in the subcrust sand in the column increased to 30 mbar.

Crusts of this type were applied to the same column for succeeding runs. Each infiltration run through a particular crust yielded one point of a curve of hydraulic conductivity versus soil suction (see Fig. 7.9). The small space between the crust surface and the cover of the cylinder was kept full of water. A Mariotte device, in a burette, maintained a constant pressure of about 3 mm water over the crust (Fig. 7.8). The infiltration rate into the soil, corresponding to the rate of movement of the water level in the burette, was recorded as soon as the tensiometers showed that equilibrium had been reached. This infiltration rate, when constant for a period of at least 4 hours, was taken to be the unsaturated K-value at the subcrust suction, when the suction gradient was zero. In some cases a suction gradient remained at steady state conditions. Hydraulic conductivity was then calculated according to: $K = v/i$, where v = infiltration rate and i = hydraulic gradient below the crust (in such a case $\neq 1$).

7.4.4. Results

Figure 7.9 gives the hydraulic conductivity versus suction curves for some horizons of four soils. These curves could be extended farther into the dry range, but this would take more time and requires that the soil be initially quite dry. The hydraulic conductivity values for saturated soil, measured with the double tube apparatus corresponded well with infiltration rates into these columns before crusts were added. One column was of glacial till, containing many stones that made use of the Bouwer tubes impossible.

The data indicate that hydraulic conductivity decreases sharply with increasing soil moisture tension. This is most evident in soil materials with coarse pores (B3, Plainfield sand) and less so in fine porous clays (B2, Hibbing), in which saturated conductivity is low. These results are important for the study of liquid waste disposal in soils. Measurement of soil moisture tensions around seepage beds of operating systems (5) indicated the occurrence of considerable soil moisture tensions. Movement of liquid, therefore, is governed by processes of unsaturated flow. A quantitative analysis of the flow system can only be given when relevant K values, as measured with this new test, are available.

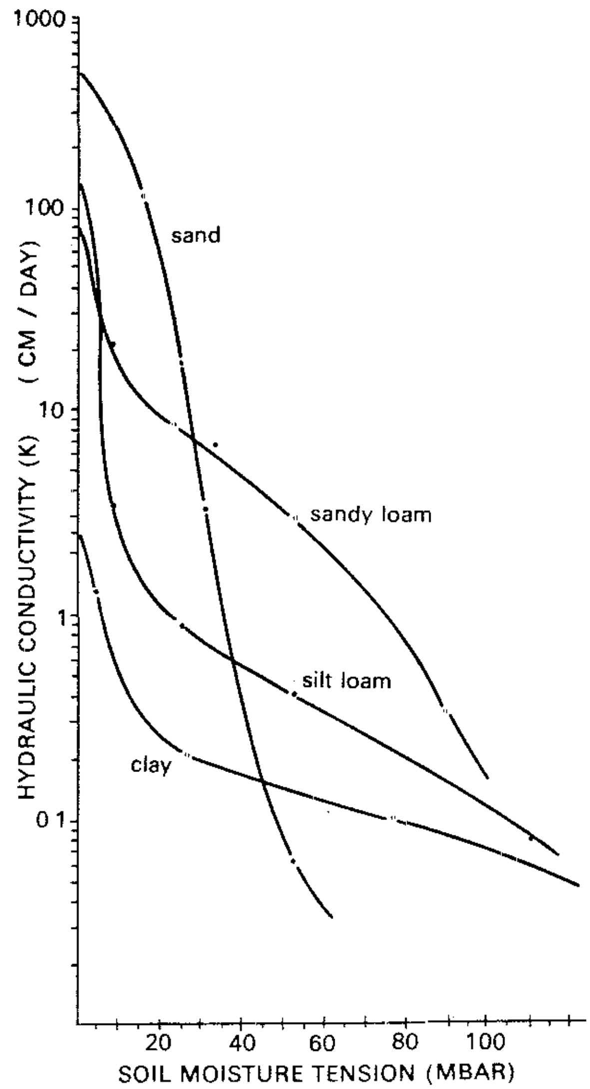

Fig. 7.9. Hydraulic conductivity (K) as a function of soil moisture tension measured *in situ* with the crust test procedure.

Appendix 7.5

7.5. The instantaneous profile method.

This method can be used to determine K-values in the field *in situ*. Several authors have described the basic method (Staple and Lehane, 1954; Ogata and Richards, 1957; Rose et al., 1965; Watson, 1966; Davidson et al., 1969; Rose and Stern, 1967; Nielsen et al., 1972 and Hillel at al., 1972). The theoretical basis of the method will be reviewed and a description of the procedure to be followed in the field will be given. Finally a completely worked out example will be presented as obtained for the Ap, B_1, and B_2 horizons of the Batavia silt loam (UW-Charmany Farm, Madison, Wisconsin).

THEORY

The general equation describing flow of water in a vertical soil profile is (see Chapter 3.3)

$$\frac{\partial \theta}{\partial t} = \frac{\partial}{\partial z} \left[K(\theta) \frac{\partial H}{\partial z} \right] \qquad (1)$$

where θ is volumetric wetness; t = time, z = vertical depth coordinate (here positive downwards), K = hydraulic conductivity; H = hydraulic head (= M + z) Integration results in:

$$\int_0^z \frac{\partial \theta}{\partial t} dz = \frac{\partial \theta}{\partial t} \cdot z = K(\theta) \frac{\partial H}{\partial z} \qquad (2)$$

where Z is the soil depth to which the measurement applies. If the soil surface is covered to prevent evapotranspiration, only internal drainage can occur. Equation (2) states that the change in water content per unit time for a given vertical distance Z equals the product of the relevant K and hydraulic head gradient at point Z. The total change in water content per unit time over depth Z may be obtained by summation of changes occuring in smaller depth intervals that, together, add up to total depth Z as follows:

$$\int_{0}^{Z_1} \frac{\partial\theta}{\partial t}\, dz + \int_{Z_1}^{Z_2} \frac{\partial\theta}{\partial t}\, dz + \int_{Z_2}^{Z_3} \frac{\partial\theta}{\partial t}\, dz \quad \text{etc.} \tag{3}$$

where $Z_1 + Z_2 + Z_3 = Z$ and the zero level represents the soil surface.

Initially, the whole profile is saturated (P = 0). Tensiometers are installed at depths Z_1, Z_2, and Z_3 and record soil moisture tensions as a function of time ($= \partial\theta/\partial t$).

The gradient of the hydraulic head can be measured and the K can be calculated by:

$$K(\theta) = \frac{(\partial\theta/\partial t) \cdot Z}{(\partial H/\partial z)} \tag{4}$$

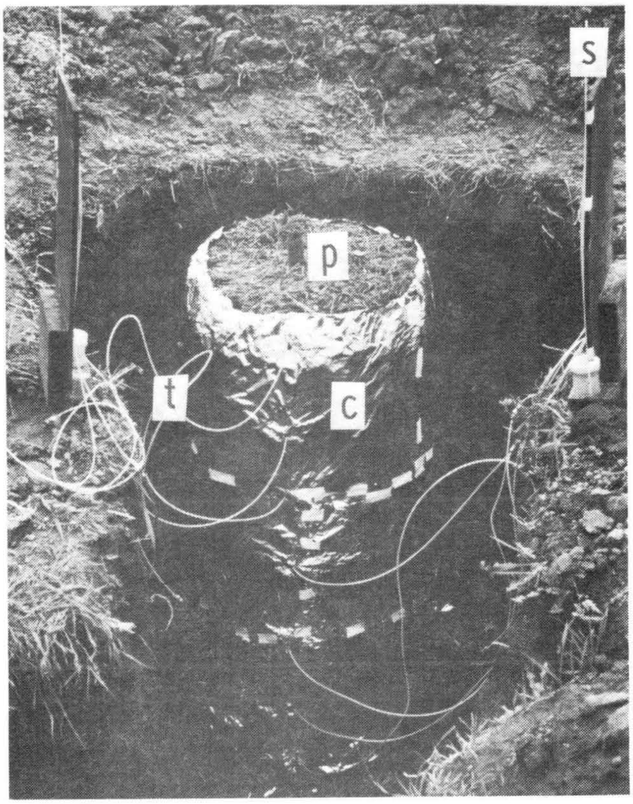

Fig. 7.10. Excavated column to be used for field determination of $K_{unsat.}$ with the instantaneous-profile method (see text). p = metal pipe for neutron probe; c = soil solumn; t = tensiometers and s = tensiometer boards with calibrated scales for reading moisture tensions.

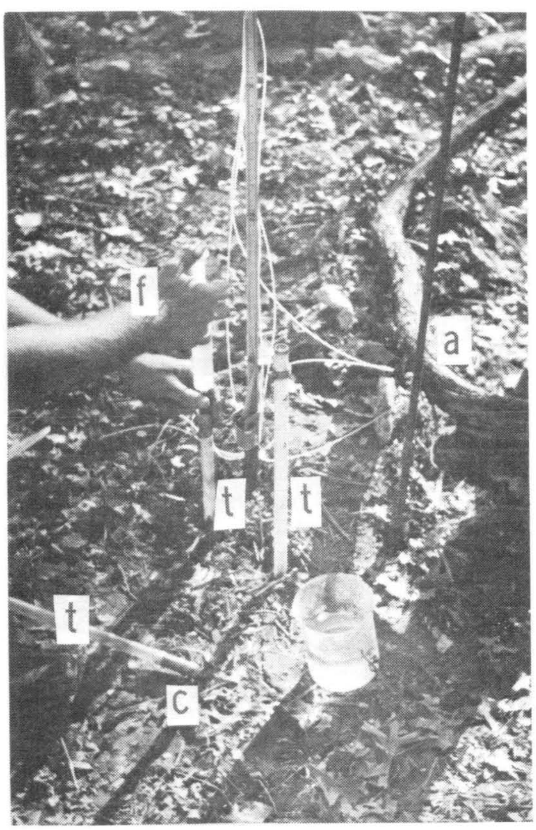

Fig. 7.11. Tensiometers used for the instantaneous profile method as applied to a large area ($10m^2$). c = porous cups cemented to plastic tubes (t) forming tensiometers, that are vertically installed in the plot by placement into vertical holes, drilled with an auger (a). The plastic tubes were filled with water (f) and connected with very samll tubes leading into mercury, following a calibrated scale. The rise of mercury in the small tubes can be used to determine the soil moisture tension. Tensiometers can be installed at different depths.

Experimental procedure.

1. A fallow plot has to be selected in the field that is sufficiently large so that processes of one-dimensional vertical flow in its center are unaffected by its boundaries. A plot of 3 x 3 m may be sufficiently large (Davidson et al., 1969). An alternative procedure is to carve out a large cylindrical column of soil down to a depth of 1.80 cm below the soil surface (Fig. 7.10). This column has to be carefully wrapped with aluminum foil to avoid any evaporation from the sidewalls of the column.

2. Tensiometers are placed at certain intervals preferably not exceeding 30 cm (Fig. 7.10 or 7.11). A morphological study of soil structure has to preceed this installation because measurement results will be most significant if tensiometers coincide with boundaries of major horizons.

3. An access tube, to be used for measurement _in situ_ of soil moisture contents with the neutron probe, can be installed in the center of the plot. An alternative procedure is to determine the moisture retention curves (desorption) for the major horizons by analyzing soil cores in the laboratory (see Appendix 7.2). The measured soil moisture tensions can be translated into moisture contents using these desorption curves. (This procedure was followed in the following example).

4. Water is ponded on top of the fallow plot or the column until all tensiometers indicate saturated conditions or constant low tensions. The soil surface is then covered with a plastic sheet to avoid evaporation and tensions in all

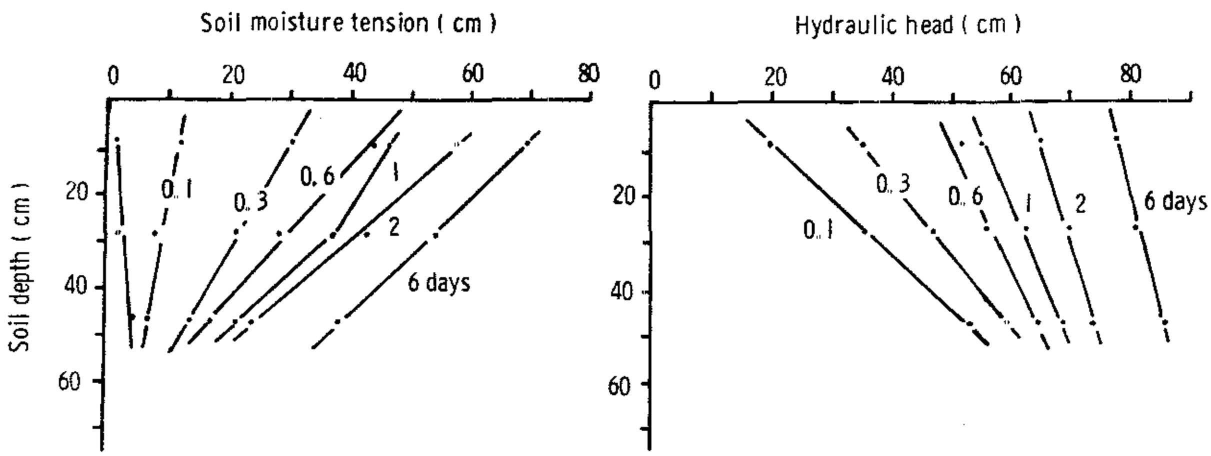

Fig. 7.12. Moisture tensions and hydraulic heads measured <u>in situ</u> at three depths in the Batavia silt loam as a function of time as part of the instantaneous profile methods.

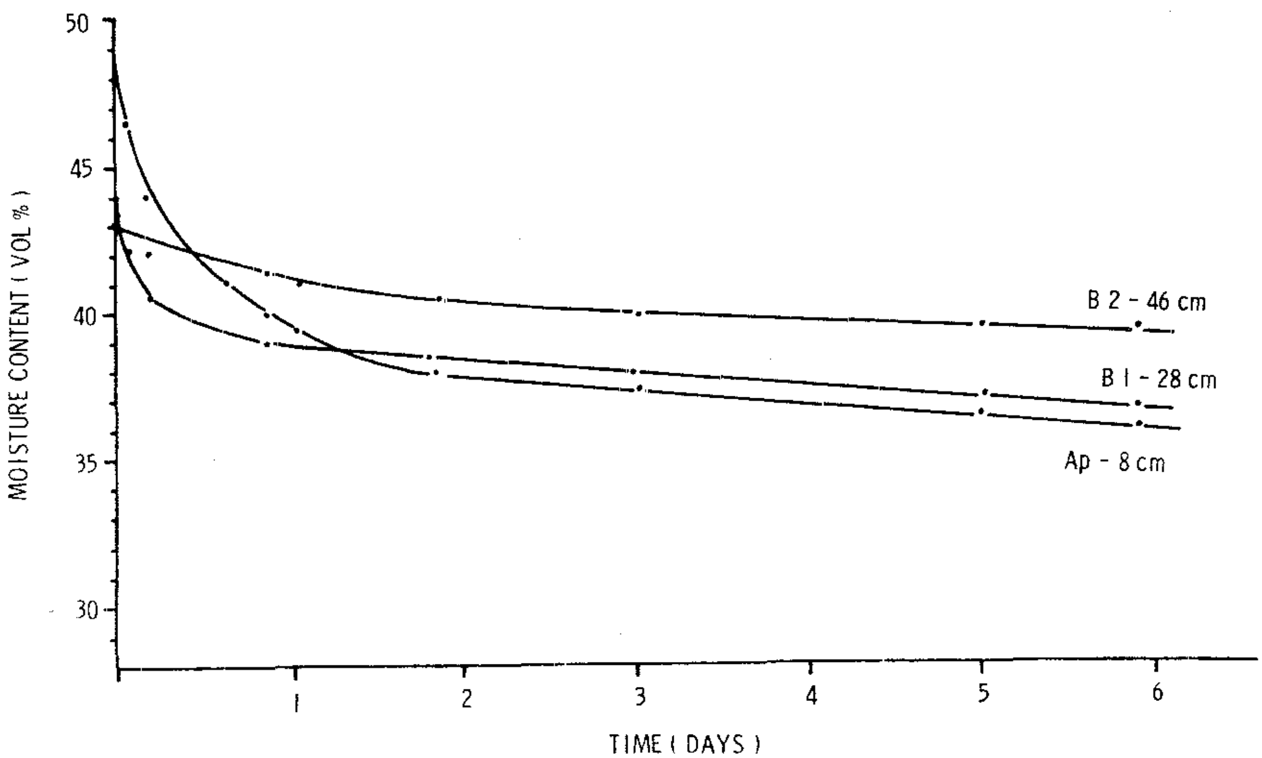

Fig. 7.13. Moisture contents derived from moisture retention data using measured moisture tensions for three depths in the Batavia silt loam.

Table 7.2: Calculation K instantaneous profile method

t	z	$\partial\theta/\partial t$	dz $(\partial\theta/\partial t)$	$q = \Sigma$ dz
0.1 day	0-8	0.190	1.520	1.520
	8-28	0.150	3.000	4.520
	28-46	0.020	0.360	4.880
0.3 day	0-8	0.068	0.544	0.544
	8-28	0.040	0.800	1.344
	28-46	0.018	0.324	1.668
0.6 day	0-8	0.050	0.40	0.400
	8-28	0.016	0.32	0.720
	28-46	0.016	0.288	1.008
1 day	0-8	0.040	0.32	0.320
	8-28	0.003	0.06	0.380
	28-46	0.007	0.126	0.506
2 day	0-8	0.010	0.080	0.080
	8-28	0.003	0.060	0.140
	28-46	0.0025	0.045	0.185

Table 7.3

Depth	q	$\partial H/\partial z$	K cm/day	$\bar{\theta}$	P
8 cm	1.520	0.86	1.75	.440	12
	0.544	0.50	1.08	.400	30
	0.400	0.45	0.85	.385	42
	0.320	0.40	0.80	.375	46
	0.080	0.20	0.40	.365	58
	0.032	0.10	0.22	.350	80
28 cm	4.520	0.86	5.30	.400	8
	1.344	0.50	2.68	.355	22
	0.720	0.30	2.15	.350	28
	0.380	0.28	1.14	.345	36
	0.140	0.20	0.70	.340	42
	0.082	0.20	0.40	.335	59
46 cm	4.880	0.86	5.65	.415	7
	1.668	0.50	3.34	.400	14
	1.008	0.30	3.00	.395	17
	0.506	0.28	1.55	.390	21
	0.185	0.25	0.74	.385	24
	0.09	0.24	0.37	.375	42

tensiometers and the moisture content are measured as a function of time. First, some hourly measurements may be needed. Later, daily measurements may suffice. The necessary frequency of measurement and the duration will vary for different soils.

Handling of Data

Data for three soil depths in the Batavia silt loam: the Ap horizon (A_1 = 8 cm depth), the B_1 horizon (Z_2 = 28 cm depth) and the B_{21t} horizon (A_3 = 46 cm depth) are presented in Figs. 7.12 and 7.13. These data include curves giving the moisture tensions (Fig. 7.12), the derived moisture contents (Fig. 7.13), and the hydraulic heads (Fig. 7.12)as a function of time at the three depths.

Calculations of soil moisture fluxes ($\partial\theta/\partial t$) are presented in Table 7.2 $\partial\theta/\partial t$ values were graphically determined from Fig. 7.13 for each depth. Table 7.3 presents the calculation of K, using the fluxes calculated in Table 1 and the slopes of the hydraulic-head curves ($\partial H/\partial z$) as graphically determined from Fig. 7.12.

The calculated K values were plotted in Fig. 7.14 as a function of P (P directly measured _in situ_). A comparison was made in Fig. 7.14 with K values measured in the same soil at the same site with the crust test (see Appendix 7.4). Agreement was quite good.

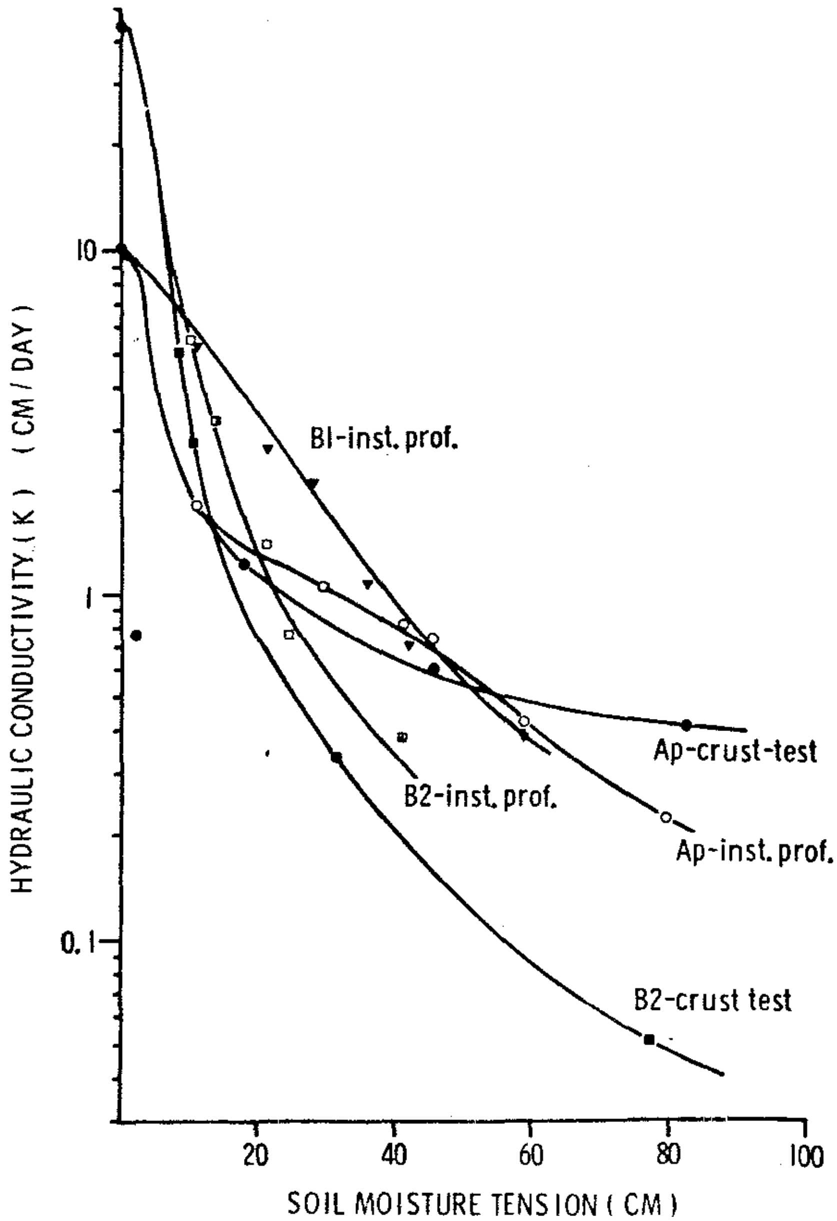

Fig. 7.14. Hydraulic conductivity (K) as a function of moisture tension, measured in situ with the crust test in the Ap and B2 horizon and with the instantaneous-profile method in the Ap, B1, and B2 horizon of the Batavia silt loam.

7.5. LITERATURE CITED

1. Davidson, J.M., L.R. Stone, D.R. Nielsen and M.E. Larue. 1969. Field measurement and use of soil water properties. Water Resources Research. Vol. 5, no. 6. 1312-1321.

2. Hillel, D.I., V.D. Krentos and Y. Stylianon. 1972. Procedure and test of an internal draingae method for measuring soil hydraulic characteristics in situ. Soil Science. Vol. 114, no. 5: 395-400.

3. Nielsen, F.R., J.W. Biggar and J.C. Corey. 1972. Application of flow theory to field situations. Soil Science. Vol. 113, No. 4: 254-264.

4. Rose, C.W., Stern, W.R. and J.E. Drummond. 1965. Determination of hydraulic conductivity as a function of depth and water content for soil in situ. Austr. J. Soil Res. 3 :1 .

5. Rose, C.W. and W.R. Stern. 1967. The drainage component of the water balance equation. Austr. J. Soil Res. 3:95-100.

6. Wattson, K.K. 1966. An instantaneous profile method for determining the hydraulic conductivity of unsaturated porous materials. Water Resources Res. 2:709-715.

7. Ogata G. and L.A. Richards. 1957. Water content changes following irrigation of bare-field soil that is protected from evaporation. Soil Sci. Soc. Amer. Proc. Vol. 21, no. 4. 355-356.

8. Staple, W.J., Lehane, J.J. 1954. Movement of moisture in unsaturated soils. Canad. J. Agri. Sci. vol 34:329-342.

Appendix 7.6. Calculation of hydraulic conductivities from moisture retention data (method of Green and Corey).

A detailed description of this method, based on a review and revision of earlier work, is given by Green and Corey (1971). Larger soil pores are progressively emptied with increasing soil moisture tension and since flow rates are strongly correlated with pore sizes (Chapter 3), a relationship between flow rates and moisture tension can be derived in principle for different soil materials using moisture retention characteristics. In addition, a pore interaction model is necessary to express the dominant hydraulic effect of small pores on the rate of flow in a complex heterogeneous pore system. The equation used by Green and Corey (1971) is as follows:

$$K(\theta)_i = (K_s/K_{sc}) \cdot (30\delta^2/\rho g \eta) \cdot (e^p/n^2) \cdot \sum_{j=1}^{m}\left[(2j+1-2i)h_j^{-2}\right]$$

$$i = 1,2, \ldots m$$

where: $K(\theta)_i$ is the calculated conductivity for a specified water content (given in cm/day); θ is water content (cm^3/cm^3); i = last water content class on the wet end: i = 1 = pore class corresponding with θ_{sat}. i = m = pore class with lowest water content for which K is calculated; K_s/K_{sc} = matching factor (= measured/calculated K); δ = surface tension of water (dynes/cm); ρ = density of water (g/cm^3); g = gravitational constant (cm/sec^2); η = viscosity of water (g/cm sec) e = porosity (cm^3/cm^3); p = parameter. Here p = 2, n = total number of pore classes between $\theta = 0$ and θ_{sat}; h_j = pressure of a given class of waterfilled pores (cm water).

The need for use of the matching factor (K_s/K_{sc}) implies that the method does not directly yield a curve at the correct level of conductivities for each moisture content or tension, but that the slope of the calculated K-curve is assumed to be correct. This method has been applied to several Wisconsin soils. Unpublished results show that calculated K-curves for sandy, apedal soil horizons agree well with those determined experimentally. Results for clayey, pedal soil horzons were quite variable, however, and use of the method for these soils is not recommended.